Three-dimensional Assessment of Facial Asymmetry in Children with Operated Unicoronal Synostosis

Thesis submitted in accordance with the
requirements of the
University of Liverpool
for the degree of
Doctorate of Dental Science
by

Emer Byrne

June 2018

Acknowledgements

I wish to express my gratitude to my supervisors Dr Dominguez-Gonzalez, Dr Flannigan and Dr Burnside for their assistance and support throughout this project. In addition I wish to thank Dr Burnside for his statistical input and advice with all stages of the project.

I wish to thank my colleague Orla for her input through the design of the project and in particular with the inter-rater reliability which was an essential element of the study. I also wish to thank John Owens and the Medical Photography team at Alder Hey Children's Hospital for their ongoing help with the use of the 3dMD imaging system.

I finally wish to thank the craniofacial team at Alder Hey and the participants for the use of the 3dMD images without whom the project would not have been possible.

Table of Contents

Table of Contents

Abstract

Three-dimensional Assessment of Facial Asymmetry in Children with Operated Unicoronal Synostosis.

E. BYRNE[1]*, N. FLANNIGAN[1], G. BURNSIDE[1] and S. DOMINGUEZ-GONZALEZ[2] ([1] Liverpool University Dental Hospital. [2] Alder Hey Children's Hospital, Liverpool)

Objectives: The primary objective was to quantitatively describe soft tissue middle and lower third facial asymmetry and facial rotation in children with Unicoronal synostosis (UCS) who have undergone surgical correction with Fronto-orbital Advancement and Remodelling (FOAR) in infancy using three-dimensional stereophotogrammetric imaging. The secondary objective was to assess if a correlation exists between facial asymmetry and age of imaging or age of surgical intervention.

Design/ Setting: A retrospective cross-sectional study undertaken at Alder Hey Craniofacial Unit, Liverpool.

Subjects: Children with nonsyndromic UCS who underwent Fronto-orbital Advancement and Remodelling in infancy and had post-operative 3D imaging with the static 3dMD head system.

Methods: Participants with nonsyndromic UCS and who underwent FOAR at Alder Hey Craniofacial Unit in infancy were identified. The quality of their static 3dMDhead images were assessed for inclusion in the study. Twenty two anthropometric landmarks were identified (eight mid-facial and seven paired bilateral landmarks) for each participant on the static 3dMDhead images. The landmarks were remarked on a random sample of 24 images to assess intra-rater and inter-rater reliability by two investigators. An asymmetry index (AI) was calculated for each landmark and linear and surface measurements between each of the paired bilateral landmarks and the landmark Nasion were measured. Deviation of the nasal tip and chin were also measured to assess the direction of facial rotation.

Results: Thirty six participants were included for analysis. The mean age of FOAR was 1yr 5 months and the average age of 3D imaging was 5yrs 6months. Intra-class correlation coefficients showed excellent agreement (ICC 0.96-0.99) for all landmarks with the exception of Nasion in the *x* direction which had good agreement (intra-rater ICC 0.66 and inter-rater ICC 0.77). The asymmetry index showed that facial asymmetry was evident in the middle and lower face and increased as you move superiorly to inferiorly away from the cranium. The AI was lowest for the landmark Nasion (0.49mm) and highest for Cheilion (7.11mm). The amount of asymmetry was generally greater in the medio-lateral direction. Average deviation of the nasal tip and Pogonion to the unfused side was 4.4 ± 3.9 degrees and 3.5 ± 2.7 degrees respectively. Significant facial rotation of the middle and lower face

towards the unfused side was evident (Chi-square analysis, $p < 0.001$). Age of imaging and age of surgical intervention did not correlate with facial asymmetry.

Conclusions: The findings of this study demonstrate that children with UCS who undergo FOAR in infancy show consistent soft tissue facial asymmetry post-operatively. FOAR does not change the direction of facial growth with continuation of the UCS phenotype of facial rotation towards the unfused side.

Chapter 1: Introduction

The cranial bones are separated by cartilaginous tissue or sutures at birth.[1] The purpose of the sutures are to facilitate moulding of the skull as it passes down the birth canal as well as allow for the expanding brain and absorption of mechanical trauma during childhood.[2] Complete closure of the sutures may not occur until adulthood. Premature fusion of these sutures results in craniosynostosis.[3]

Unicoronal synostosis (UCS) results from premature fusion of one of the coronal sutures and commonly results in pronounced craniofacial asymmetry.[4,5] The characteristic facial features of untreated individuals with UCS has been well documented in the literature.[6–10] The goal of surgical intervention in these patients is to allow adequate intracranial volume for the expanding brain and it is also aimed at providing more optimal conditions for normal or symmetrical facial growth.[11,12]

Studies have shown that symmetry in the human body is theoretical and even in faces which are considered aesthetically pleasing a degree of asymmetry is evident.[13] Several studies have investigated the amount of post-operative facial asymmetry in children with UCS who have undergone surgical intervention in infancy.[6,14–18] Different methods have been used to assess facial asymmetry including direct anthropometric measurements, two-dimensional imaging techniques including the use of cephalograms as well as three dimensional techniques such as CT imaging.[6,14–18] CT imaging facilitates assessment of the hard tissues but does not allow soft tissue assessment and requires exposure to ionizing radiation. More recent studies have focused on the use of non- invasive 3D imaging including stereophotogrammetry to allow assessment of soft tissue facial asymmetry in UCS subjects.[9,11] These techniques have been shown to be reliable and have a high degree of precision.[19–22] This study aims at assessing the degree of soft tissue facial asymmetry in a group of children with Unicoronal synostosis who underwent surgical intervention in infancy.

Chapter 2: Literature review

2.1: Normal Development of the Skull Bones

The cranial bones are formed during the first weeks of foetal life by membranous ossification which continues during the second and third months.[23] The skull consists of flat bones; the paired frontal bones, the paired parietal bones, the lateral walls are made of the squamosal part of the temporal bone and the greater wing of the sphenoid and the anterior part of the occipital bone also makes up the skull bones.[24–26] At birth the cranial bones are separated by connective tissue, the sutures and the fontanelles.[23] There are six major sutures; metopic and sagittal sutures which are single sutures and the paired coronal and lambdoid sutures as illustrated in Figure 1.[27,28] The metopic suture forms between the paired frontal bones and the sagittal suture between the paired parietal bones. In a transverse direction the coronal sutures are found between the frontal and parietal bones and the lambdoid suture connects the parietals with the occipital bone. The points where the cranial bones meet the sutures remain wide and these are called the fontanelles.[29] These allow a degree of moulding of the skull as it passes down the birth canal. The sutures and fontanelles fuse at different ages with the fontanelles generally closed by 18 months of age.[10,28] Closure of the posterior fontanelle usually proceeds closure of the anterior fontanelle.[1,30] The metopic suture starts to fuse at 9 months but may persist until up to two years of age. Complete closure of the coronal, sagittal and lambdoid sutures can persist well into adulthood as shown in Figure 2.[28] As well as facilitating moulding, the function of the suture is to allow adjustment for the expanding brain and absorption of mechanical trauma in childhood.[2]

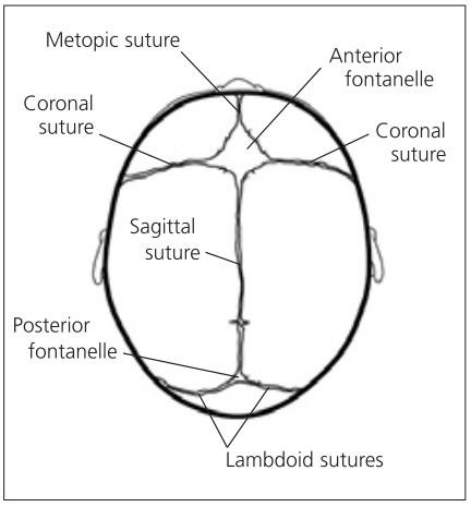

Figure 1. The cranial vault of newborn demonstrating the sutures and fontanelles. Adapted from Kabbani et al. [28]

Growth of the cranial vault is in response to pressure of the intracranial tissues which passively displaces the bones of the skull at the sutures. In response to this displacement, the intramembranous bones of the cranium grow by compensatory bone growth at the sutures as well as remodelling along the external and internal surfaces. The process of growth along the sutures must be closely regulated with new bone formation occurring in equilibrium with bone displacement or separation so as to maintain patency. If this is not the case then premature fusion of one of more of the sutures can occur resulting in craniosynostosis.[3]

Cranial Suture	Closure Begins (yrs)
Interfrontal (metopic)	2
Interparietal (sagittal)	22
Frontoparietal (coronal)	24
Occipitoparietal (lambdoid)	26
Temporoparietal (squamosal)	35-39

Figure 2. Timing of closure of craniofacial sutures. Adapted from Meikle et al. [31]

2.2: Craniosynostosis

2.2.1: Definition

Craniosynostosis is a craniofacial malformation characterized by premature fusion of one or more of the cranial sutures.[4,10,23,29,32,33] The consequence of this premature fusion is abnormal skull growth resulting in a characteristic distorted head shape and an increased risk of elevated intracranial pressure.[4,23]

2.2.2: Prevalence

The prevalence is variable but has been quoted in the literature as between 3 and 6.4 cases per 10,000 live births.[29,32,34–37] It has been observed in many racial groups including Caucasian, Asian, native American, African and Australian populations.[10]

The incidence of nonsyndromic craniosynostosis has been shown to have increased by 2.5% per year between 1982 and 2008.[37] Cornelissen et al.[4] investigated the prevalence of craniosynostosis in the Netherlands between 2008 and 2013. They found the prevalence to be 7.2 per 10,000 live births and that total craniosynostosis, sagittal and metopic synostosis had all demonstrated a significant increase in prevalence of 12.5%, 11.7% and 20.5% respectively over this period. They were unable to identify a

specific cause for this increase but hypothesised this may have resulted from a true raised prevalence or as a consequence of raised awareness and therefore greater detection of such cases.[4]

2.2.3: Classification

Craniosynostosis can be classified according to three sub-categories as demonstrated in Figure 3 depending on: [2,10,23,29,38]

1. The number of sutures involved. In simple craniosynostosis, only one suture is involved such as sagittal, coronal, metopic or lambdoid, whereas in complex craniosynostosis two or more sutures prematurely fuse. Single suture craniosynostosis results in deformities in head shape depending on which suture is involved.[1]
2. Aetiology. Craniosynostosis can be classified as either primary, where there is an intrinsic defect in the suture and occurs in isolation or secondary where premature fusion occurs alongside other medical conditions such as thalassemia, hyperthyroidism, haematologic and metabolic disorders. Primary craniosynostosis is more common than secondary craniosynostosis.
3. Whether it is nonsyndromic or syndromic. Nonsyndromic craniosynostosis, also known as isolated craniosynostosis occurs without any other evident abnormalities other than those associated with the premature fusion. This contrasts with syndromic craniosynostosis which is accompanied by other developmental defects and involves multiple systems such as cardiac, genitourinary and musculoskeletal systems. Syndromic craniosynostosis includes syndromes such as Apert syndrome and Crouzon syndrome which are the most common. Others include Carpenter syndrome, Muenke syndrome and Saethre-Chotzen syndrome.

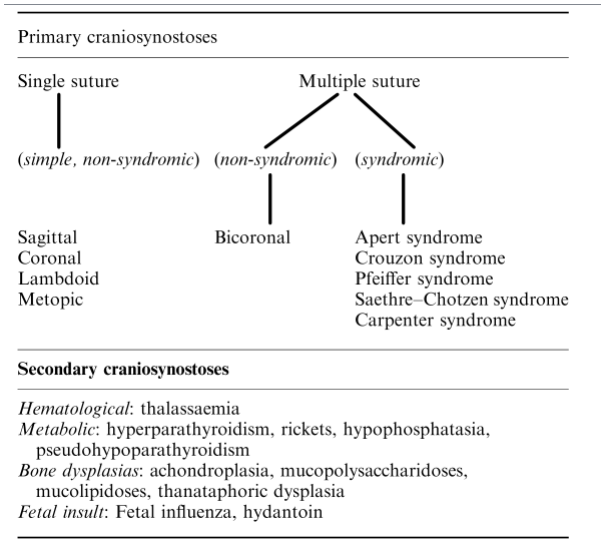

Figure 3. Anatomical Classification of craniosynostosis. Adapted from Aviv et al.[23]

2.2.4: Sagittal suture synostosis

Sagittal synostosis is the most common form of simple craniosynostosis accounting for 40% to 58% of all cases.[2,33] It most commonly affects males with a male to female ratio of 3.5:1 and estimated prevalence of 1.9 to 2.8 per 10,000 live births.[10,36,39] Lajeunie et al. found that the defect is transmitted as an autosomal dominant disorder with 38% penetrance and 72% sporadic cases.[39] Genetic analysis showed that 6% of families demonstrated a high degree of familial aggregation.[39] Risk factors are thought to include twinning, increased parity, maternal smoking and constraint of the intrauterine head.[10,33]

Sagittal synostosis although not directly, indirectly involves the skull base.[40] Due to growth inhibition in a direction perpendicular to the affected suture, transverse growth of the skull is inhibited. There is continuing growth in an anteroposterior direction. As such sagittal suture synostosis results in anteroposterior lengthening of the skull, also known as dolichocephaly or scaphocephaly, and appearance is of a boat shaped skull (Figure 4 and Figure 7).[10,27,29,41,42] Ridging of the sagittal suture is palpable.[10] The metopic and coronal sutures are still patent and therefore there is unrestricted growth of these sutures. Clinical features include an inclined anterior forehead, frontal bossing and increased intra-orbital distance. Occipital bulging is also a feature due to unrestricted growth at the patent lambdoid suture.[29]

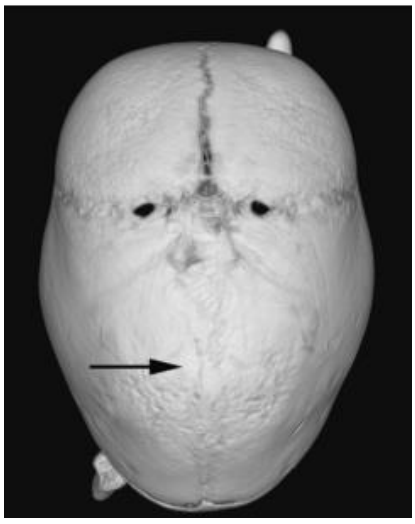

Figure 4. Sagittal suture synostosis. Nagaraja et al.[29]

2.2.5 Metopic suture synostosis

Metopic synostosis accounts for approximately 4% to 10% of all craniosynostosis cases with an incidence of 1.9 per 10,000 births.[36] Similar to sagittal synostosis it has a male predominance with a male to female ratio of 3.3:1. [2,33,43] Kweldman et al. found that the incidence is increasing as shown by a 6% increase per year between 1997 and 2007.[36]

The two frontal bones are separated by the metopic suture at birth and suture closure can begin as early as 3 months, making it the first in the skull to fuse physiologically. Fusion usually occurs by the 9th month although there is individual variation and may take up to 2 years without any pathological consequences.[29,44–46]

Premature fusion of the metopic suture results in a triangular shaped head or trigonocephaly as shown in Figure 5 and Figure 7.[27,42,44] There is compensatory expansion at the patent sagittal and coronal sutures.[23] Clinically the head demonstrates a pointed forehead and the eyebrows may appear "pinched".[10] Features also include depressions over the lateral aspect of the pterions (the region on the side of the skull, behind the temple where the frontal, parietal, temporal and sphenoid join together) and hypotelorbitism or reduced distance between the orbits.[40]

Approximately 75% of cases are isolated while 25% are associated with a syndrome.[29] Lajeunie et al. however, in an analysis of 237 patients with trigonocephaly showed that only 5.6% of cases were associated with a family history.[43] Other risk factors which have been identified are multiple births, premature birth, low birth weight, increasing maternal age, and emergency caesarean births. Males are also more commonly affected. Syndromes which have been identified to be associated with metopic synostosis include Baller-Gerold, Jacobsen (including 11q24.1 deletion), chromosome 9p deletion, Opitz C syndrome and Chiari I malformation.[2,29,33,37,43,47]

Figure 5. Fused metopic suture resulting in trigonocephaly. Adapted from Weinzweig et al.[44]

2.2.6: Lambdoid suture synostosis

Lambdoid craniosynostosis is uncommon accounting for only 2% to 4% of all nonsyndromic craniosynostosis cases.[2] The resulting cranial vault deformity is known as posterior plagiocephaly. It can be unilateral or bilateral. The majority of cases are unilateral resulting in asymmetric posterior plagiocephaly or an asymmetric shape of the posterior cranium as demonstrated in Figure 6 and Figure 7.[32,42] However it can be mistaken for deformational plagiocephaly and therefore care should be

taken.[29,48,49] With lambdoid synostosis the posterior cranial fossa is reduced in the anteroposterior dimension and resultant compensatory growth occurs at the parietal and frontal regions on the contralateral sides.[29,41] The posterior cranial base deviates to the fused side.[41] Bilateral lambdoid synostosis results in widening and flattening of the occipital region.[2] It has been suggested that possible risk factors for lambdoid craniosynostosis are a male predominance, intrauterine constraint and pre-term babies.[42,50]

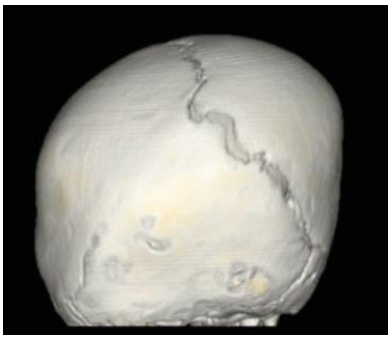

Figure 6. CT image of unilateral lambdoid synostosis. Adapted from Garza et al.[32]

2.2.7: Coronal suture synostosis

Coronal suture synostosis was previously the second most common form of craniosynostosis accounting for 13-16% of all cases. However it is now considered the third most common type, following sagittal and metopic craniosynostosis.[51] UCS is four to seven times more common than bicoronal and the ratio of right to left side involvement is 2:1.[35,51] Estimated incidence of UCS is 0.8 to 1 per 10,000 live births and has a female predominance with 60-75% of cases involving females.[2,42,51,52] Premature fusion of a coronal suture unilaterally results in anterior plagiocephaly or brachycephaly if there is bilateral involvement, as demonstrated in Figure 7.[42] In comparison to other single suture craniosynostosis types it has been suggested that coronal synostosis has a higher genetic component.[2,10,42] Single gene mutations have been shown in approximately one third of cases of coronal synostosis with 37.5% of bicoronal and 17.5% of unicoronal synostosis patients demonstrating such a mutation.[33,53,54]

2.2.8: Multiple suture involvement

Multiple suture involvement accounts for 5% of craniosynostosis cases. It is further subdivided clinically into two suture diseases which include bicoronal synostosis or complex diseases involving more than two sutures. Nonsyndromic bicoronal synostosis or brachycephaly is twice as common in females and has been associated with increasing paternal age and an increased familial involvement.[27] Complex craniosynostosis is associated with developmental delay due to increased intracranial

pressure. This contrasts with patients with two suture fusion who have similar long term neurodevelopment to those with simple craniosynostosis. However they have a higher rate of re-operation.[2]

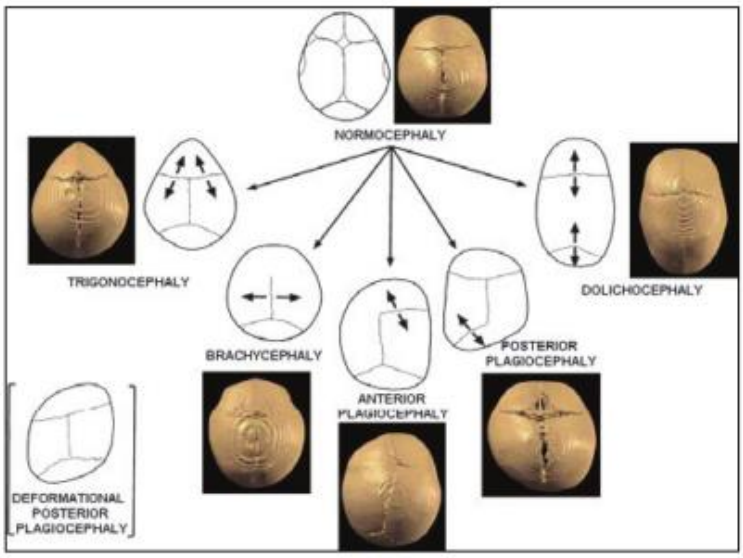

Figure 7. Schematic presentation of the calvarial sutures and the skull deformities resulting from synostosis of individual sutures. Boyadjiev et al. [42]

2.2.9: Aetiology and pathogenesis

In 1791 Von Soemerring first associated premature cranial suture fusion with dysmorphic cranial growth. However it was not until 1851 that Virchow was the first to propose a theory on the pathophysiology of craniosynostosis. [23,55,56]

Normal calvarial vault growth occurs in planes perpendicular to the sutures, however Virchow proposed that with premature fusion of a suture bony expansion or growth ceases perpendicular to the suture and compensatory growth occurs in the opposite direction. It does not affect growth parallel to the suture nor does it directly affect sutures which are not involved in the abnormal process. This compensatory growth results in skull distortion. [2,32,41,56]

Virchow's theory was that the primary cause is an abnormality in the suture itself.[56,57] However this remains controversial and differing theories have been proposed such as that by Moss.[57,58] His theory involves abnormal tensile forces which develop in the skull base attachments and are then transmitted upward to the skull causing synostosis of the cranial suture. Further studies, however, have questioned Moss's theory and have shown that the dura does not play as significant role as he may have believed. [40,41,57–59]

Recent theories have focused on genetic influences.[53] Craniosynostosis is likely to result from alteration in the equilibrium between proliferation and differentiation of osteoprogenitor cells in the cranial sutures resulting from disturbances in signalling, tissue interactions or a combination of the both.[25] Transcription factor, growth factor receptors and cytokine expression have been linked with premature fusion in nonsyndromic craniosynostosis.[32]

Mutations in the fibroblast growth factor signalling pathway have been shown to play a central role.[2] The fibroblast growth factor receptor (FGFR) genes which have been identified to play a role are FGFR1, FGFR3 and more frequently mutations in FGFR2. These FGFR's bind to fibroblast growth factor and initiate signal transduction therefore are central in growth and differentiation of mesenchymal and neuroectodermal cells.[54,60] Defects in this signal transduction due to mutations in FGFR's results in arrested growth of the midface and cranium.[54,61] Syndromes such as Pfeiffer, Apert, Crouzon, Beare-Stevenson, Jackson-Weiss and Muenke syndrome most frequently are associated with bicoronal synostosis. These syndromes have been associated with such mutations in FGFR1 to FGFR3.[25,26]

Noggin, is an antagonist to bone morphogenetic proteins and belongs to the transcription growth factor family which normally induce suture patency. Downregulation of this antagonist has been proposed to likely be involved in premature suture fusion. [32] Mutations in TWIST genes have also been associated with syndromic craniosynostosis. More than 100 different mutations in transcription factor TWIST1 gene ranging from nucleotide substitutions, deletions, insertions, duplications to complex rearrangements have been linked with syndromic craniosynostosis.[2]

Mutations in muscle segment homeobox 2 (MSX2) genes have also been associated with the syndromic Boston-type craniosynostosis.[62] An increase in MSX2 levels has been linked with enhanced calvarial bone formation. Animal models have shown that this enhancement in bone formation results from an increase in osteoblasts and therefore osteogenesis.[53,62] Garza et al. discussed that better understanding of these genes and their expression in relation to the cranial bones may lead to future targeted gene therapy for prevention of premature fusion.[32]

2.2.10: Risk factors for Craniosynostosis

Craniosynostosis has been found to be associated with increasing maternal age, maternal race, multiple births, gender and birth weight, although there is conflicting evidence within the literature. [35,63] Lajeunie et al.[52] did not find maternal age to be associated with an increased risk of sagittal synostosis. This contrasts however with Boulet et al.[35] who did find an association with sagittal and metopic synostosis. Infants born to Caucasian mothers have also been shown to have a higher incidence of craniosynostosis compared to those from other ethnic groups.[35,52] Sagittal synostosis is more prevalent in males compared to females and with birth weight >4,000g. In contrast low birth

weight has been shown to be associated with metopic and lambdoid synostosis.[35,63] Maternal anticonvulsant use and increasing paternal age has also been linked with syndromic craniosynostosis such as Crouzon, Apert and Pfeiffer syndromes.[36]

2.2.11: Functional considerations

Intracranial hypertension can occur in children with craniosynostosis if the capacity of the cranial vault is insufficient to accommodate the volume of the brain.[27] Those with single suture involvement are less likely to experience elevated intracranial pressure in comparison to syndromic cases where there is often multiple sutures involved.[64] It is also unlikely to occur after 6 years of age.[64] Bristol et al. showed increased intracranial pressure to occur in only 4-14% of single suture cases. [65] Hydrocephalus occurs in 5 to 10% of subjects although again is not commonly seen in those with premature fusion of a single suture.[27] Elevated intracranial pressure can lead to visual impairment. If left untreated optic atrophy can occur leading to partial or complete blindness.[1,27] Cognitive, behavioural and speech-related disorders have also been associated with craniosynostosis although those with single suture synostosis are generally shown not to be at an increased risk.[27] Despite this however, the potential for such side effects means that appropriate diagnosis of these patients is essential.

2.2.12: Diagnosis of craniosynostosis

Diagnosis is by clinical and radiographic examination. The need for radiography is controversial however and clinical examination may be sufficient for diagnosis.[51] Clinical evaluation involves inspection of the head shape and palpation of the skull for patency of the sutures, ridging, projection of the supraorbital rims and presence of the fontanelles.[27] Radiographic evaluation can be with plain skull radiographs, ultrasonography, CT imaging and magnetic resonance imaging (MRI).[29] The majority of cases can be diagnosed on plain radiographs with patent sutures being seen as a radiolucent line. If this is not evident in the normal anatomic position then craniosynostosis may be suspected. Other features include bony bridging at the suture, sclerosis and straightening or narrowing of the suture. Ultrasonography is only reliable up to approximately one year of age. After this the anatomy of the suture can be difficult to interpret. CT imaging allows assessment of suture patency, extent of the synostosis, calvarial deformity in all dimensions as well as assessment of cranio-cerebral disproportion.[28,51]

2.3: Unicoronal synostosis (UCS)

2.3.1: Definition

Unicoronal synostosis or Unilateral Coronal synostosis (UCS) develops due to premature fusion of one of the coronal sutures and results in frontal or anterior plagiocephaly as shown in Figure 7. [5,42,66]

2.3.2: Prevalence

Unicoronal synostosis was previously the second most common type of craniosynostosis with a prevalence of 0.8-1 in 10,000 live births and accounting for 20-30% of all craniosynostosis cases.[2,51,52] However in recent years there has been a change in the different subtypes of nonsyndromic craniosynostosis resulting in anterior plagiocepahly now being considered the third most common type behind scaphocephaly and trigonocephaly. Unicoronal synostosis is four to seven times more common than bilateral involvement of the coronal sutures. Females are affected in 60-75% of cases and the right side is twice as likely to be affected in comparison to the left side.[35,51,52,67]

2.3.3: Pathogenesis and risk factors for Unicoronal Synostosis

Approximately 15-30% of all craniosynostosis cases are syndromic with single gene mutations or chromosome abnormalities being identified in more than 20% of all cases.[33,54,68] These single gene mutations are more frequently detected in coronal synostosis in comparison to other single suture synostosis with 37.5% of bicoronal and 17.5% of unicoronal cases demonstrating a single gene mutation.[33,53] Unicoronal synostosis has been shown to have a higher proportion of familial cases and an association with increased paternal age is suggestive of a higher genetic component in coronal synostosis in comparison to other single suture craniosynostosis types.[10,54]

Similar to the other forms of craniosynostosis, patency of the coronal suture is dependent on the interplay of factors including transcription factors, cytokines, fibroblast growth factor receptors and extracellular matrix molecules.[25] As seen in sagittal and metopic synostosis mutations in TWIST1 have been associated with UCS as well as pro250arg FGFR3 mutations.[29,69]

Single suture synostosis has been linked with Caucasian mothers, multiple births and birth weights less than 1,500g or greater than 4,000g. Kallen et al.[70] has demonstrated an association between increasing maternal age and coronal synostosis. In contrast Boulet et al.[35] failed to find a link with coronal synostosis and found increasing maternal age to be a risk factor for sagittal and metopic synostosis only. Unlike other suture involvement coronal suture synostosis has not been shown to have an association with maternal smoking.[35,70]

2.3.4: Clinical features

Premature fusion of one of the coronal sutures and compensatory growth of the remaining sutures results in characteristic frontal, orbital, nasal and malar asymmetry.[6] As well as affecting the calvaria, the dysmorphology extends to involve the entire craniofacial region including the base of the skull. It results in facial asymmetry in the sagittal, vertical and transverse direction as well as lower facial asymmetry.[7,8,11]

Characteristic features on the fused side are unilateral retrusion of the supraorbital region and forehead which results in a flattened appearance.[7,9] The supraorbital rim is also elevated and displaced laterally on the fused side.[12] The orbit is shallow while the palpebral fissure is rounded and shortened transversely but has increased vertical dimension on the affected side.[51] The harlequin phenomenon (elevation of the greater wing of sphenoid) can be observed radiographically and a raised eyebrow on the ipsilateral side is also evident as well as deviation of the nasal root towards the fused side and the tip towards the unfused side.[5,10,71] Studies have shown that the angle of deviation of the nose towards the non-fused side at the hard tissue level is 6.6 ± 2.9˚ and at the soft tissue level the deviation of the dorsum of the nose to the non-fused side was 5.4 ± 3.4 ˚.[5] A significant deviation of the tip of the nose towards the unfused side in UCS patients compared to controls has also been shown to be in the region of 2.2 ± 1.2 ˚.[5]

In relation to the orbits a degree of protrusion of the affected ocular globe may be evident as well as strabismus on upward gaze due to the abnormal configuration of the orbit cavity.[51] Beckett et al.[72] in a retrospective study to explore the morphology of both the ipsilateral and contralateral UCS orbits in comparison to controls showed that the bony volume of the ipsilateral orbital cone was significantly smaller (approximately 6%) than the contralateral side and significant dysmorphology of both the ipsilateral and contralateral eyes were also evident. Morphologically the ipsilateral orbit is tall and narrow compared to the contralateral one which is vertically short and wide. This contrasted to the unaffected controls who demonstrated orbital symmetry in both volume and morphology.[72]

Analysis of a dry skull with plagiocephaly showed that the maxilla and mandible are shorter on the fused side compared to the unfused due to compensatory asymmetric development resulting from the primary asymmetry of the cranial base.[8] However conflicting evidence has been shown in the literature in relation to mandibular asymmetry with some studies showing it to be found in the ramus and condyle whereas others have demonstrated that it is the mandibular body length which is shorter by approximately 5% on the affected side.[8,73] In older children a reduction in the height of the ipsilateral maxilla and mandible has been associated with an occlusal cant [8,10] A decrease in the size of the face on the affected side results in facial asymmetry as well as elevation and anterior displacement of the ipsilateral ear which are also characteristic features.[74]

On the contralateral side features include frontal and temporal bossing or bulging of the forehead and the middle and lower face is rotated toward the non-fused side.[9,71] In addition to the nasal tip being deviated towards the non-fused side the chin has also been shown to deviate in a similar direction.[12,51] If left uncorrected these facial and calvarial asymmetries have been shown to persist and even worsen with growth.[75]

2.3.5: Anthropometric proportion indices in Unicoronal synostosis

Farkas et al.[76] demonstrated the pre-surgical craniofacial changes in those with isolated coronal synostosis using the proportion indices. The study consisted of 73 participants of North American origin aged between 0-5 months and 20 years with unilateral and bicoronal synostosis. Prior to any surgical intervention 10 projective linear measurements were carried out on the face which included two measurements in each of the cranial, facial, orbital, nasal and oral regions. These measurements were compared with already established norms for healthy North American Caucasians. They found that for right sided synostosis all the participants showed normal proportions in the oral region while 88.9% of males and 88.2% of females showed normal measurements for the facial and orbital regions. A lower proportion of normal indices was seen in the cranial region, with only 66.7% of males and 52.9% of females showing normality. For left sided synostosis 100% of males and 61.1% of females showed normal proportions in the nasal region. They found that the effect of the synostosis decreased as you move away from the cranium with the oral region showing no abnormalities.[76] As this study involved direct anthropometric analysis these findings are likely to be affected by the soft tissues and not just the underlying hard tissues.

2.3.6: Surgical Management of UCS

Management of patients with UCS requires a multidisciplinary approach including input from oral and maxillofacial surgeons, craniofacial surgeons, plastic surgeons, neurosurgeons, dentists/ orthodontists, ophthalmologists, audiologists, geneticists, paediatricians, psychologists and Speech and Language Therapists. [33] One goal of craniofacial surgical intervention in these patients is to provide adequate intracranial volume to allow brain development and therefore to reduce any neurologic or ophthalmologic complications. However in cases of single suture synostosis the incidence of raised intracranial pressure has been shown to be low at 4-14% therefore is not the primary goal in most cases. Fronto-orbital symmetry is also an aim of surgical correction and it is hoped that this would result in more satisfactory growth of the craniofacial region and create an aesthetically normal skull shape and facial appearance. It is assumed that nasal, cheek, chin and asymmetry of the ears will improve with growth or will be masked with growth therefore these anomalies are not addressed with primary surgery. Craniofacial anomalies such as cleft lip and palate and craniosynostosis have been found to be associated with psychosocial problems including social, academic and attention problems. Surgical intervention is also aimed therefore at improving the psychosocial development of the child. [11,12,14,77]

Surgical management of UCS is generally with Fronto-orbital Advancement and Remodelling (FOAR) which aims to correct the frontal volumetric restrictions and also to correct the asymmetry of the frontal bone and supraorbital bar.[18,66,78] One of the benefits of this technique is that it does not rely

on expansion from the growing brain to achieve the desired contour and is therefore still indicated in older children who have matured past the age of rapid brain expansion which occurs by 2 years of age.[48] Historically a unilateral advancement approach was adopted while a bilateral approach is now advocated. Bartlett et al.[15] found that there was no statistically significant difference in the results obtained by using a unilateral or bilateral approach and they concluded that either procedure can produce favourable results in the majority of patients.[15,16] However in more recent times a bilateral approach has become current practice.

Both procedures involve access to the anterior cranial vault via a bicoronal incision. The frontal bone is removed and if carrying out a bicoronal procedure the supraorbital bar is mobilised. Reshaping of the segment is performed by advancement of the synostotic side and the shape of the contralateral side is adjusted. Following split of the forehead in the midline the resulting bone fragments are adjusted and positioned in the most optimal position on top of the supraorbital bar. Historically, if a unilateral technique was used it was only the ipsilateral half of the supraorbital bar which was mobilised and adjusted.[66]

While open surgical procedures are generally used to normalize skull shape, there has been an interest in minimally invasive approaches to craniosynostosis such as endoscopic sutural release and helmet therapy. However these techniques are limited to between 3 and 5 months of age and the variable degree of patient compliance with the helmet protocols means these techniques are not routinely performed.[79]

The challenge in these patients is to be able to carry out the correction in a single surgery and avoid the need for a second operation with associated increased morbidity. Selber et al.[80] found that re-operations were required in 14.3% of cases. This is higher, however, than reoperation rates found in other studies. Wall et al.[81] in a retrospective study showed the need for a second surgical procedure was only required in 5.15% of cases when a single suture was involved. Re-operations may be required due to supraorbital rim dystopia, relapse of the fronto-orbital region and temporal hollowing.[80] In order to prevent the need for secondary procedures reconstruction with a hyper corrected surgical technique is advocated in order to facilitate an element of relapse.[79]

2.3.7: Age of Fronto-orbital Advancement and Remodelling

The optimal timing for Fronto-orbital Advancement and Remodelling is controversial. [48] Okada et al.[48] discussed that delaying surgical intervention until at least 6 months of age reduces the risks of surgery. Prior to this age the bones are too malleable to retain the surgical correction and therefore recurrence can occur. It has also been argued that early surgery can have negative consequences on further craniofacial development.[14,80] Some advocate that FOAR is performed between 4 and 13 months of

age and stable results have been demonstrated at 1 year postoperatively.[48] Further studies have found that the optimal timing for surgical intervention is before the age of 12 months so as to prevent raised intracranial pressure.[66,79,80] This risk of raised intracranial pressure, however, is rarely a problem in single suture craniosynostosis cases.[64]

2.3.8: Facial asymmetry following Fronto-orbital Advancement and Remodelling

In patients with UCS an improvement in facial symmetry has been shown following FOAR.[6,14–16,82] McCarthy et al.[14] found that 25 of 32 cases had complete correction of their nasal deformity while the remaining 7 showed an improvement towards symmetry. 72% of the subjects were considered to have either an "excellent", "good", "very satisfactory" or "acceptable" result.[14] Raposa-Amaral et al.[83] aimed to assess facial symmetry obtained in patients with UCS surgically treated by 2 different techniques. It this prospective study participants were randomly allocated to either total frontal reconstruction with transferring of onlay bone grafts to the recessive superior orbital rim or unilateral fronto-orbital advancement. Computerized photogrammetric analysis measured vertical and horizontal axis of the nose and the orbital globe in the pre-operative and post-operative periods. The study showed a significant reduction of the nasal and orbital globe axis in the post-operative period in the 2 groups indicating that facial symmetry was achieved in the patients with UCS who underwent surgery regardless of surgical technique. [83]

Hansen et al.[12] used direct anthropometry to assess the outcomes of three surgical techniques; unilateral fronto-orbital advancement, bilateral fronto-orbital advancement and bilateral fronto-orbital advancement with closing wedge nasal osteotomy. Post-operative asymmetry was seen in all the groups with elevation and retrusion of the supraorbital rim on the ipsilateral side compared to the contralateral side. Persistent deviation of the nasal root was also evident in those who did not have the additional closing wedge nasal osteotomy.[12]

Following surgical correction temporal hollowing has also been shown to be a common feature and is usually located lateral and cranial to the lateral apex of the eyebrow.[15,66] Cornelissen et al.[66] evaluated the development of temporal hollowing pre and post operatively as well as the influence of the operative technique (unilateral approach verses bilateral approach) on temporal hollowing. The study consisted of 48 participants from a single centre who had undergone surgical correction before 2 years of age between 1979 and 2010. Cephalometric and photographic analysis was used pre and post-surgery to assess the presence and severity of temporal hollowing and the width of the forehead and supraorbital bar. They showed that pre-operative osseous asymmetry improved significantly after surgery. The occurrence of temporal hollowing can be reflective of the surgical technique. 73% of cases managed with FOAR demonstrated post-operative temporal hollowing with those treated

bilaterally showing more severe temporal hollowing (23%) compared to unilaterally treated patients (6%). This difference however, was not shown to be statistically significant. The authors discussed that the timing of treatment is generally considered to be optimal before the patient reaches 1 year of age in order to prevent raised intracranial pressure. However the timing did not influence the occurrence of severe temporal hollowing.[66] Although FOAR was unable to achieve normal growth in the temporal region in a large proportion of the patients, symmetry was improved.[7]

The success or efficiency of the surgical technique can only be evaluated by using an accurate and reliable measuring tool whereby quantitative measurements will allow objective assessments of surgical outcome and comparison with what is "normal" in the population around them.

2.3.9: Facial asymmetry following FOAR assessed using 3D imaging techniques

Three-dimensional imaging in patients with craniofacial deformities where facial asymmetry is pronounced and more difficult to treat can be used to aid in detailed diagnosis.[84]

Three-dimensional computed tomographic imaging has been used to look at the long term morphologic outcome of surgical intervention. Becker et al.[18] looked at three populations of UCS subjects; group 1 had surgical intervention in infancy and had reached dentoskeletal maturity, group 2 were untreated UCS patients and group 3 were a subset of group 1 patient's one year post-surgical treatment. Thirty five osseous landmarks were identified on thin slice computed tomography scans by a single operator. Euclidean distance matrix asymmetry analysis was used and they found there was more statistically significant ipsilateral-contralateral asymmetric pairs in those who had reached dentoskeletal maturity compared to those who were only one year post-operative, but fewer statistically significant asymmetric pairs than in the untreated group. These results show that surgical treatment in infancy does result in improved craniofacial symmetry post-operatively. However, with further growth there is partial retrusion. Families and patient's need to be advised regarding this possibility of relapse. Limitations of the study are that it may have been subject to participant bias in that those who volunteered to take part may have been those with the less favourable long term outcome or conversely may have had a more favourable outcome. A further limitation is that all subjects in the long term follow up group may not have reached dentoskeletal maturity and could have had further growth potential.[18]

More recently stereophotogrammetry has been used to assess post-operative soft tissue facial asymmetry. Oh et al.[9] described middle and lower facial asymmetry using the 3dMDface System in adolescents and adults with corrected UCS. The study involved 15 patients (14F, 1M) with a mean age at fronto-orbital advancement of 8 months (range 3-14 months). Images using the 3dMDface system were taken on average at 14 years (range 11-29 years) and six anthropometric landmarks were

identified by a single operator to compare the ipsilateral to the contralateral side of the face. They found a statistically significant decrease in the mean middle facial depth of 5.1 ± 3.2mm and lower facial depth of 2.7 ± 2.5mm on the fused side compared to the unfused. Deviation of the nasal tip (5.0 ± 1.2˚) and facial midline (3.4 ± 0.7˚) towards the unfused side was also evident. Rotation of the middle and lower face towards the unfused side was also seen in all participants. Asymmetry was not shown to correlate with age of FOAR or digital imaging. These findings looking at soft tissue facial symmetry are consistent with those assessing the osseous dysmorphology in that they indicate that post-operatively there is continued middle and lower facial asymmetry.[9,18]

Similar findings have also been shown by Owall et al.[11] who in a retrospective follow up study assessed soft tissue facial asymmetry in post-operative UCS children (mean age 6.5 years) in comparison to controls. Twenty two non-syndromic UCS children who had surgical intervention within the first 19 months and underwent 3D imaging with the 3dMDtrio system were included. The control group was matched for age and sex. A detailed map of 3D asymmetry demonstrating the asymmetry in the sagittal, vertical and transverse directions were calculated for six facial sub regions. They found that there was significantly more facial asymmetry in the UCS group in comparison to the controls for all facial regions. Only 10% of the UCS patient's had a degree of craniofacial asymmetry within the range of the control group. The facial features were similar to that of untreated UCS individuals with the nasal root deviating towards the ipsilateral side and chin deviation towards the contralateral side. In the vertical direction the eyebrow and temporal area were elevated on the ipsilateral side and in the sagittal direction frontal retrusion on the affected side and frontal bossing on the unaffected side were evident. These findings again suggest that there is post-surgical retrusion to the untreated form.[11]

2.3.10: Attractiveness in children with single suture craniosynostosis

Collett et al.[85] investigated laypersons ratings of attractiveness in children with and without single suture craniosynostosis (SSC) including sagittal, metopic, unilateral lambdoid and unicoronal synostosis. In this longitudinal cohort study photographs of 196 children with SSC and 186 controls aged 18-36 months were rated by 8 blinded observers on a Likert type scale. Photographs were taken at three time points; prior to surgery, 18 and 36 months post-surgery. Children with SSC were found to have lower ratings compared to the healthy controls at each time point and there was minimal change following surgery. In both groups appearance ratings decreased over time and those with UCS and lambdoid synostosis had the lowest ratings of attractiveness. Better outcomes were associated with earlier surgery. They concluded that the appearance of the head does not fully normalize post-operatively. However without surgical intervention asymmetrical head shape would likely have worsened. Potential limitations of the study were that it was restricted to frontal views of the face

which may not have been able to capture the perception of the person as seen in a social perspective.[85]

2.4: Facial asymmetry

2.4.1: Normal facial asymmetry

Symmetry and averageness of the face has been shown to be correlated with good health and attractiveness.[13] However perfect symmetry in the human body is largely a theoretical concept with mild asymmetry being a common biological characteristic even found in faces considered aesthetically pleasing.[86–90] Research has shown that faces which are seen as beautiful may have asymmetry between the right and left sides of the face. In fact studies involving hemi-facial duplication of the right and left sides of the face have shown that perfect facial symmetry is actually seen as unattractive and a degree of asymmetry is preferred.[90] It is only when facial asymmetry becomes more severe, however, that it becomes clinically evident and this has a negative impact on facial aesthetics.[91] In clinical terms symmetry means balance whereas significant asymmetry represents an imbalance.[92]

2.4.2: Left to right differences in facial asymmetry

Right sided dominance has been shown in the literature in both males and females.[88,89,93] Ferrario et al.[94] found that the chin rotated towards the left rather than the right side.[88] A similar trend of right sided dominance was also shown by Peck et al.[93] in a study looking at postero-anterior cephalograms of 52 well balanced and aesthetically pleasing Caucasian adults although this was not found to be statistically significant.[93] The left side of the face, however, has been shown to be more attractive in both females and males by Blackburn et al. in a study of 10 females and male images viewed from both sides of the face by 37 observers.[95] Quantification of facial asymmetry is necessary in order to determine if a patients asymmetry lies within the normal range for the population or if complex treatment if required for aesthetic and or functional rehabilitation.[96]

2.4.3: What is normal facial asymmetry?

Lu et al. found that only facial asymmetries greater than 3% are clinically detectable.[97] Farkas and Cheung[87] analysed facial asymmetry in 308 normal North American Caucasians (154 F and 154 M) aged 6-18 years using direct anthropometry to compare the right to the left side of the face. They found that average differences between the right and left side of the face was in the order of 3mm or 3% with the right side being more dominant. Sex and age did not have a significant effect on prevalence of facial asymmetry.[87]

Peck et al.[93] attempted to quantify subclinical asymmetries in clinically symmetrical faces. They analysed skeletal facial asymmetry using postero-anterior cephalograms of 52 well balanced and aesthetically pleasing Caucasian adults and found that asymmetry reduced and dimensional stability increased as you moved towards the cranium. The mean asymmetry in the latero-superior orbit was 0.87mm (range 0-4mm), which increased to 2.25mm (range 0-9mm) at the lateral zygoma and the greatest amount of asymmetry was observed at the gonion with a mean of 3.54mm (range 0-12mm). A difference of up to 4mm in the right left latero-superior orbital region can be present without detectable asymmetry.[93] Farkas also found a degree of facial asymmetry in normal individuals which was less than 2% in the orbital region, less than 7% for the nasal region and in the oral region was higher at approximately 12%.[98,99] These findings are consistent with that of Peck et al. which in that facial asymmetry increases as you move away from the cranium.[93]

Facial features have been shown by Wang et al. in a recent systematic review to have a "threshold of perception" beyond which facial asymmetry is detectable to the eye.[100] The eyelid is the area of the face which is most sensitive to facial asymmetry. We fixate on the eyes when viewing an unfamiliar face followed be the nose and mouth.[100] Laypeople have been shown to detect a 2mm asymmetry in eyelid position whereas up to 3mm asymmetry in eyebrow was considered symmetrical and only an asymmetry of 4mm or greater was seen as asymmetrical.[101] The nose plays an important role in our perception of facial symmetry in both laypeople and clinicians with nasal asymmetries being rated as more negative in comparison to the same degree of asymmetry of the chin. Meyer-Marcotty et al.[102] found a 4mm nasal tip deviation on either side of the face to be the perceived as asymmetric by both laypeople and clinicians where as 6mm deviation of the chin was perceived as asymmetric. Deviations of the chin to the right is seen as more asymmetric which contrasts with the nose where left sided deviations are perceived to more asymmetric.[102] Kwak et al.[103] used frontal photographs to assess what was "normal", "acceptable" and "needing surgical correction" in terms of nasal tip deviation. They concluded that a deviation of 2.92 degrees was the point of recognition and the upper limit of acceptable was 4.25 degrees for men and 4.32 degrees for females.[103] Chu et al.[104] showed at least 3mm of asymmetry of the oral commissure has been shown to be required before detectable by laypeople but only an asymmetry of greater than 5mm is deemed as unacceptable or needing intervention.[104] These threshold values do need to be viewed with caution however due to limitations in the studies. The majority involved manipulation of a single image which may show a more unnatural appearance.[100]

2.4.4: Methods of measuring facial asymmetry

Facial asymmetry is a three-dimensional problem. Despite this a lot of research has involved two-dimensional imaging techniques such as the use of clinical photographs and cephalograms.[105,106] Two-

dimensional imaging has the advantage of being simple, low cost, non-invasive in the case of clinical photography and allows rapid acquisition.[20] However the limitations of these methods are that they do not take into account the three-dimensional nature of facial asymmetry.[105]

Facial anthropometry involves taking measurements between landmarks defined on the head, face and ears. Traditionally this was performed by directly measuring on a subject with the use of calipers or metric tape or indirectly by placing the landmarks on two-dimensional images.[98] Direct anthropometry required direct contact with the subject and while indirect anthropometry carried out with the use of photogrammetry does not require direct contact with the subject it has been shown to be prone to measurement error.[21,107]

2.5: 3D imaging techniques

To overcome the limitations of two-dimensional imaging, 3D imaging techniques have been developed.[105] 3D imaging can provide information about hard and soft tissues. Techniques include computerized tomography (CT), cone beam computerized tomography (CBCT), morphanalysis, 3D laser scanning, structured light technique, stereophotogrammetry or 3D surface imaging, 3D facial morphometry, 3D ultrasound and magnetic resonance imaging (MRI).[108]

2.5.1: Computerized tomography (CT)

CT imaging generates cross-sectional images of the body and there are two types of CT machines: fan beam and cone beam.

2.5.1.1: Fan beam computerized tomography

With fan beam CT machines, the source and detectors within a circular metal frame rotate around the patient who is in a horizontal position. One rotation lasts approximately one second. This generates a narrow, fan-shaped beam which takes a snapshot image of a section of the patient's body for each rotation. A single or multiple cross-sectional images are then reconstructed by stacking the slices.[108,109]

2.5.1.2: Cone beam computerized tomography (CBCT)

With Cone beam computerized tomography (CBCT) the x-ray source and detector synchronously move around the patients head and involves only a single 360˚ rotation. Single projection images are acquired at particular degree intervals and this series of images is known as the projection data which is used to generate the 3D image. It has a number of advantages compared to conventional CT which include that due to collimation small regions of the face can be scanned, reduced radiation dose, improved resolution, rapid scan time due to single rotation and reduced artefacts.[109] However it also has a limited capacity for soft tissue imaging.[108] Further limitations of CT are high cost and exposure to high dose radiation, the need for general anaesthesia in young patients and poor resolution.[109,110]

2.5.2: Laser scanning

Laser scanning has the advantage that it is easy to use and non-invasive.[111]. The laser scanner is composed of two sources of fanned laser beams which are projected at an oblique angle onto the surface to create pre-merged scans and these are then used to produce a composite whole face and surface co-ordinates (Figure 8 and 9). The images are obtained by laser triangulation where objects length, width and depth can be detected by triangulating distances between the laser beam and the scanned surface [111–113] It has been shown to be an accurate and reliable method of recording three dimensional data. [111,114] However due to the relatively slow capture time (up to 20 seconds) distortion can occur on the image and lack of surface texture is also a disadvantage.[20,108,115]

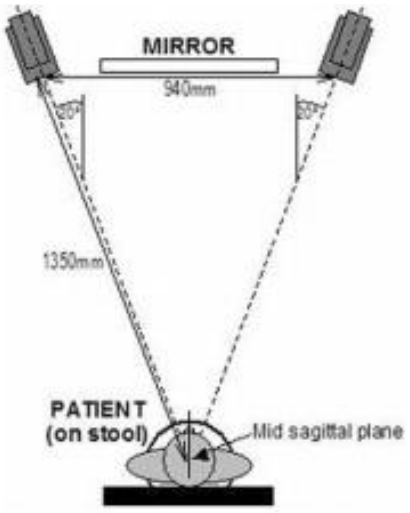

Figure 8. Example of setup of laser scanner with two sources of laser beams projected onto the scanned surface. Adapted from Kau et al.[114]

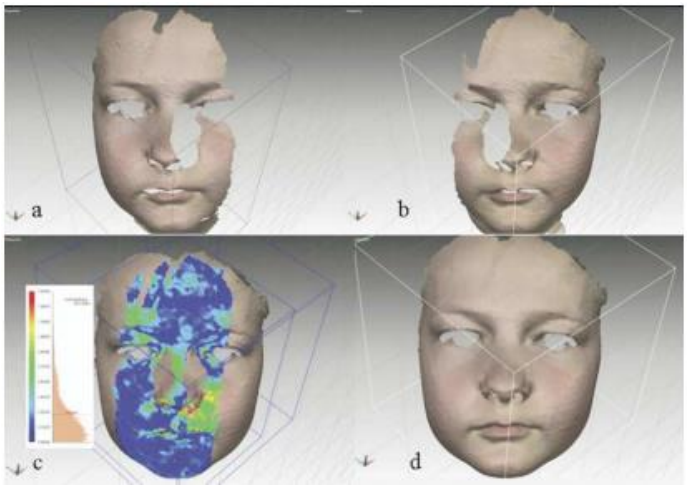

Figure 9 Example of composition of face using 3D laser scanning A) Right scan; B) left scan; C) shell deviation colour map; D) merged whole face. Adapted from Kau et al.[114]

2.5.3: Structured light technique

Structured light technique reconstructs the 3D surface of an object by deformation of a projected pattern such as stripes or dots onto the surface of the object. The objects image overlaid by the projected pattern is captured by a camera which is positioned at a different angle than the projector so that the deformed projected pattern is visible. This enables estimation of the 3D surface and a surface image to be produced.[116] However often the pattern of light needs to be projected several times in order to capture the face which increases the capture time and the likelihood of the subject moving.[117]

2.5.4: Magnetic Resonance Imaging (MRI)

Magnetic resonance Imaging (MRI) was originally a method of 2D imaging but it has become a valuable 3D technique.[113] A magnetic tomograph is used for MRI which is a large electromagnet that is cylindrically shaped and has coils, transmitters and receivers of radio waves. The electromagnet generates a magnetic field around the patient which causes polarization of hydrogen atoms in the tissues. The emission from the subsequent depolarization of the tissues is detected by the receivers, converted to numbers and the data is processed to produce the magnetic resonance image. MRI is the medical imaging technique with the highest contrast resolution.[108]

More recent developments have the advantage of software which transforms the MRI images into 3 dimensions. This facilitates rotation of the images, allows geometric calculations and more in depth analysis of specific regions. Reassembly of the slices allow visualization of a 3D image of the head and neck.[113]

MRI is used for analysis of soft tissues but has limited use for hard tissues due to their low hydrogen concentration. Its advantages are that it can provide excellent soft tissue resolution without exposing the patient to ionizing radiation, it is particularly useful for investigation of the TMJ and can also allow examination of inflammatory processes, scar tissues and tumours. It is useful in the diagnosis of osteoarthritis, condylar resorption and avascular necrosis involving the TMJ.[118] It can also be used in those with an allergy to contrast agents. The disadvantages are the expense, the time required for imaging and metals such as orthodontic appliances can produce artefacts in the image. There is also issues with access to MRI machines.[108,113] MRI techniques are also unable to provide skin texture or a natural photographic appearance to the face.[105]

2.5.5: Stereophotogrammetry

3D stereophotogrammetry uses multiple digital cameras which obtain images simultaneously from multiple angles and reconstruct a 3D image by triangulation. The image is visualized as a collection of

points, known as a “point cloud” resulting from the reconstructed craniofacial surface. The surface data involves a collection of points which are interrelated by their position along an x, y and z co-ordinate system and the distance between these points can be computed. Indirect anthropometric landmarks can be identified on the images which deform to the facial contour and appear as colour points. Each landmark has reference co-ordinates in the x, y and z axis which can be saved for analysis.[20]

Stereophotogrammetry can be divided into three categories: active, passive and hybrid. Active stereophotogrammetry involves projection of a pattern onto the objects surface with two or more cameras which capture the pattern deformation and is based on the structured light technique. Triangulation is used to produce the 3D image and involves combining the information about the set-up such as the camera position and the captured 2D images of the cameras. This differs from passive stereophotogrammetry which does not involve projection of a pattern but relies on the natural patterns on the surface of the object. Unlike active stereophotogrammetry lighting needs to be carefully controlled as the surface detail can be affected by ambient light. Active stereophotogrammetry is also better at showing variation between dark and light patterns or skin tones. Hybrid involves combination of both active and passive features resulting in improved quality of the surface image.[116,119]

The advantages of stererophotogrammetry are the fast capture time of approximately 1.5ms which reduces the potential for artefacts resulting from movement of the subject and therefore particularly beneficial with younger subjects. It has the ability to measure linear surfaces, surface areas, volumes, angles and the potential to extract x, y and z co-ordinates allowing statistical shape analysis.[19,21] It also allows measurements without the need for direct contact of the instruments with the facial surface and preventing distortion of the soft tissues.[19,20,22,120] Disadvantages include expense, lack of a normal database as well as difficulty in imaging shadowed or transparent surfaces.[20,21,110]

Several types of 3D stereophotogrammetry systems have been described in the literature and one such system is the static 3dMDhead system. This system utilizes active stereophotogrammetry to calculate the 3D surface image from a series of individual photographs generated from the system's array of synchronized, industrial-grade machine vision cameras. It incorporates five modular camera units (MCUs) and external white light flash units positioned around the subject's head and facial complex to achieve optimal 360˚ 3D surface coverage.

The five MCUs and external white light flash units are synchronized for a 1.5ms capture window. Initially the 10 white light speckle projectors are simultaneously triggered with the five pairs of

monochrome stereo cameras. The five colour cameras located in the centre of each MCU are triggered in conjunction with the external white light flash units following half a millisecond.

3dMD's active stereophotogrammetry technique software uses proprietary stereo triangulation algorithms to identify and match unique external surface features recorded by each pair of monochrome (stereo) cameras, enabling the system to yield a single 360˚ 3D surface image of the subject's full head. Once the 3D anatomical shape contour information has been generated, another software algorithm then matches and merges the images from the colour cameras to generate a corresponding colour texture map. The 3dMD software automatically generates a continuous 3D polygon surface mesh with a single x, y and z co-ordinate system from all synchronized stereo pairs of the image. The resultant 3dMDhead image in conjunction with the measurement software has been verified to consistently record a geometric accuracy of <0.2mm RMS (root mean square). 3dMD Vultus is the visualisation software developed by 3dMD.[121]

2.5.6: Accuracy and reliability of anthropometric landmarks using 3dMD systems

Much of the published literature involving stereophotogrammetry has involved landmarked based methods although more recently some studies have used landmark independent methods. Studies investigating the accuracy and reliability of the 3dMD system have been documented in the literature.[19–22,122–124] Weinberg et al.[19] compared craniofacial measurements obtained from mannequin heads using three methods; direct anthropometry, Genex 3D laser imaging system and 3dMD imaging system to assess intra-rater precision. Statistically significant differences were found between the three methods for 9 of the 12 anthropometric variables. However in practical terms these were all less than 1mm, therefore, have no clinical significance and could have been due to measurement error. For intra-observer precision all three methods were shown to be precise, although was carried out on mannequins and not human faces.[19] Wong et al.[9] also assessed the validity and reliability of the 3dMDface System in comparison to direct anthropometry on 20 normal adults. Eighteen landmarks were identified twice by a single operator with a minimum of 24 hours between each measurement session. They showed that for the majority of the linear distances measured (17 out of 18 measurements) the 3dMD system was accurate when compared to direct anthropometry. Similar to Weinberg et al. the precision of the digital measurements was within 1mm and the reliability was high.[19,20]

Aldridge et al.[21] also investigated the precision, error and repeatability of anthropometric landmarks using the 3dMDface System. Twenty anthropometric landmarks (6 mid-facial and 7 bilateral) were landmarked twice by a single operator, with a minimum of 24 hours apart. They showed the data to be highly repeatable and precise with the average error associated with placement of landmarks to

be less than 1mm, comparable to that found in other studies.[19,20] Fourteen of the 20 landmarks displayed a very high degree of precision in all three co-ordinate planes. Three of the landmarks; Nasion, Tragion right and Tragion left showed error of greater than 1mm but less than 2mm while Glabella, left and right Gonion showed they were less precise with an error greater than 2mm. The less precise finding with Tragion may be due to the subject's hair casting shadow on the image obscuring these features. Gonion and Glabella are also difficult to locate without direct palpation resulting in less precision. This high degree of precision and reliability of the 3dMDface system means it is useful in evaluating clinical dysmorphology.[21]

A more recent study by Aynechi et al.[22] again investigated the accuracy and precision of the 3dMDface system. However they looked to see if there was a difference between with and without landmark labelling before image acquisition. Eighteen linear craniofacial measurements were obtained from 10 adults who underwent 3dMDface imaging and landmarks were labelled before and after acquisition and compared to direct anthropometry. Intra-rater reliability was assessed by identifying the landmarks on two occasions one week apart. They showed statistically significant differences between direct anthropometry and 3dMDface system for seven measurements, however, the magnitude of these were not clinically significant at less than 2mm. For the seven measurements two of these involved the ear, two used bony landmarks (Zygion and Gnathion) and three used the landmark Stomion. Similar to Aldridge et al.[21] landmarks on the ear showed less precision, which may be due to the 3dMD face system having a 180˚ capture of information and therefore unable to capture all the data is this area. The bony landmarks required palpation for accurate location and are therefore more difficult to locate on the 3D image. They concluded that 3dMDface system showed good accuracy and precision in comparison to direct anthropometry, regardless of landmarking before or after acquisition.[22]

As well as assessing intra-rater reproducibility, inter-rater reproducibility and reliability of 49 soft tissue landmarks were evaluated on 20 patients by *Plooij et al*.[122] They showed intra-rater and inter-rater reproducibility and reliability was high with the landmarks in the midline being more precise than bilateral landmarks. The researchers agreed with previous literature that landmarks on the ear (Porion and Tragion) and the nose (Alare and Alar curvature) were less accurate and more difficult to identify.[122]

As well as looking at the accuracy of identifying landmarks on 3dMD images of normal individuals the accuracy has also been assessed in children with non-synostotic cranial deformities and those with cleft lip.[123,124] Schaaf et al.[123] assessed the intra and inter-rater agreement on 100 3dMD images of children aged between 4 and 20 months with non-synostotic cranial deformities. Measurements were

carried out 5 times by 5 separate clinicians and they showed excellent inter-rater agreement on those subjects with plagiocephaly (ICC 0.97) showing that it is a reliable tool in children as well as adults.[123]

2.5.7: Asymmetry Index as a method of assessing facial asymmetry

An Asymmetry Index (AI) was first developed by Katsumata et al.[106] as a method of evaluating facial asymmetry on 3D-CT images. They used a 3D-CT image based co-ordinate system to define an AI, measured in millimetres, for each anatomical landmark. Three reference planes were identified; the mid-sagittal (x), axial (y) and coronal (z) reference planes and the distance between each anatomical point and the three planes were measured in millimetres and defined as dx, dy and dz. The differences in these values between the right and left side of the face were used to calculate the AI using the formula in Figure 10, where R=right and L=left. They defined an anatomical landmark as asymmetric when the asymmetry index was greater than the mean asymmetry indices plus one standard deviation of the mean of that seen in the control subjects. A landmark was said to have marked asymmetry if its AI was outside two standard deviations of the control mean.

Since its development the AI has been modified to take into account the right-left side deviation for each landmark and has been adopted by other studies in the literature as a method of evaluating soft tissue facial asymmetry.[96,106,125]

$$\text{Asymmetry index} = \sqrt{(R\,dx - L\,dx)^2 + (R\,dy - L\,dy)^2 + (R\,dz - L\,dz)^2}$$

Figure 10. Asymmetry index (AI) measured in mm for each landmark, where R= right and L= left[96,125]

2.5.8: Assessment of facial asymmetry in normal individuals using 3D imaging

Various methods for assessing soft tissue facial asymmetry using non-invasive 3D imaging methods have been developed and are described in the literature. Some of these involve landmark dependent methods while landmark independent methods have also been developed but none have been universally accepted.[88,96,105,125,126]

Huang et al.[125] used 3D surface imaging to assess the degree of normal facial asymmetry in adults who appeared to have symmetrical faces. Sixty healthy Chinese adults (30M and 30F) had surface imaging with a GENEX 3D FACE CAM system and 16 facial landmarks were identified on each image. An asymmetry index was calculated for each landmark and the mean asymmetry index ranged from

0.76mm for Glabella to 2.82mm for the landmark Cheilion. For the midline landmarks the AI was greater for the lower face compared to the upper face and the largest midline AI was seen for the landmark Menton (1.54mm ± 1.50). Bilateral landmarks also showed a similar trend with increased asymmetry in the lower face. Potential limitations of the study were that they only included Chinese participants who were all recruited from a single centre and therefore may lack external generalisability. The capture time of the scan with the GENEX 3D FACE CAM system was also slow at 400ms per scan therefore increasing the potential for dynamic movement.[125]

Alqattan et al.[96] aimed to collect reference values for soft tissue facial asymmetry of British Caucasian adults. They obtained this by carrying out landmark and surface based analysis on 3D facial laser scans of 85 individuals (29 males: 56 females) aged 19-54 years from Cardiff Dental Hospital staff and students. For the landmark analysis seven mid-facial (Glabella, Nasion, Pronasale, Subnasale, Labiale Superius, Labiale Inferius, and Pogonion) and seven bilateral anthropometric landmarks (Endocanthion, Exocanthion, Palpebrale Superius, Palpebrale Inferius, Alare, Crista Philtri, and Cheilion) were placed on each scan by one operator using the definitions by Farkas.[96,98] Medial landmark asymmetry was measured in the x direction and for the bilateral landmarks the asymmetry was measured in each co-ordinate plane. An asymmetry Index was also calculated to show the total amount of asymmetry for the bilateral landmarks. The lowest AI for the medial landmarks was for Pronasale at 0.1mm in males and 0.2mm in females and the highest AI was the landmark Pogonion with an AI of 1.5mm in males and 1.8mm in females. With the exception of Pronasale the asymmetry in medial landamarks increased as they moved down the face. For the bilateral landmarks, the lowest AI was found for the landmark Crista Philtri with a median of 2.2mm in males and 1.6mm in females. The highest AI was seen for the landmark Cheilion at 3.2mmin males and 3.5mm in females. Surface based analysis showed the degree of asymmetry in the order of 0.7mm (0.5-0.9mm) for males and 0.6mm (0.5-0.7mm) for females. Limitations of the study are that the landmarks were only identified by a single operator and all subjects were staff and students of Cardiff University therefore lacks external generalisability. As the study used laser scanning the capture time is also slower. In order to keep this to a minimum surface data was lacking from behind the Zygoma which may have impacted on asymmetry analysis.[96]

Chapter 3: Rationale for Research

Assessing facial asymmetry in patients with UCS is an important surgical outcome which should be evaluated. Previous research in this area has shown that following post-surgical correction there may be reversion back to the untreated UCS phenotype. This may be as a result of reversion of the cranium to the untreated form.[9,11,18]

Various methods have been used to assess facial asymmetry with more recent studies using 3D stereophotogrammetric imaging techniques allowing assessment of soft tissue facial asymmetry without the need for exposure to ionizing radiation. As far as the authors are aware no previous studies however, have assessed facial asymmetry in a UCS population using these 3D techniques in a UK population. Previous research using these methods are based on small sample sizes with the largest being 22 participants. They also have only assessed intra-rater agreement of landmark identification and do not consider the inter-rater agreement of these methods.[11]

The aim of this study is therefore to assess the degree of soft tissue facial asymmetry in a UCS population who have undergone surgical correction in infancy using 3D stereophotogrammetric imaging.

Chapter 4: Study Aims and Objectives

4.1: Primary Study Aim

- To describe soft tissue facial asymmetry in a group of children with surgically corrected Unicoronal synostosis.

4.2: Secondary Study Aim

- To describe the effect that age of imaging and age of surgical correction has on soft tissue facial asymmetry.

4.3: Study Objectives

4.3.1: Primary Study Objective

- To evaluate middle and lower third soft tissue facial asymmetry in a group of children with surgically corrected UCS using three-dimensional surface imaging with the static 3dMD head system.
- To assess asymmetry with a landmark based approach by comparison of mid-facial and paired bilateral landmarks using an x, y, z co-ordinate system, an asymmetry index and linear and surface measurements.
- To assess if a relationship exists between side of fusion and the direction of facial rotation.

4.3.2: Secondary Study Objective

- To assess if age of digital imaging and age of surgical correction has an effect on soft tissue facial asymmetry.

Chapter 5: Methods and Participants

5.1: Study Design

This study was a retrospective observational study which was cross-sectional in nature, assessing the degree of facial asymmetry in a group of subjects with surgically corrected Unicoronal synostosis.

5.2: Sample

5.2.1: Participants

The sample consisted of children with UCS who had undergone imaging with the Static 3dMDhead System in Alder Hey Children's Hospital, Liverpool, which is one of four Craniofacial Units in the United Kingdom, following surgical correction with Fronto-orbital Advancement and Remodelling.

Post-operative 3D surface imaging with the Static 3dMDhead System forms part of the routine follow up of these patients at Alder Hey Children's Hospital and participants were identified from a database of UCS patients who have been seen in the Craniofacial Department. The records of the patients on the UCS database were reviewed for dates of any imaging with the 3dMD head system and these were accessed from Alder Hey's secure hard drive.

5.2.2: Inclusion criteria

Participants were included if they:

- Had premature fusion of one of the coronal sutures,
- Had undergone surgical correction with FOAR and had post-operative 3D surface imaging with the Static 3dMDhead System at least three months post-surgical intervention,
- Were under 16 years of age,
- Were of either gender; male or female,
- Had digital imaging which was of acceptable quality for assessment of facial asymmetry as described in section 5.4.
- Informed consent had previously been gained from the participant's parents/ guardians for use of the images for research purposes.

5.2.3: Exclusion criteria

Participants were excluded if they:

- Were over 16 years of age,
- Had synostosis affecting cranial sutures other than a single coronal suture or if they had multiple suture involvement,
- Had not undergone surgical correction with FOAR,

- Had any known or suspected craniofacial syndrome or had been diagnosed with any congenital clefts of the lip or palate, had a history of facial trauma or had complications post-surgery requiring secondary surgical intervention.
- The images were taken less than three months post-surgery or if they were not of acceptable quality to be included in the study which is described in section 5.4.
- If the images did not show the participant in a relaxed natural head position or pose such as eyes closed, smiling or mouth open.
- Participant's guardians or parents had not previously consented for use of their images for research purposes.

5.3: Ethics and Regulatory Approvals

The protocol and related documents were submitted to Alder Hey's Research Committee. Due to the retrospective nature of the study, the records forming part of the routine management of these participants and that consent had been previously gained for use of the images for research purposes following review by the Director of Research for Alder Hey it was agreed that Research Ethics Committee (REC) or Health Research Authority (HRA) approval was not required. (Appendix 1).

5.3.1: Data Handling

The chief investigator (NF) is acting as custodian for the study data. All data collected was anonymised by allocation of a study identifier. All anonymised data was stored on a password protected computer and all analysis was kept in a locked drawer in the investigators office (EB). The master sheet which linked patient details to the ID number was stored within the Medical Photography Department, Alder Hey Hospital.

5.4: Assessment of image quality for inclusion or exclusion of images

To determine whether an image was satisfactory for inclusion in the study each image was assessed independently by a panel of assessors. This consisted of 5 members; two Orthodontic Consultants (NF and SDG), two Orthodontic registrars (EB and OC) and one member of Alder Hey's imaging team who is involved in taking the Static 3dMDhead system images.

Each panel member assessed the images independently to determine whether they felt that it was of satisfactory quality to be included in the study and this was carried out over two sessions. Following viewing of the image on the 3dMD Vultus software each member simply ticked "Yes"(appropriate for inclusion) or "No" (to be excluded) on a table which had been provided (Appendix 2). If they ticked "No" they were also asked to provide a reason as to why the image should be excluded. A total of three assessors were required to say "Yes" for an image to be included in the study.

Prior to this all members of the panel discussed and agreement was reached as to the necessary criteria for inclusion. It was agreed that if the subjects did not appear to have relaxed facial muscles, were smiling and had eyes closed they were to be excluded. A degree of mouth opening was deemed acceptable as these were young children and incompetent lips is a common feature, although if a panel member deemed this to be excessive they were to say “No” to this image . Missing data on the images or presence of clothing or other artefacts which would have resulted in inaccurate landmark positioning and image analysis were to be excluded.

5.5: Review of Clinical case notes

The handwritten clinical case notes at Alder Hey are scanned and these notes were reviewed along with any clinical letters stored on MediSec by a single investigator (EB) to identify the following:

- Demographic information for each participant
- Side of Unicoronal synostosis
- Age at imaging
- Date of FOAR
- Any known or suspected craniofacial syndrome, involvement of cranial suture other than a single coronal suture, diagnosis of any congenital clefts of the lip or palate, history of facial trauma or any complications following FOAR requiring secondary surgical intervention. If there was a positive history for any of these factors then the participant was excluded from the study.

If following assessment of image quality and review of the notes there was more than one image per participant then the eldest image only was retained for inclusion in the study.

5.6: Method

5.6.1: Static 3dMDhead System

3D stereophotogrammetric images using the Static 3dMDhead System have been routinely taken following FOAR in UCS patients since 2011. Experienced 3D imaging technicians captured all of the images and were obtained using a commercially available camera system [Static 3dMDheadT System (2011 Model), 3dMD LLC, Atlanta, USA, http://www.3dMD.com].[121] The static 3dMDhead System utilizes a software-driven technique called "active stereophotogrammetry" to calculate the 3D surface image from a series of individual photographs generated from the system's array of synchronized, industrial-grade machine vision cameras. It incorporates five modular camera units (MCUs) and

external white light flash units positioned around the subject's head and facial complex to achieve optimal 360˚ 3D surface coverage of the subject's head.

The five MCUs and external white light flash units are synchronized for a 1.5ms capture window. First the 10 white light speckle projectors are simultaneously triggered with the five pairs of monochrome stereo cameras. Following this, the five colour cameras located in the centre of each MCU are triggered in conjunction with the external white light flash units.

3dMD's active stereophotogrammetry technique software uses proprietary stereo triangulation algorithms to identify and match unique external surface features recorded by each pair of monochrome (stereo) cameras, enabling the system to yield a single 360˚ 3D surface image of the subject's full head. Once the 3D anatomical shape contour information has been generated, another software algorithm then matches and merges the images from the colour cameras to generate a corresponding colour texture map. The 3dMD software automatically generates a continuous 3D polygon surface mesh with a single x, y and z coordinate system from all synchronized stereo pairs of the image. The resultant 3dMDhead image in conjunction with the measurement software has been verified to consistently record a geometric accuracy of <0.2mm RMS (root mean square).[121]

The system at Alder Hey is recalibrated on a daily basis. Multiple images are taken with the patient at rest and under standard lighting conditions. The image data is stored in Digital Imaging and Communications in Medicine (DICOM) format on a secure centralised hard drive and can be manipulated in three dimensions using the 3dMD Vultus analytical software.

5.6.2: Software training

Training on the use of the 3dMDhead system and Vultus analytical software was provided by 3dMD to two investigators (EB and OC). This included two sessions over the telephone and one in house training day with a 3dMD technician.

5.6.3: Orientation of the images: 3D photograph based reference frame

In order to allow standardisation of each image in three co-ordinate planes a three-dimensional photograph based reference system was used to orientate and reference the images. Similar reference plane systems have been used in previous studies such as that by Plooij et al. 2009[122] To reference the images five bilateral landmarks were identified and marked on the images. These landmarks were;

- Exocanthion Right (ExoR) and Exocanthion Left (ExoL),

- Endocanthion Right (EnR) and Endocanthion Left (EnL),
- Pupil Right (PuR) and Pupil Left (PuL),
- Preaurale Right (PRAR) and Preaurale Left (PRAL),
- Supraaurale Right (SAR) and Supraaurale Left (SAL)

The reference plane system uses the above landmarks to generate the natural head position and the "Pupil Reconstructed Point", defined as the point located at the midline of the nose at the level of the inter pupillary line to register the image. The reference plane was generated on each included image prior to landmark identification by a single operator (EB).

5.6.4: Identification of the Landmarks

The DICOM file was imported into the 3dMD Vultus analysis software. Twenty two anthropometric landmarks; 8 mid-facial and 7 bilateral, (Figure 11, Table 1 and 2) were identified and marked on the 3dMDhead system images by one operator (EB). The 3dMDvultus software was used to generate x, y and z co-ordinate data for each landmark in millimetres which were extracted into an excel document for analysis. The landmarks identified have been used in previous studies[96,125,127–129] of 3D facial imaging and were defined according to Farkas (1994).[98]

Figure 11. Example of the twenty two anthropometric landmarks (8 mid-facial and 7 bilateral) identified on the static 3dMD head system images

Landmark	Description of soft tissue landmark
Glabella (g)	*Most prominent midpoint between the eyebrows*
Soft tissue Nasion (n)	*Deepest point of the nasal bridge*
Pronasale (prn)	*Most protrusive point of the nasal tip*
Subnasale (sn)	*The midpoint of the angle at the columella base where the lower border of the nasal septum and the surface of the upper lip meet*
Labrale Superius (ls)	*The midpoint of the upper vermillion line*
Stomion (sto)	*Midpoint of the mouth orifice*
Labrale Inferius (li)	*The midpoint of the lower vermillion line*
Pogonion (pg)	*The most prominent midpoint of the chin*

Table 1. **Mid-facial anthropometric soft tissue landmarks**

Landmark	Description of soft tissue landmark
Endocanthion (en)	*Inner commissure of the eye fissure*
Exocanthion (exo)	*Outer commissure of the eye fissure*
Palpebrale Superius (ps)	*The highest point in the mid portion of the free margin of each upper eyelid*
Palpebrale Inferius (pi)	*The lowest point in the mid portion of the free margin of each lower eyelid*
Alare (al)	*The most lateral point on the alar contour*
Cheilion (ch)	*Point at the corner of the mouth at the labial commissure*
Crista Philtri (cph)	The point on each elevated margin of the philtrum above the vermillion line

Table 2. **Bilateral soft tissue anthropometric landmarks**

5.7: Evaluating facial asymmetry

5.7.1: Landmark based analysis of facial asymmetry

The distance of each of the 22 anthropometric landmarks to the reference plane was measured in millimetres as the x, y and z co-ordinates. The values of x, y and z for the Pupil reconstructed point which was used to register the images was zero. The co-ordinates were collected from the software and saved in an excel spreadsheet.

The asymmetry of the eight medial landmarks: Glabella, Nasion, Pronasale, Subnasale, Labrale Superius, Stomion, Labrale Inferius and Pogonion were measured only in the x direction, therefore the distance of each mid-facial landmark in mm from the mid-sagittal plane (x co-ordinate) indicates its asymmetry. For the bilateral landmarks: Endocanthion, Exocanthion, Palpebrale Superius, Palpebrale Inferius, Alare, Cheilion and Crista Philtri the asymmetry was measured in each of the 3 co-ordinate planes. Absolute values of the differences in the co-ordinates between the unfused and fused side of the face were used to indicate the amount of asymmetry.

5.7.2: Asymmetry Index

In addition to the assessment of facial asymmetry in each plane, an asymmetry index which has been used in previous studies investigating facial asymmetry was modified and calculated to show the total amount of asymmetry for the bilateral landmarks.[96,125]

The formula used to calculate the asymmetry index (AI) was:

$$\sqrt{(X_{unfused} - X_{fused})^2 + (Y_{unfused} - Y_{fused})^2 + (Z_{unfused} - Z_{fused})^2}$$

Where X, Y, Z are the co-ordinates of a landmark, *unfused* stands for the unaffected coronal suture and the *fused* represents the side with the synostosis. For perfect symmetrical paired bilateral landmarks, the discrepancy for the asymmetry would equal zero.

5.7.3: Landmark based analysis looking at the direction of facial asymmetry

Using the 3dMD Vultus software the Euclidean distance (linear distance) between the seven bilateral anthropometric landmarks (Exocanthion, Endocanthion, Palpebrale Superius, Palpebrale Inferius, Alare, Cheilion, Crista Philtri) and the mid-facial landmark of Nasion were compared between the unfused and the fused sides of the face which were landmarked by one investigator, EB.

Surface measurements taking into account the soft tissue contour of the face were also measured between the same seven bilateral anthropometric landmarks and the mid-facial landmark of Nasion to compare the distances between the unfused and fused sides of the face. This is demonstrated in Figure 12.

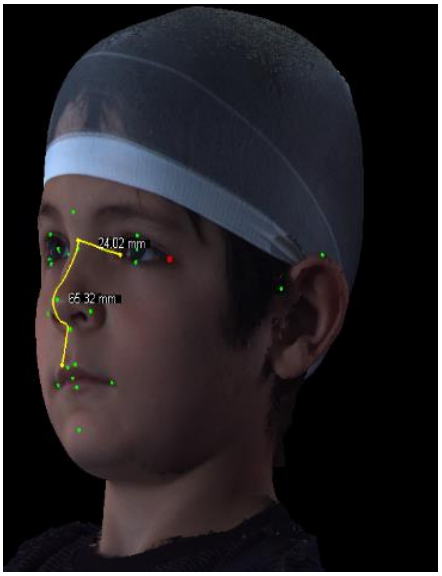

Figure 12. Example of surface measurements taking into account the soft tissue contour of the face.

5.7.4: Direction of facial rotation

Two angular measurements were generated to assess the deviation of the nasal tip and the chin and therefore the direction of facial rotation using the 3dMD Vultus software. These were;

1. **Angle Plane to Pronasale :**

   This is the angle constructed from the following points:

   - Projected Nasion point (P_PRN) 5mm below the Nasion point on the true vertical that passes through Nasion point.
   - Nasion point (N)
   - Pronasale point (PRN)

2. **Angle Plane to Pogonion**:

   This is the angle constructed from the following points:

   - Projected Nasion point (P_PG) 5mm below the Nasion point on the true vertical that passes through Nasion point.
   - Nasion point (N)
   - Pogonion point (PG)

In order to be able to say if the Pronasale or Pogonion point were deviated towards the right or left side of the Nasion point (because the angle always has a positive value), after registering the 3dMD image the PRP (Pupil Reconstructed Point) had an x co-ordinate of 0. The x co-ordinate of the Pronasale or Pogonion points were compared to Nasion's x co-ordinate to determine whether it is to the right or the left side as shown by a positive or negative value.

Figure 13. Angular measurement to assess deviation of the nasal tip or Pronasale.

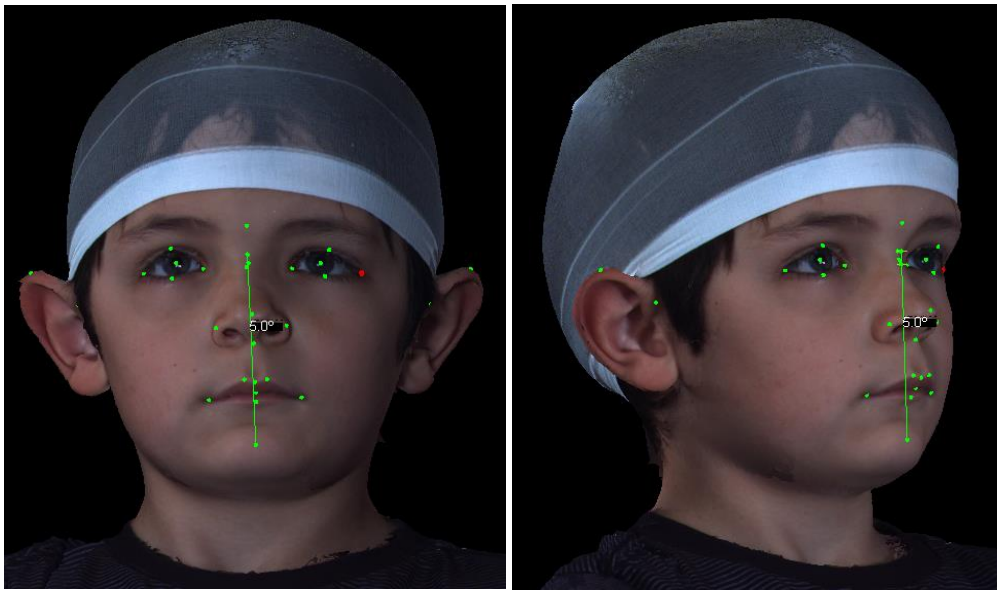

Figure 14. Angular measurement to assess deviation of the chin or Pogonion.

5.8: Intra and inter-examiner reliability

5.8.1: Intra-observer agreement

The intra-observer landmark reliability was determined by observer EB identifying the twenty two anthropometric landmarks on twelve randomly selected UCS 3dMDhead system images and re-identifying the landmarks at least two weeks apart. The twelve images were randomly selected from the original sample using a computer generated list (generated by GB) in an attempt to reduce bias. A sample of twelve images was decided upon following discussion with the statistician as 10% of the

sample was felt to be too small to test reliability and twelve images had been selected as part of a parallel study which was also assessing facial asymmetry using 3dMD imaging in children in the North West of England.[130]

The Euclidean distance between each landmark and Nasion was compared to assess the intra-observer reliability as this measurement would be used to assess facial asymmetry. The landmark Nasion was assessed separately as it was used as a reference for the other 21 anthropometric landmarks. To determine the intra-observer agreement of Nasion the individual x, y and z co-ordinates in millimetres were assessed for each of the 12 images.

5.8.2: Inter-observer agreement

Inter-observer reliability was assessed by two investigators (EB and OC) identifying the twenty two anthropometric landmarks on 24 images. Twelve of these images were the same UCS images used for the intra-observer reliability and twelve images were randomly selected from a parallel study being carried out looking at facial asymmetry in a population of children in the North West of England.[130] The twenty four images were selected at random by GB from the original sample using a computer generated random sequence to reduce bias.

Similar to the intra-observer reliability the Euclidean distance between each landmark and Nasion was compared to assess the inter-observer reliability as this measurement would be used to assess facial asymmetry. The landmark Nasion was assessed separately by comparing the individual x, y and z coordinates in mm for each of the 24 images.

5.9: Statistics

5.9.1: Reliability

Intra-class correlation coefficients (ICC) and Bland and Altman plots were used to assess intra and inter observer agreement and investigate for random and systematic errors. An ICC of <0.40 was classed as poor agreement, 0.40-0.59 fair agreement, 0.60-0.74 good agreement and 0.75-1.00 excellent agreement. The Bland and Altman analysis makes the assumption that the mean difference between two repeated measurements should be zero. The 95% limits of agreement assess whether the limits of agreement are acceptable in terms of absolute difference in mm.[131,132]

5.9.2: Statistical methods and analysis

Statistical analysis was carried out using SPSS 24. *StatsDirect 3* was used to calculate the Intra-class correlation coefficients for each landmark.

Histograms and Shapiro-Wilk tests were used to check the normality of the facial asymmetry parameters. Data was analysed using paired t tests to evaluate differences between fused and non-

fused sides. Chi square analysis was used to assess the direction of facial rotation. The association between facial asymmetry with age of imaging and age of surgery was analysed using Pearson correlation coefficients. A Bonferroni correction was used to adjust for multiple comparisons.

5.10: Dissemination of results

It is intended that the results of the study will be reported and disseminated at international conferences and in peer-reviewed scientific journals. The information also forms part of a research thesis submitted in partial fulfilment of a DDSc at the University of Liverpool.

5.11: Financial Aspects

Money was sought from the DDSc research fund (Orthodontic Department) to buy a laptop for viewing the 3D images within Alder Hey Hospital.

Chapter 6: Results

6.1: Descriptive statistics of the sample

Fifty eight participants with UCS who had attended Alder Hey's Craniofacial Unit and had undergone digital imaging with the static 3dMDhead system were identified. Some of these participants had undergone three-dimensional imaging on more than one occasion and therefore 97 images belonging to these 58 participants were assessed for image quality.

Following review of the image quality, 11 participants (27 images) were excluded and on review of the clinical case notes a further 11 participants (15 images) were excluded. Three participants/ four images were excluded due to an associated craniofacial syndrome, two participants/ three images did not undergo surgical correction and six participants/ eight images were pre-surgical or less than 3 months post FOAR resulting in a sample of 36 participants who met the inclusion criteria.

Eleven of these 36 participants had multiple post-operative images which met the inclusion criteria therefore the most recent image only for each participant was assessed resulting in a sample size of 36 participants each with a single image.

Of the 36 participants in the final sample: 24 were female and 12 were male which reflects the literature that UCS is more common in females than males. Mean age of Fronto-orbital Advancement and Remodelling was 17 months (SD 7.4 months) with a range from 11 to 48 months.

Mean age at imaging was 5yrs 6 months (SD 2yr 7 months), ranging from 1yr 7 months to 11yrs 6 months. Eighteen patients had fusion of the right coronal suture and 18 patients had involvement of the left coronal suture.

6.2: Reliability

6.2.1: Intra-observer reliability

The intra-observer landmark reliability was determined by observer EB landmarking the twenty two anthropometric landmarks on twelve randomly selected UCS 3dMDhead system images and re-identifying the landmarks at least two weeks apart. The twelve images were randomly selected using a computer generated list (generated by GB) in an attempt to reduce bias. Twelve images were selected as 10% of the sample was felt to be too few to assess reliability and twelve images were selected in a parallel study assessing three-dimensional facial asymmetry in a child population of the

North West of England.[130] Intra-class correlation coefficients and Bland and Altman Plots were used to assess the intra-observer agreement.

The Euclidean distance between each landmark and Nasion were compared to assess the intra-observer reliability as this measurement would be used to assess facial asymmetry. The landmark Nasion was assessed separately as it was used as a reference for the other 21 anthropometric landmarks and will be discussed in section 6.3.

The intra-class correlation coefficients for the twenty one anthropometric landmarks ranged from 0.97 to 0.99, which was classed as excellent agreement and shown in Table 3. This is also demonstrated in the Bland and Altman Plots for each landmark (Figure 15-18 and Appendix 3).

Landmark	Intra-class correlation coefficient	Mean difference in Euclidean distance to Nasion (mm)	95% limits of agreement
Glabella	0.98	0.21	-0.72, 1.13
Endocanthion Right	0.98	-0.07	-0.80, 0.66
Endocanthion Left	0.97	-0.03	-0.9, 0.90
Exocanthion Right	0.99	-0.18	-1.32, 0.96
Exocanthion Left	0.99	-0.10	-1.33, 1.14
Palpebrale Superius Right	0.97	0.06	-1.04, 1.17
Palpebrale Superius Left	0.97	0.26	-0.86, 0.80
Palpebrale Inferius Right	0.99	0.30	-0.34, 0.91
Palpebrale Inferius Left	0.98	-0.04	-0.98, 0.91
Pronasale	0.99	-0.08	-0.99, 0.83
Subnasale	0.99	-0.22	-1.43, 0.99
Alare Right	0.99	0.20	-0.82, 1.22
Alare Left	0.99	0.15	-0.95, 1.25
Labrale Superius	0.99	-0.46	-1.37, 0.45
Stomion	0.99	-0.40	-1.53, 0.72
Labrale Inferius	0.99	-0.34	-1.31, 0.63
Cheilion Right	0.99	-0.34	-1.46, 0.79
Cheilion Left	0.99	-0.35	-1.02, 0.33
Crista Philtri Right	0.99	-0.38	-1.33, 0.56
Crista Philtri Left	0.99	-0.40	-1.28, 0.47
Pogonion	0.99	0.21	-1.10, 1.52

Table 3. Table to summarise the intra-observer reliability for landmark identification including intra-class correlation coefficient (one way random effects), the mean difference in Euclidean distance between the 21 anthropometric landmarks and Nasion and the 95% limits of agreement.

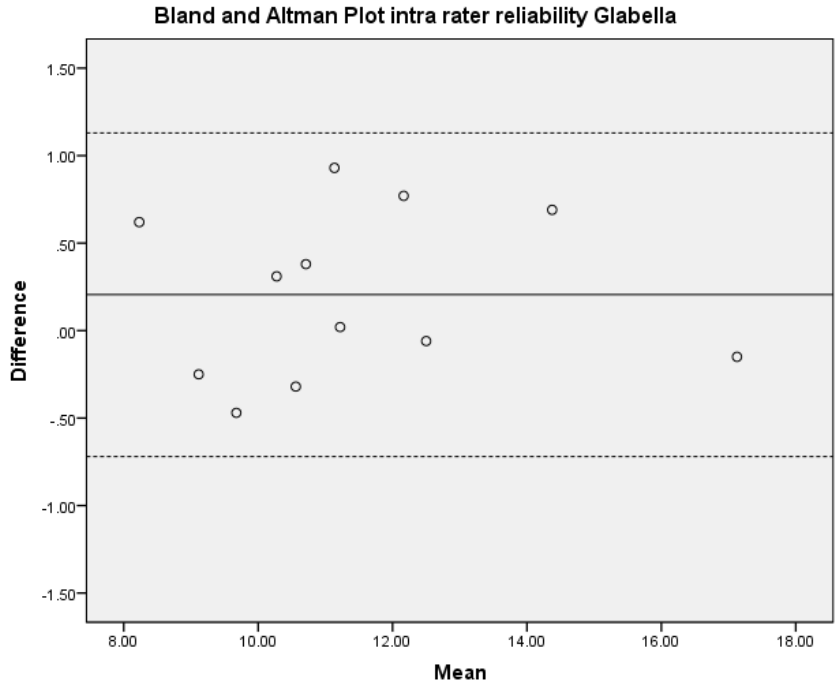

Figure 15. Bland and Altman Plot showing EB intra-observer agreement for Glabella - Nasion; mean difference 0.21mm, 95% Limits of agreement = -0.72 to 1.13 mm

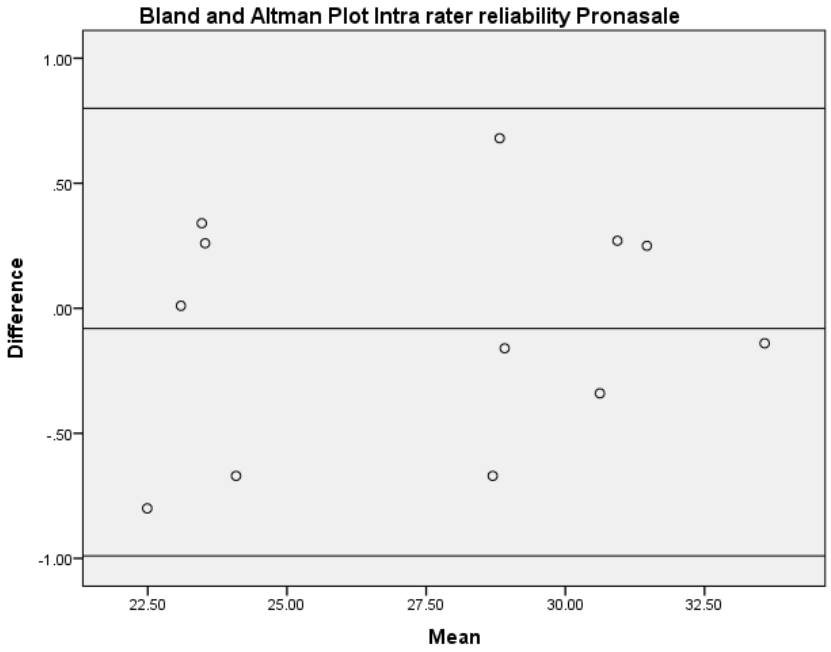

Figure 16. Bland and Altman Plot showing EB intra-observer agreement for Pronasale - Nasion; mean difference -0.08mm, 95% Limits of agreement = -0.99 to 0.83mm

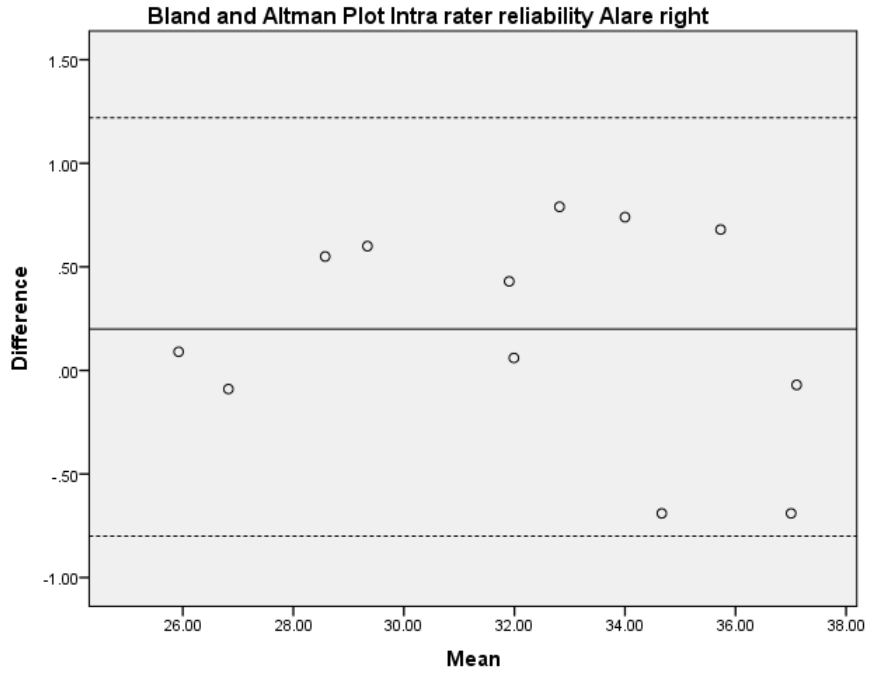

Figure 17: Bland and Altman Plot showing EB intra-observer agreement for Alare Right - Nasion; mean difference 0.20mm, 95% Limits of agreement = -0.82 to 1.22mm

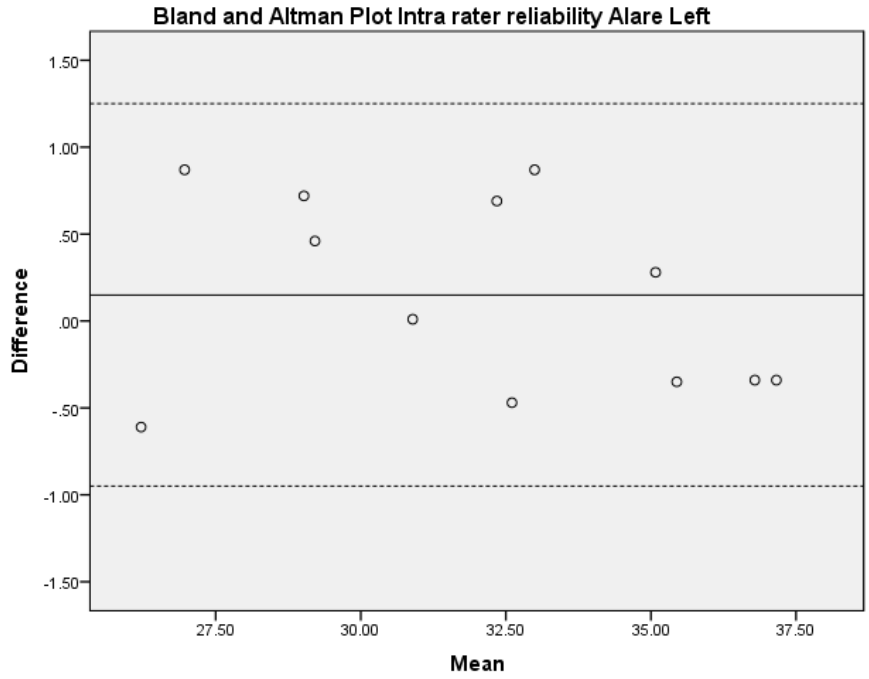

Figure 18: Bland and Altman Plot showing EB intra-observer agreement for Alare Left - Nasion; mean difference 0.15mm, 95% Limits of agreement = -0.95 to 1.25mm

6.2.2: Inter-observer reliability

To assess the inter-observer agreement of landmark identification, two investigators EB and OC, identified the twenty two anthropometric landmarks on 24 images. Twelve of these images were the same UCS images used for the intra-observer reliability and twelve images were randomly selected from a parallel study assessing facial asymmetry in a non UCS population.[130] The twenty four images were selected at random using a computer generated random sequence by GB from the original sample to reduce bias.

The Euclidean distance between each landmark and Nasion were compared to assess the inter-observer reliability. The landmark Nasion was assessed separately as it was used as a reference for the other 21 anthropometric landmarks and will be discussed in section 6.4. Intra-class correlation coefficients and Bland and Altman plots were used similar to the intra-observer agreement.

This was initially carried out on 24 images. However it was felt that agreement could be improved and therefore following further training inter-observer agreement was assessed on a new set of randomly selected 24 images which showed acceptable agreement. The intra-class correlation coefficients (one way random effects) ranged from 0.96 to 0.99, which was classed as excellent agreement as demonstrated in Table 4. This is also demonstrated in the Bland and Altman Plots for each landmark (Figure 19-22 and Appendix 4).

Landmark	Intra-class correlation coefficient	Mean difference in Euclidean distance to Nasion (mm)	95% Limits of agreement
Glabella	0.96	0.19	-1.34 to 1.71
Endocanthion Right	0.98	0.25	-0.53 to 1.04
Endocanthion Left	0.97	0.43	-0.32 to 1.18
Exocanthion Right	0.99	0.08	-0.98 to 1.08
Exocanthion Left	0.99	0.13	-1.01 to 1.28
Palpebrale Superius Right	0.96	-0.50	-1.47 to 0.47
Palpebrale Superius Left	0.97	0.15	-0.99 to 1.30
Palpebrale Inferius Right	0.98	-0.04	-1.15 to 1.07
Palpebrale Inferius Left	0.98	0.27	-0.71 to 1.25
Pronasale	0.99	0.22	-0.95 to 1.39
Subnasale	0.99	0.06	-1.01 to 1.14
Alare Right	0.99	-0.22	-1.60 to 1.16
Alare Left	0.99	0.13	-1.31 to 1.57
Labrale Superius	0.99	0.27	-0.66 to 1.19
Stomion	0.99	0.52	-0.31 to 1.34
Labrale Inferius	0.99	0.38	-0.72 to 1.48
Cheilion Right	0.99	0.05	-0.83 to 0.94
Cheilion Left	0.99	0.20	-0.72 to 1.11
Crista Philtri Right	0.99	0.04	-1.11 to 1.19
Crista Philtri Left	0.99	0.01	-1.00 to 1.02
Pogonion	0.99	-0.04	-1.70 to 1.62

Table 4. Table to summarise the inter-observer reliability for landmark identification including the intra-class correlation coefficient (one way random effects), mean difference in Euclidean distance between the 21 anthropometric landmarks and Nasion and the 95% limits of agreement.

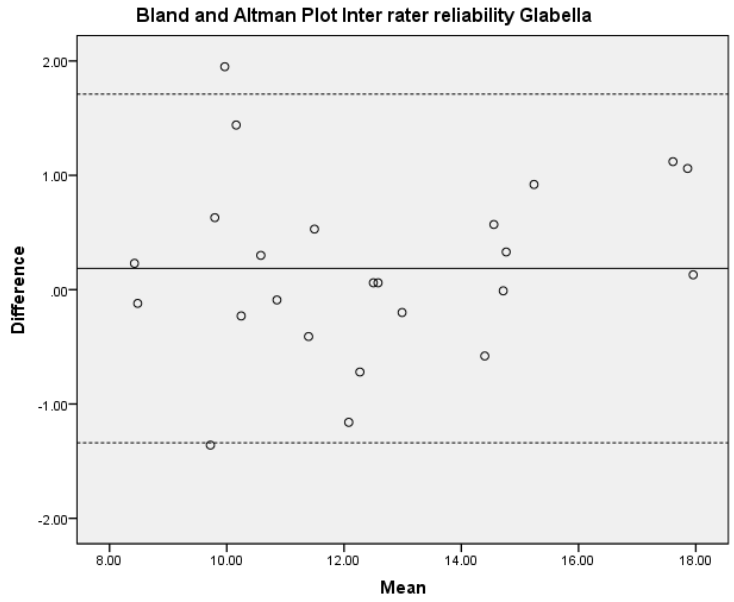

Figure 19. Bland and Altman Plot showing inter-observer agreement for Glabella - Nasion; mean difference 0.19mm, 95% Limits of agreement = -1.34 to 1.71mm

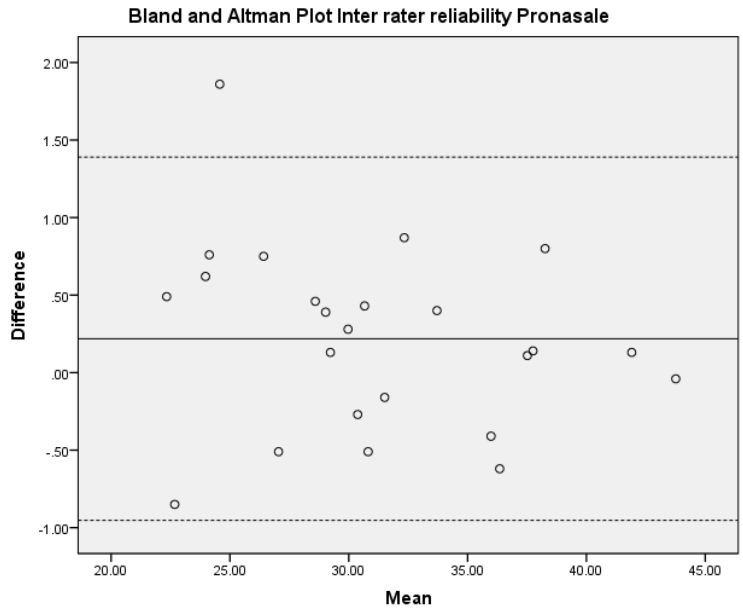

Figure 20. Bland and Altman Plot showing inter-observer agreement for Pronasale - Nasion; mean difference 0.22mm, 95% Limits of agreement = -0.95 to 1.39mm

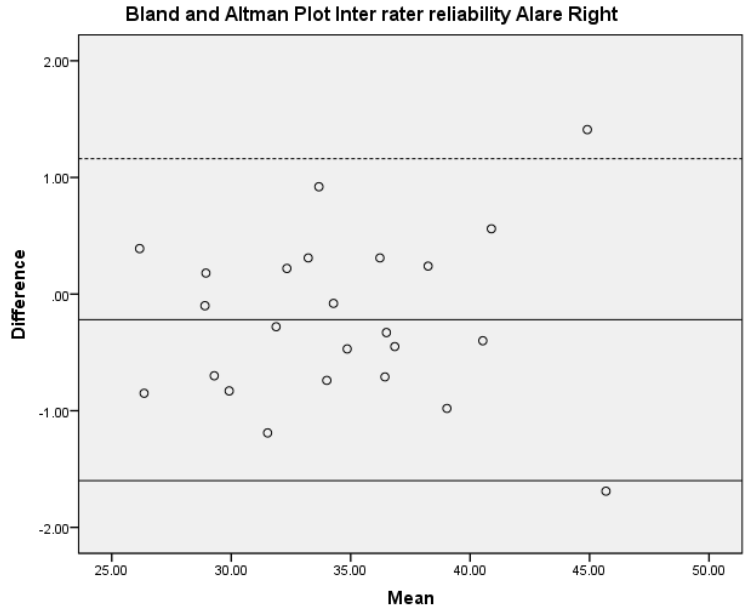

Figure 21. Bland and Altman Plot showing inter-observer agreement for Alare Right - Nasion; mean difference -0.22mm, 95% Limits of agreement = -1.60 to 1.16mm

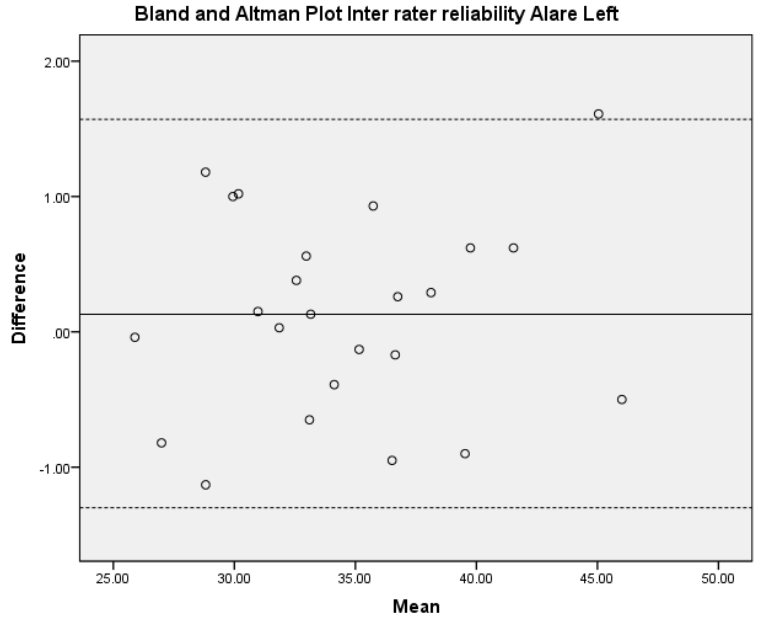

Figure 22. Bland and Altman Plot showing inter-observer agreement for Alare Left - Nasion; mean difference 0.13mm, 95% Limits of agreement -1.31 to 1.57mm

6.3: Intra-observer reliability for landmark Nasion

To assess the intra-observer reliability of identifying the landmark Nasion the individual x, y and z co-ordinates were analysed on the same 12 UCS images for observer EB which was landmarked and then re-identified at least two weeks later. Intra-class correlation coefficients and Bland and Altman Plots were used to assess the intra observer reliability in the x, y and z planes.

6.3.1: Intra-observer reliability of landmark Nasion in x co-ordinate plane

The intra-class correlation coefficient (one way random effects) for Nasion in the x co-ordinate (mediolateral plane) was 0.66, which although lower than the other landmarks is classed as good agreement. The mean difference was low at -0.05mm. This is displayed in the Bland and Altman Plot as shown in Figure 23.

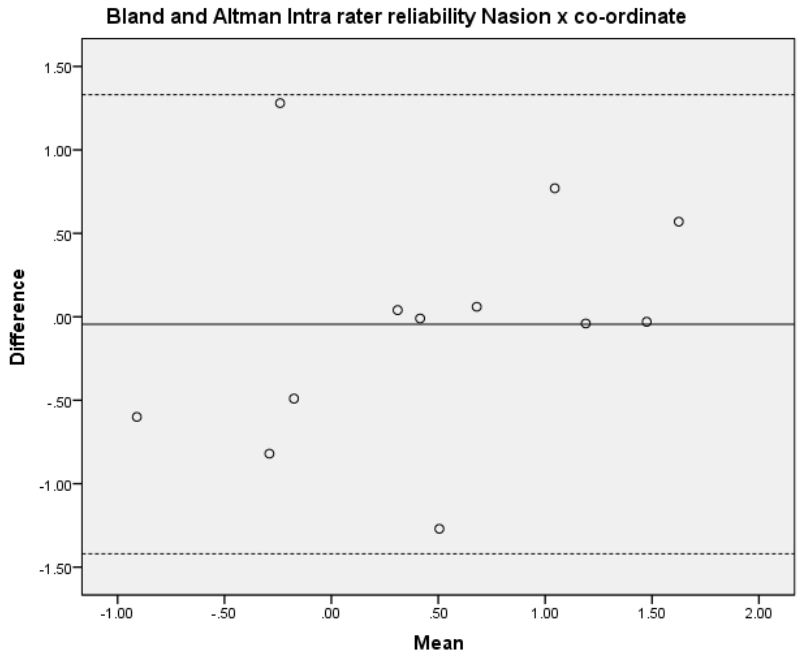

Figure 23. Bland and Altman Plot showing EB intra-observer agreement for Nasion in the x co-ordinate: mean difference -0.05mm, 95% Limits of agreement = -1.42 to 1.33mm

6.3.2: Intra-observer reliability of landmark Nasion in y co-ordinate plane

The intra-class correlation coefficient (one way random effects) for Nasion in the y co-ordinate (superoinferior plane) was 0.95, which shows excellent agreement. This agreement is also shown in the Bland and Altman Plot (Figure 24).

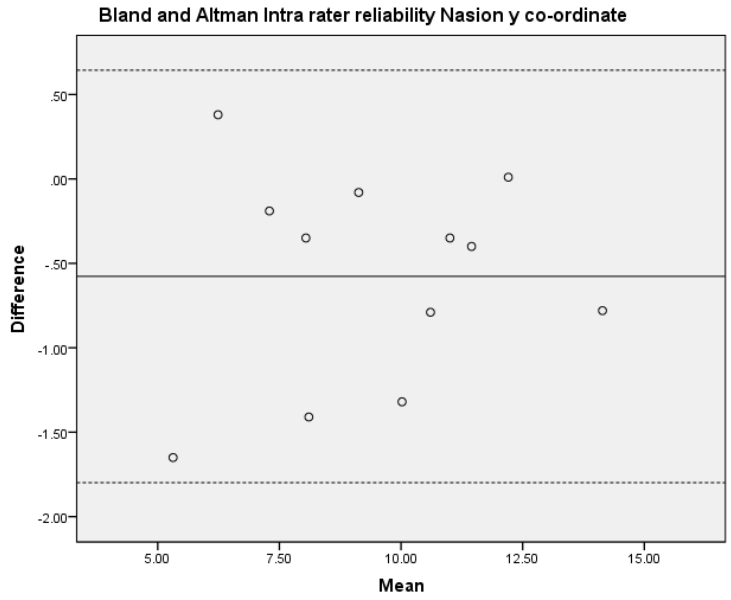

Figure 24. Bland and Altman Plot showing EB intra-observer agreement for Nasion in the y co-ordinate: mean difference -0.58mm, 95% Limits of agreement = -1.80 to 0.64mm.

6.3.3: Intra-observer reliability of landmark Nasion in z co-ordinate plane

The intra-class correlation coefficient (one way random effects) for Nasion in the z co-ordinate (anteroposterior plane) was 0.99, which shows excellent agreement. This agreement is also shown in the Bland and Altman Plot (Figure 25).

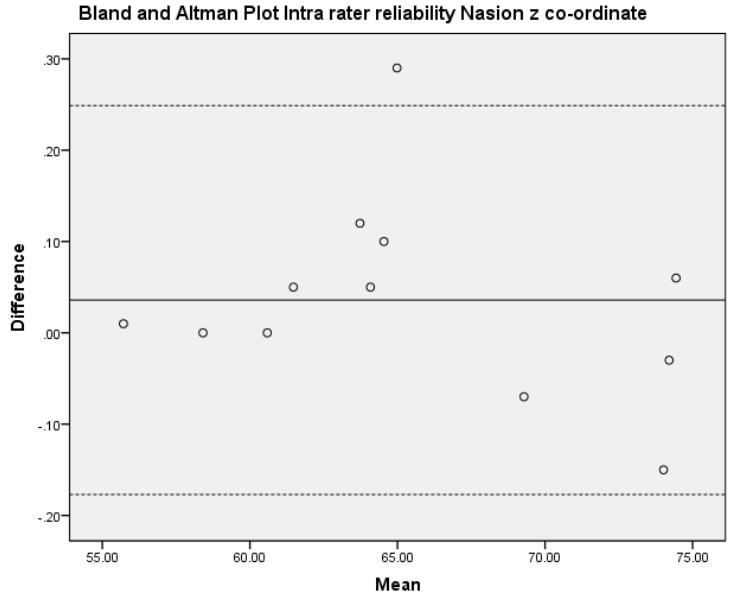

Figure 25. Bland and Altman Plot for EB intra-observer agreement for Nasion in the z co-ordinate: mean difference 0.04mm, 95% Limits of agreement = -0.18, 0.25mm

Co-ordinate	Intra-class correlation coefficient (ICC)	Mean difference (mm)	Limits of agreement
X	0.66	-0.05	-1.42, 1.33
Y	0.95	-0.58	-1.80, 0.64
Z	0.99	0.04	-0.18, 0.25

Table 5. Table to summarise the intra-observer reliability for Nasion in the x, y and z co-ordinates including intra-class correlation coefficient (one way random effects), the mean difference and the limits of agreement from the Bland and Altman Plots.

6.4: Inter-observer reliability for landmark Nasion

To assess the inter-observer reliability of identifying the landmark Nasion the individual x, y and z co-ordinates were assessed on the same 24 images used in 6.2.2 for the observers EB and OC. Intra-class correlation coefficients and Bland and Altman Plots were used to assess the inter-observer reliability in the x, y and z co-ordinate planes.

6.4.1: Inter-observer reliability of landmark Nasion in x co-ordinate

The inter-class correlation coefficient (one way random effects) for Nasion in the x co-ordinate was 0.77, which is classed at good agreement. This is displayed in the Bland and Altman Plot as shown in Figure 26.

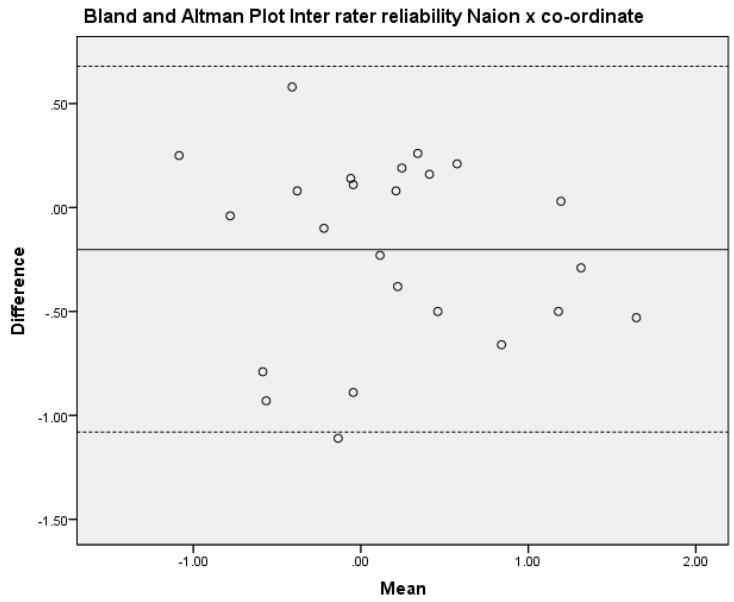

Figure 26. Bland and Altman Plot for inter-observer agreement for Nasion in the x co-ordinate: mean difference -0.20mm, 95% Limits of agreement = -1.08, 0.68mm

6.4.2: Inter-observer reliability of landmark Nasion in y co-ordinate

The inter-class correlation coefficient (one way random effects) for Nasion in the y co-ordinate was 0.99, which shows excellent agreement. The Bland and Altman Plot also demonstrates excellent agreement as seen in Figure 27.

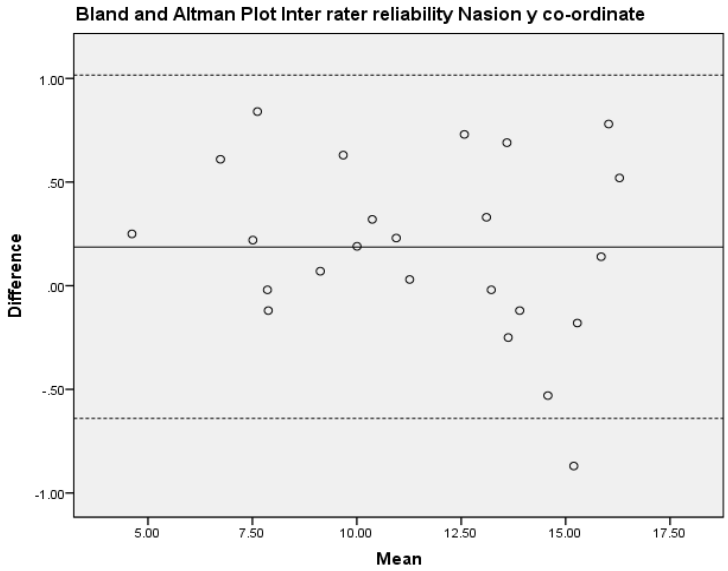

Figure 27. Bland and Altman Plot for inter-observer agreement for Nasion in the y co-ordinate: mean difference 0.19mm, 95% Limits of agreement = -0.64, 1.02mm

6.4.3: Inter-observer reliability of landmark Nasion in z co-ordinate

The inter-class correlation coefficient (one way random effects) for Nasion in the z co-ordinate was 0.99, which shows excellent agreement. There was one outlier with a mean difference of -0.63mm however this was considered to be acceptable as less than 1mm. Overall there was excellent agreement as seen on the Bland and Altman Plot in Figure 28.

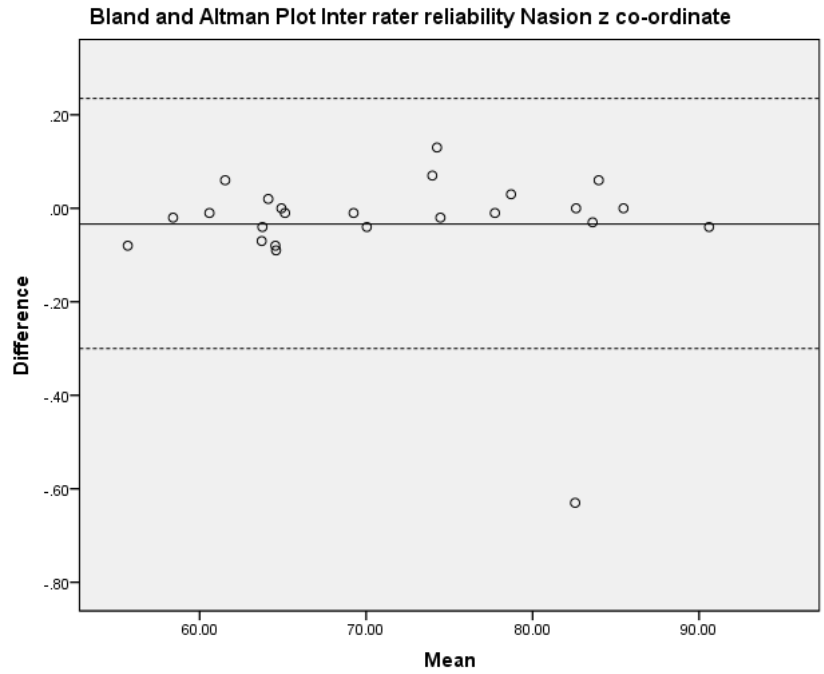

Figure 28. Bland and Altman Plot for inter-observer agreement for Nasion in the z co-ordinate: mean difference -0.03mm, 95% Limits of agreement = -0.30 to 0.24mm.

Co-ordinate	Intra-class correlation coefficient (ICC)	Mean difference (mm)	Limits of agreement
X	0.77	-0.20	-1.08, 0.68
Y	0.99	0.19	-0.64, 1.02
Z	0.99	-0.03	-0.30, 0.24

Table 7. Table to summarise the inter-observer reliability for Nasion in the x, y and z co-ordinates including intra-class correlation coefficients (one ay random effects), the mean difference and the limits of agreement from the Bland and Altman Plots.

6.5: Landmark based analysis of facial asymmetry

Eight mid-facial and seven bilateral anthropometric landmarks were placed on each of the 36 images by operator EB according to the definitions by Farkas[98] which are described in the methods chapter. The asymmetry of the eight medial landmarks: Glabella, Nasion, Pronasale, Subnasale, Labrale Superius, Stomion, Labrale Inferius and Pogonion were only measured in the x direction, therefore the distance of each mid-facial landmark in millimetres from the mid-sagittal plane (x co-ordinate)

indicates its asymmetry. Absolute values of the differences in x co-ordinate between the unfused and fused side of the face were used to indicate the amount of asymmetry but not its direction.

6.5.1: Asymmetry of the medial landmarks in medio-lateral direction (x co-ordinate)

The results for medial landmark asymmetry are presented in table 8. Normality was assessed using histograms and Shapiro-Wilk tests for each of the landmarks. The majority of the data was skewed as demonstrated in Appendix 5 and following discussion with the statistician the median values and the interquartile range (IQR) are reported as they are less sensitive to outliers.[133]

The median asymmetry ranged from between 0.49mm (IQR 0.26, 1.03) which was found for the landmark Nasion and 3.40mm (IQR 1.78, 5.50) for Pogonion. With the exception of Nasion the asymmetry of the medial landmarks increased as we move down the face (cranial to caudal).

Landmark	Median in mm (IQR)	Minimum, Maximum (mm)
Glabella	0.62 (0.24,0.98)	0.02, 2.85
Nasion	0.49 (0.26, 1.03)	0.04, 2.50
Pronasale	1.66 (0.87,2.52)	0.32, 4.22
Subnasale	2.13 (1.54, 3.15)	0.23, 4.70
Labrale Superius	3.11 (2.42, 4.02)	0.36,5.99
Stomion	3.20 (2.36, 3.87)	0.36, 5.64
Labrale Inferius	3.30 (2.53, 4.86)	0.50, 6.50
Pogonion	3.40 (1.78, 5.50)	0.48, 8.75

Table 8. The asymmetry (in mm) of mid-facial anthropometric landmarks in 36 children with UCS.

6.5.2: Asymmetry of the bilateral landmarks

For the seven bilateral landmarks (Endocanthion, Exocanthion, Palpebrale Superius, Palpebrale Inferius, Alare, Crista Philtri and Cheilion) the asymmetry was measured in each of the three coordinate planes (x, y, and z). Similar to the medial landmarks the absolute values were used to show the amount of asymmetry only for each of the landmarks and not its direction. Despite some of the data being reasonably symmetric as seen by the histograms and Shapiro-Wilks this was not the case

for all the data with some of the landmarks being skewed. Similarly to the mid-facial landmarks median values and IQR were used as they are more sensitive to outliers (Appendix 6, 7 and 8).[133]

The asymmetry in the x direction ranged between 0.39mm (IQR 0.17, 1.01) for Palpebrale Inferius and 6.18mm (IQR 3.83, 7.88) for Cheilion. The asymmetry in the y direction ranged between 0.00mm for Exocanthion and 1.08mm (IQR 0.69, 1.56) for the landmark Alare. The asymmetry in the z direction ranged between 0.59mm (IQR 0.37, 0.95) for Crista Philtri and 2.95mm (IQR 1.45, 4.86) for Exocanthion as shown in Table 9.

	X co-ordinate plane		Y co-ordinate Plane		Z co-ordinate Plane	
Landmark	Median in mm (IQR)	Min, Max	Median in mm (IQR)	Min, Max	Median in mm (IQR)	Min, Max
Endocanthion	0.69 (0.21,1.54)	0.07, 3.70	0.38 (0.18,0.77)	0.03, 1.22	1.84 (1.05,2.59)	0.17, 4.64
Exocanthion	1.27 (0.52,1.68)	0.05, 3.56	0.00 (0.00,0.00)	0.00, 0.68	2.95 (1.45,4.86)	0.30, 8.08
Palpebrale Superius	0.52 (0.17,0.77)	0.04, 9.22	0.84 (0.35,1.47)	0.01, 3.66	1.82 (0.77,2.85)	0.01, 8.99
Palpebrale Inferius	0.39 (0.17,1.01)	0.01,3.02	0.64 (0.32,1.02)	0.01, 1.76	2.17 (1.46,3.15)	0.07, 6.76
Alare	2.98 (2.34,4.79)	0.67, 8.68	1.08 (0.69,1.56)	0.08, 2.70	1.76 (0.90,2.90)	0.05, 4.27
Crista Philtri	6.17 (4.59,7.44)	0.61,10.84	0.36 (0.18,0.61)	0.00, 1.41	0.59 (0.37,0.95)	0.02, 1.89
Cheilion	6.18 (3.83,7.88)	0.55,10.83	0.87 (0.45,1.84)	0.01, 2.93	2.37 (1.66,3.11)	0.34, 5.73

Table 9. The asymmetry (in mm) of bilateral anthropometric landmarks in each co-ordinate plane for 36 children with UCS.

6.5.3: Asymmetry Index

In addition to the assessment of facial asymmetry in each plane, an asymmetry index (AI) which has been used in previous studies investigating facial asymmetry *(*Huang et al.,[125] Alqattan et al.[96]*)* was calculated to show the total amount of asymmetry for the bilateral landmarks.

The formula used to calculate the asymmetry index (AI) was:

$$\sqrt{(X_{unfused} - X_{fused})^2 + (Y_{unfused} - y_{fused})^2 + (Z_{unfused} - Z_{fused})^2}$$

Where X, Y, Z are the co-ordinates of a landmark, *unfused* stands for the unaffected coronal suture and *fused* represents the side with the synostosis. For perfect symmetrical paired bilateral landmarks, the discrepancy for the asymmetry would equal zero.

The smallest asymmetry index was exhibited by the landmark Palpebrale Superius with a median AI of 2.30mm (IQR 1.33, 3.17) although the range was wide from 0.48mm to 14.68mm. The largest AI was seen for Cheilion with a median of 7.11mm (IQR 4.69, 8.94). The asymmetry index for the bilateral landmarks demonstrates a similar finding to the mid-facial landmarks that there is greater asymmetry in the lower part of the face compared to the middle thirds. This is demonstrated in Table 10.

Landmark	Median in mm (IQR)	Minimum, Maximum (mm)
Endocanthion	2.33 (1.49, 3.19)	1.11, 4.88
Exocanthion	3.52 (2.25, 5.12)	1.13, 8.09
Palpebrale Superius	2.30 (1.33, 3.17)	0.48, 14.68
Palpebrale Inferius	2.84 (1.81, 3.42)	0.75, 19.23
Alare	4.22 (3.02, 6.07)	0.99, 9.29
Crista Philtra	6.21 (4.63, 7.55)	0.72, 11.0
Cheilion	7.11 (4.69, 8.94)	1.53, 12.22

Table 10. Asymmetry index (AI) for the bilateral landmarks measured using the formula: AI = $\sqrt{(X_{unfused} - X_{fused})^2 + (Y_{unfused} - y_{fused})^2 + (Z_{unfused} - Z_{fused})^2}$

6.6: Landmark based analysis looking at the direction of facial asymmetry

6.6.1: Linear distances

The Euclidean distance (linear distance) between the seven bilateral anthropometric landmarks (Exocanthion, Endocanthion, Palpebrale Superius, Palpebrale Inferius, Alare, Cheilion, Crista philtri) and the mid-facial landmark of Nasion were compared between the unfused and the fused sides of the face which were landmarked by one investigator, EB. Histograms and Shapiro-Wilk tests demonstrated the continuous linear measurements showed no statistically significant departure from normality as evident in Appendix 9 therefore *paired t tests* were used to test for statistically significant differences in bilateral landmarks between the fused and unfused sides.

A Bonferroni correction was used to adjust for multiple comparisons and statistical significance for the *paired t tests* was set at $P<0.007$ (α value 0.05/7).

Statistically significant differences were found for the bilateral landmarks Exocanthion, Palpebrale Inferius and Cheilion with the differences for these landmarks being statistically significant at a *p* value

of <0.007. The mean difference for Exocanthion was 1.84mm (SD 1.93) shorter on the fused side which contrasts with Palpebrale Inferius where the mean difference was 0.85mm (SD 1.72) and Cheilion 1.14mm (1.12) shorter on the unfused side compared to the fused. This is demonstrated in table 11.

Landmark	Mean unfused (mm)	Mean fused (mm)	Mean Difference (mm)	95% CI	Sig (2-tailed)
Exocanthion	44.61 (SD 3.93)	42.77 (SD 3.40)	1.84 (SD1.93)	1.19, 2.50	**<0.001***
Endocanthion	20.42 (SD 2.63)	19.96 (SD 2.13)	0.46 (SD1.77)	-0.14. 1.06	0.131
Palpebrale Superius	29.67 (SD 2.5)	30.15 (SD 2.99)	-0.49 (SD1.99)	-1.16, 0.19	0.151
Palpebrale Inferius	31.11 (SD 2.75)	31.96 (SD 3.0)	-0.85 (1.72)	-1.44, -0.27	**0.005***
Alare	32.54 (SD 3.40)	32.57 (SD 3.55)	-0.02 (1.11)	-0.39, 0.35	0.896
Crista Philtri	48.54 (SD 4.91)	48.70 (SD 4.9)	-0.16 (0.40)	-0.03, -2.50	0.018
Cheilion	59.98 (SD 4.58)	61.12 (SD 4.74)	-1.14 (1.12)	-1.52, -0.76	**<0.001***

Table 11. Results of paired t tests testing facial asymmetry with regards to linear distances in bilateral landmarks comparing the unfused to fused side. Statistically significant differences were found for only three of the landmarks (Exocanthion, Palpebrale Inferius and Cheilion) with a p value of <0.007.

6.6.2: Surface distances

In addition to the Euclidean distances the surface measurements which take into account the soft tissue contours of the face were also measured between the same seven bilateral anthropometric landmarks (Exocanthion, Endocanthion, Palpebrale Superius, Palpebrale Inferius, Alare, Cheilion, Crista Philtri) and the mid-facial landmark of Nasion to compare the distances between the unfused and fused sides of the face. For the majority of landmarks normality tests demonstrated the data showed no statistically significant difference from normality as seen in Appendix 10. Therefore *paired*

t tests were used to test for statistically significant differences in bilateral landmarks between the unfused and fused sides.

A Bonferroni correction was used to adjust for multiple comparisons and statistical significance for the paired t tests was set at P<0.007 (α value 0.05/7). Statistically significant differences were found for the bilateral landmarks Exocanthion and Palpebrale Inferius with the differences for these landmarks being statistically significant at a p value of <0.007. The mean difference for Exocanthion was 2.15mm (SD 2.26) and Palpebrale Inferius 1.44mm (SD 1.94) shorter on the fused side (Table 12) in comparison to the unfused side.

Landmark	Mean unfused (mm)	Mean fused (mm)	Mean Difference (mm)	95% CI	P value
Exocanthion	48.36 (SD 4.75)	46.21 (SD 3.93)	2.15 (2.26)	1.39, 2.92	**<0.001***
Endocanthion	21.12 (SD 2.86)	20.73 (2.32)	0.39 (1.97)	-0.28, 1.06	0.243
Palpebrale Superius	31.58 (SD 3.42)	31.33 (SD 3.34)	0.25 (2.50)	-0.60, 1.10	0.548
Palpebrale Inferius	34.75 (SD 3.75)	33.31 (SD 3.21)	1.44 (1.94)	0.78, 2.10	**<0.001***
Alare	33.02 (SD 3.57)	33.10 (SD 3.42)	-0.09 (1.30)	-0.53, 0.35	0.680
Crista Philtri	58.71 (SD 5.90)	58.64 (SD 5.84)	0.07 (1.52)	-0.45, 0.58	0.786
Cheilion	72.03 (SD 5.60)	72.43 (SD 5.98)	-0.41 (4.0)	-1.76, 0.95	0.548

Table 12. Results of paired t tests testing facial asymmetry with regards to surface distances in bilateral landmarks comparing the unfused to fused side. Statistically significant differences were found for the landmarks Exocanthion and Palpebrale Inferius with a p value of <0.007.

6.7: Direction of facial rotation

Two angular measurements, the deviation of the nasal tip (angle constructed between projected Nasion point, Nasion and Pronasale) and deviation of the chin (angle constructed between projected Nasion point, Nasion and Pogonion) were assessed using a true vertical that passes through Nasion point. The relationship between the side of fusion and the direction of facial rotation was analysed using a chi-square analysis (1 degree of freedom).

6.7.1: Deviation of the nasal tip

Of the 18 participants with left sided UCS 15 participants (83%) had a nasal tip which deviated towards the right side or unfused side and 3 participants nasal tip deviated toward the side of fusion (17%). Of the 18 participants who had right sided UCS all 18 participants (100%) had deviation of the nasal tip towards the left or unfused side.

The mean nasal tip deviation towards the unfused side was 4.4 degrees (SD 3.9) as seen in Table 13. The null hypothesis that nasal tip deviation is zero is rejected (chi-square=25.714 with 1 degree of freedom, P <0.001).

	Mean Angulation (SD)	X^2	df	Significance (2 sided)
Deviation of Nasal tip to unfused side	4.4 ± 3.9	25.714	1	**<0.001***

Table 13. Chi square analysis for deviation of nasal tip showing the mean angulation of 4.4 degrees (SD 3.9 degrees) toward the unfused side.

6.7.2: Deviation of chin

Similar to the deviation of the nasal tip for the 18 participants with left sided UCS 15 participants (83%) had a Pogonion which deviated towards the right or unfused side and 3 participants (17%) had a Pogonion which deviated toward the side of fusion. All eighteen participants (100%) with right sided fusion showed a Pogonion which deviated towards the unfused or left side.

The mean Pogonion deviation towards the unfused side was 3.5 degrees (SD 2.7) as demonstrated in Table 14. The null hypothesis that deviation of the chin is zero is rejected (chi-square = 25.714 with 1 degree of freedom, p < 0.001).

	Mean Angulation (SD)	X^2	Df	Significance (2 sided)
Deviation of Pogonion to unfused side	3.5 ± 2.7	25.714	1	**<0.001***

Table 14. Chi square analysis for deviation of Pogonion showing the mean angulation of 3.5 degrees (SD 2.7 degrees) toward the unfused side.

6.8: Age of imaging and facial asymmetry

To determine if there was any possible association between facial asymmetry for bilateral landmarks and age in years of imaging, Pearson product-moment correlation coefficients were calculated. Following application of a Bonferroni correction the significance level was set at $p < 0.007$ (α value 0.05/7). Only weak correlation as seen in Table 15 was found between facial asymmetry and age of imaging, indicating that the participants do not become more or less asymmetric with age.

Landmark	Pearson correlation	Significance (2-tailed)
Exocanthion	0.223	0.192
Endocanthion	0.154	0.371
Palpebrale Superius	0.101	0.559
Palpebrale Inferius	-0.019	0.914
Alare	0.040	0.817
Cheilion	0.124	0.471
Crista Philtri	0.090	0.600

Table 15. Pearson correlation coefficients demonstrating there is no significant relationship between facial asymmetry and age of imaging at the p <0.007 level of significance.

6.9: Age of surgery and facial asymmetry

To determine if there was any possible association between facial asymmetry for bilateral landmarks and age of fronto-orbital advancement and remodelling, Pearson product-moment correlation coefficients were calculated as shown in Table 16. Following application of a Bonferroni correction the significance level was set at $p < 0.007$ (α value 0.05/7).

Mean age of fronto-orbital advancement and remodelling was 17 months (SD 7.4 months) with a range from 11 to 48 months. Cheilion shows reasonable correlation was a coefficient of 0.352 which was significant at the 0.05 level of significance. However after application of the Bonferroni correction this was no longer significant and no relationship was found between facial asymmetry and age of FOAR indicating that early or late intervention does not impact on facial asymmetry. However this should be viewed with caution due to 27 of the participants having surgery prior to 18 months while only 9 had surgery after 18 months of age.

Landmark	Pearson correlation	Significance (2-tailed)
Exocanthion	0.283	0.095
Endocanthion	0.217	0.203
Palpebrale Superius	0.008	0.961
Palpebrale Inferius	0.049	0.779
Alare	0.227	0.183
Cheilion	0.352	0.035
Crista Philtri	0.034	0.842

Table 16. Pearson correlation coefficients demonstrating there is no relationship between facial asymmetry and age of FOAR at the 0.007 level of significance.

Chapter 7: Discussion

7.1: Demographics of the study

The primary aim of the study was to describe the soft tissue facial asymmetry in a group of children with surgically corrected Unicoronal Synostosis. The study consisted of thirty six participants diagnosed with UCS who underwent FOAR in infancy and had post-operative three-dimensional imaging with the static 3dMD head system.

Of the 36 participants included 24 were female (66%) and 12 were male (33%) which reflects the literature that UCS has a female predominance with between 60-75% of cases occurring in females.[2,42,52] Previous studies have found that the right side is more commonly affected however in this study 50% of participants had involvement of the right coronal suture and 50% had left sided involvement.[35,51,52,67]

Fronto-orbital Advancement and Remodelling has been the surgical technique used at Alder Hey Craniofacial Unit since 2003. The mean age of FOAR was 17 months (SD 7.4 months) with a range between 11 and 48 months. Mc Carthy et al.[14] defines early surgery as that before eighteen months of age and in this current study 27 participants were operated on before this age while nine participants had surgery later than 18 months. The mean age of FOAR in this study is later than that of other studies in the literature,[9,11,14,18,79] however, the standard protocol at Alder Hey Craniofacial Unit is to aim to carry out surgical correction in these patient's between 12 and 18 months of age. The slightly older mean age of surgical intervention may be reflective of these patient's being treated under the National Health Service where there is a waiting time for treatment.

7.2: Reliability testing

Reliability refers to the reproducibility of the measurement when repeated at random in the same subject. When assessing facial asymmetry using facial landmarks this has to be interpreted with regards to the reliability of identification of these landmarks; that is the random method of the error.

7.2.1: Intra-observer repeatability

Intra-observer repeatability was assessed on twelve UCS images which were randomly selected and the twenty two anthropometric landmarks were identified on two occasions at least two weeks apart by operator EB. The linear measurements of twenty one landmarks to Nasion were measured to assess their repeatability. Agreement was analysed using intra-class correlation coefficients as well as Bland and Altman plots to assess for random and systematic errors. The intra-class correlation coefficients ranged from 0.97 to 0.99 for the twenty one anthropometric landmarks which indicated excellent

agreement. The reliability was seen for the landmarks to be within a mean difference of 0.50mm which again indicates a high level of agreement and is comparable to other studies looking at the precision of landmarking using the 3dMD system.[20–22] The Bland and Altman plots generally showed that the spread of the data was random, with no systematic errors or over or under measuring (Appendix 3).

7.2.2: Inter-rater reliability

Inter-rater reliability was assessed by landmarking the same anthropometric landmarks on 24 images, 12 UCS images and 12 images from a parallel study.[130] This was carried out by two operators and similarly to the intra-rater reliability, the Euclidean distance between each landmark and Nasion was assessed for repeatability. The intra-class correlation coefficients showed excellent agreement for the twenty one landmarks with ICC ranging from 0.96 to 0.99. A mean difference between the two operators of less than 0.50mm was seen for 19 of the 21 landmarks. Only Palpebrale Superius Right and Stomion had a mean difference greater than this with 0.50mm and 0.52mm respectively and still indicated a high level of agreement. Generally the Bland and Altman plots showed that the data was random. However some evidence of a systematic trend was noted for the landmark Subnasale as seen in Appendix 4. The limits of agreement show that with the exception of four landmarks (Glabella, Alare Right, Alare Left and Pogonion) these were within 2.5mm. The finding in this study that there may be a slight systematic trend for Subnasale and that the limits of agreement were generally wider when carrying out inter-rater agreement reflects the fact that generally inter-rater agreement is more difficult to achieve in comparison to intra-rater agreement. It is for this reason that studies such as that by Oh et al.[9] assessing facial asymmetry in UCS patients only used a single rater and was potentially open to observer bias. The current study did however show that the majority of landmarks had a mean difference of less than 0.50mm between the two observers indicating excellent agreement and increasing the generalisability of the results.

7.2.3: Intra-rater and Inter-rater reliability Nasion

Intra-rater and inter-rater reliability for the landmark Nasion was assessed by looking at the individual x, y and z co-ordinates as it was the reference point from which all linear and surface measurements were made. The x axis is the medio-lateral plane, the y axis is along the supero-inferior plane and the z axis along the antero-posterior plane. Soft tissue Nasion was selected as its reproducibility is superior to that of other anatomical facial landmarks.[125] In this study the intra-class correlation co-efficient for the y and z axes were 0.95 and 0.99, again indicating excellent agreement. However for the x axis while still showing good agreement the ICC was lower at 0.66 suggesting that Nasion is more difficult to identify in the right to left direction. The Bland and Altman plots for the three co-ordinate planes did not generally show any systematic error or under or over measuring. Despite the ICC for the x axis being 0.66 the mean difference was low at 0.05mm.

For the inter-rater agreement the x axis (medio-lateral plane) had an ICC of 0.77, which although is still seen as a good level of agreement is lower than the y axis (supero-inferior plane) and the z axis (antero-posterior plane) which each had an ICC of 0.99. Despite this the mean difference was only 0.20mm for the x axis, 0.19mm for the y axis and 0.05mm for the z axis between the two operators. This is still a high level of precision as seen in other studies examining the reliability of landmarking who showed that differences of less than 1mm were clinically insignificant.[19,20] When examining the 95% limits of agreement these were generally quite narrow and were less than 2mm. These findings contrast with that of Alqattan et al.[96] who while only assessing intra-observer agreement showed that reliability of Nasion was lower in the y co-ordinate plane whereas the current study found the agreement with the x co-ordinate or medio-lateral plane to be lower. Aldridge et al.[21] while also only assessing the intra-observer repeatability using the 3dMD system, found that Nasion was one of six landmarks which showed an error in precision of greater than 1mm. The findings in the current study demonstrated greater precision than Aldridge et al.[21] with a mean difference for intra-rater and inter-rater agreement in all three co-ordinate planes of below 1mm.

7.3: Amount of facial asymmetry

An Asymmetry Index has been used to assess the absolute amount of asymmetry in previous studies of three-dimensional imaging involving "standard" populations and was employed in this study.[96,125] To the authors knowledge this is the first use of this method of assessing facial asymmetry in a UCS population. Although the AI does not give an indication of the direction of facial asymmetry, as employs the absolute values, it does give an indication of the total amount of asymmetry and where these lie.

For the medial landmarks, with the exception of Nasion, which was within the limits of agreement for the intra-rater reliability, the asymmetry increased as you move from the upper to the lower face. The lowest mid-facial AI was 0.49mm (IQR 0.26mm, 1.03mm) for Nasion and greatest for Pogonion at 3.40mm (IQR 1.78mm, 5.50mm).

For the bilateral landmarks, the asymmetry was assessed in each off the three co-ordinate planes as well as using the asymmetry index. For the seven pairs of bilateral landmarks the smallest AI was evident for Palpebrale Superius with a median AI of 2.30 mm (IQR 1.33mm, 3.17mm). When looking at the individual co-ordinate planes the greatest asymmetry for this landmark was evident in the x direction or medio-lateral plane rather than in a supero-inferior or antero-posterior direction. The greatest AI was evident for Cheilion with an AI of 7.11mm (IQR 4.69mm, 8.94mm). Similar to Palpebrale Superius, the greatest asymmetry was seen in the medio-lateral direction (6.18mm) rather than in the superior-inferior (0.87mm) or antero-posterior (2.37mm) direction. The bilateral

landmarks followed the same trend as seen in the medial landmarks with asymmetry increasing as you move down from the cranium. Asymmetry was also generally greater for the bilateral landmarks in comparison to mid-facial landmarks due to it being exhibited in all three co-ordinate planes, whereas, for the mid-facial axis this was only measured from the mid-sagittal plane. For all of the bilateral landmarks the asymmetry as seen by the Asymmetry Index is outside the limits of agreement for intra-rater reliability indicating a difference between the two sides of the face in UCS patients which cannot be explained by the error of the method.

No previous UCS studies found in the literature used the AI to assess facial asymmetry. However comparison can be made to those involving "standard" populations. A study carried out using laser scans by Huang et al.[125] on 60 healthy Chinese adults looked at the asymmetry of seven medial and four bilateral landmarks. The mean asymmetry index ranged from 0.76mm (SD 0.59) for Glabella to 2.82mm (SD 1.42) for Cheilion. When comparing to the current study these findings highlight that there is a trend in both the "standard" population and the UCS population for asymmetry to generally increase as we move from the upper to the lower face. However the asymmetry index in the current UCS study was generally higher than those seen by Huang et al. with the exception of the landmark Glabella. This indicates that patients with UCS post FOAR still tend to have a higher degree of asymmetry when compared to a non UCS population. In comparison to a mean AI of 2.82mm (minimum 0.40mm, maximum 6.50mm) for the landmark Cheilion found by Huang et al.,[125] in the current study, the median AI was much higher at 7.11mm and had a wider range of 1.53mm to 12.22mm. There were, however, differences in the methodology between the two studies and we need to view any direct comparisons with caution. Huang et al.[125] used laser scans and the study only included a Chinese population which is different to our predominantly Caucasian sample. The laser scanning used has a much slower capture time of 400ms in contrast to the static 3dMD head system capture time of 1.5ms, therefore, there was more possibility for dynamic movement and motion error during laser scanning. They also used a symmetry plane to compare the right to the left side of the face which was different to our method of referencing the images. They did not discuss the normality of their data. As such they used means and standard deviations in relation to their asymmetry scores whereas the current study used medians and interquartile range which are less sensitive to the influence of outliers.[133]

Huang et al.[125] also only assessed intra-operator and not inter-operator repeatability and while they report that this ranged between 0.31mm - 0.95mm with a mean value of 0.52mm they did not provide any further detail of which landmarks showed the greatest method error. Despite these differences in methodology comparison does suggest a greater degree of asymmetry in a UCS population compared to their non UCS sample.

Alqattan et al.[96] similarly used the index for twenty one landmarks to create reference values for facial asymmetry in a population of 85 “normal” British Caucasian adults. They showed that the asymmetry score with the exception of Pronasale, which was within the limits of the intra-examiner reliability, tended to increase as you move down the face and that it was greater for bilateral landmarks rather than medial landmarks. These findings are similar to those in the current study. Unlike Huang et al.[125] they do discuss the normality of their data and as positively skewed they used medians and IQR making comparison to the current study easier. No statistically significant difference was found between males and females, therefore, in the current study the genders were combined. Also due to the small sample size of the UCS population males and females were not assessed independently. Although the findings in the current study show a similar trend of increasing asymmetry as we move from cranium to chin, the asymmetry index was again higher in the UCS population compared to standard British Caucasian adults as evident in table 17 and 18. This highlights that patient’s with UCS despite being post-surgical correction tend to show a greater degree of facial asymmetry. Caution must again be used when making direct comparisons to this study however as they also involved laser scanning with a likely slower capture time. It also involved adult subjects with a mean age of 28.1yrs ± 9.5yrs (range 19-54 yrs) who would have completed growth in contrast to the current study of UCS children where the mean age at imaging was much lower at 5yrs 6 months (range 1yr 7months -11yrs 6months) and these subjects still had a lot of growth potential remaining.

Landmark	Median Asymmetry Index in mm *(IQR). Alqattan et al. 2015.*	Median Asymmetry Index in mm (IQR). *Current study UCS.*
Glabella	M 0.9 (0.6, 1.5), F 1.0 (0.5,2.2)	0.62 (0.24,0.98)
Nasion	M 0.8 (0.4,1.4), F 1.2 (0.4, 2.0)	0.5 (0.26, 1.03)
Pronasale	M 0.1 (0.0, 0.3), F 0.2 (0.1, 0.3)	1.66 (0.87,2.52)
Subnasale	M 0.8 (0.4, 1.4), F 0.7 (0.3, 1.1)	2.13 (1.54, 3.15)
Labrale Superius	M 1.1 (0.7, 1.5), F 1.2 (0.3, 1.7)	3.11 (2.42, 4.02)
Stomion	NA	3.20 (2.36, 3.87)
Labrale Inferius	M 1.2 (0.4, 1.8), F 1.3 (0.4, 2.2)	3.30 (2.53, 4.86)
Pogonion	M 1.5 (0.6, 3.0), F 1.8 (0.7, 2.5)	3.40 (1.78, 5.50)

Table 17. Comparison of the median mid-facial Asymmetry Index (AI) and IQR for Alqattan et al.[96] and current study. Alqattan et al. showed that the difference between males and females is small and not statistically significant therefore in the current study males and females were combined.

Landmark	Median Asymmetry Index in mm *(IQR). Alqattan et al. 2015.*	Median Asymmetry Index in mm (IQR). *Current study UCS.*
Endocanthion	M 2.8 (1.9, 3.4), F 3.1 (2.2, 4.8)	2.33 (1.49, 3.19)
Exocanthion	M 3.1 (2.2, 4.8), F 3.0 (2.2, 4.8)	3.52 (2.25, 5.12)
Palpebrale Superius	M 2.7 (1.7, 4.8), F 3.1 (1.9, 4.9)	2.30 (1.33, 3.17)
Palpebrale Inferius	M 2.9 (1.6, 4.7), F 2.8 (1.9, 4.1)	2.84 (1.81, 3.42)
Alare	M 2.8 (1.9, 4.4), F 2.8 (1.9, 4,1)	4.22 (3.02, 6.07)
Crista Philtri	M 2.2 (1.6, 3.0), F 1.6 (0.9, 3.5)	6.21 (4.63, 7.55)
Cheilion	M 3.2 (2.1, 4.1), F 3.5 (2.4, 5.0)	7.11 (4.69, 8.94)

Table 18. Comparison of the median bilateral Asymmetry Index (AI) and IQR for Alqattan et al.[96] and current study.

7.4: Direction of facial asymmetry

Paired t tests were used to assess for any statistically significant differences in linear measurements (Euclidean distances) and surface measurements which took into account the soft tissue contour of the face between the fused and unfused sides. Due to the multiple comparisons made a Bonferroni correction was applied and significance was set at a P value <0.007. For linear measurements statistically significant differences were found for the landmarks Exocanthion with a mean difference of 1.84mm (95% CI 1.19, 2.50mm) shorter on the fused side whereas for Palpebrale Inferius and Cheilion the mean distance was shorter on the unfused side with a mean difference of -0.85mm (95% CI -1.44mm, -0.27mm) and -1.14mm (95% CI -0.76, -1.52mm).

When the surface measurements were analysed statistically significant differences were found only for Exocanthion and Palpebrale Inferius with mean differences towards the unfused side of 2.15mm (95% CI 1.39, 2.92mm) and 1.44mm (95% CI 0.78, 2.10mm) respectively. Although only two landmarks showed statistical significance there was a general trend for the surface measurements, with the exception of Alare and Cheilion, to be greater on the nonfused compared to the fused side.

Oh et al.[9] found no significant difference in linear measurements between the fused and unfused sides of the face for medial canthus to midline measurements, measured as the distance from Sellion to Endocanthion. Although in this current study the midline landmark used was Nasion rather than Sellion, similarly no significant difference was evident between the fused and unfused sides for Endocanthion to Nasion. Becker et al.[18] in a CT study looking at long term osseous morphologic outcome of surgically treated UCS patient's found that at one year post-operatively only 25 of 135 pairs of landmarks were asymmetric and that the midface appeared symmetric. Although the participants in this current study had a mean age of 5yrs 6months with the mean age of FOAR at 1yr 5 months and therefore the majority were greater than one year post- operative, generally a degree of symmetry is seen, with only three paired linear measurements and two surface measurements showing a significant difference.

No significant difference was seen for Endocanthion to Nasion. However the landmarks Exocanthion to Nasion did show significance with the distance being shorter on the fused rather than the unfused side of the face. Although statistically significant, the mean difference between the two sides is still relatively small with the measurement being 1.84mm shorter on the fused side for the linear measurements and 2.15mm shorter for the surface measurements. Previous literature however, has shown that post FOAR there is a trend of partial retrusion to the pre-operative features.[9,11,18] In untreated individuals the nasal root has been shown to deviate towards the fused side.[5] In the current study while no difference is seen for Endocanthion to Nasion the shorter distance of Nasion to

Exocanthion on the fused side suggests that the nasal root is deviated towards the ipsilateral side and therefore similar to previous studies, with an element of retrusion to the UCS phenotype.

7.5: Direction of facial rotation

Two angular measurements were used to assess the deviation of the nasal tip and the deviation of the chin. There was consistent deviation of the nasal tip in 33 of the 36 participants towards the non-fused side and a similar trend for deviation of Pogonion towards the unfused side. Of the participants, however, who did not follow this trend and demonstrated either nasal tip deviation or Pogonion deviation towards the fused rather than the unfused side, only one of the subjects showed this pattern for both the nasal tip and Pogonion. Four subjects had either nasal tip or Pogonion deviation towards the non-fused side. All of these five subjects had left sided UCS. The mean nasal tip deviation towards the non-fused side was 4.4 degrees (SD 3.9 degrees) and the mean deviation of Pogonion towards the non-fused side was 3.5 degrees (SD 2.7 degrees).

The consistent rotation of the nasal tip and Pogonion is similar to that described in untreated individuals. Camargos et al.[5] showed that in a group of 20 UCS subjects prior to surgical correction there was significant deviation of the tip of the nose towards the unfused side (2.2± 1.2˚) compared to normal controls.[5] Surprisingly the degree of angulation in this current study of post-operative UCS children is greater than that observed by Camargos et al. in an untreated sample. This may be explained by the difference in the methodology of the study with Camargos et al. using CT scans in comparison to stereophotogrammetry.[5] Despite the difference in the size of the angulation, the current findings demonstrate that the deviation of the nasal tip is similar in direction to untreated individuals.

This contrasts with McCarthy et al.[14] who found that nasal tip deviation was corrected in 25 of their 32 participants who had pre-operative nasal deformity following FOAR and that the remaining 7 patient's showed improvement.[14] However, there are a number of limitations with this study in that facial asymmetry was determined using two-dimensional photographs which does not reflect the three-dimensional nature of facial asymmetry. They also appear to have only subjectively assessed nasal tip deviation and did not carry out a quantitative analysis which may reflect the difference in the findings between the studies.

Previous research have shown that there is a degree of post-surgical reversion of the cranium towards the untreated phenotype. [18,79] When comparing the findings to studies assessing the direction of facial rotation, the findings are consistent. Oh et al.[9] similarly used 3dMD images to assess post-operative facial asymmetry in UCS patients. They found that all demonstrated rotation of the middle and lower face towards the non-fused side with a mean nasal tip deviation of 5 degrees (SD 1.2 degrees) and

mean deviation of the facial midline towards the non-fused side of 3.4 degrees (SD. 0.7 degrees). They did however, use different anthropometric landmarks in comparison to the current study. Nasal tip was measured as Sellion to Pronasale and the midline was analysed using the landmarks Sellion to Subnasale to Gnathion. They also had a much smaller sample size of only 15 participants and the mean age at imaging was older than in the current study at 14years (range 11-29 years). This difference in method may reflect the slight difference in the angulations. Despite this the trend of rotation of the face towards the unfused side is the same as that demonstrated by Oh et al.[9]

7.6: Effect of age of imaging and age of surgical correction on facial asymmetry

A Pearson product-moment correlation co-efficient was used to assess for any correlation between facial asymmetry and age of imaging/ age of surgical correction. No significant correlation was evident between facial asymmetry and age of digital imaging, indicating that they do not become more or less asymmetric with age. The mean age of the participants in the study however was only 5yrs 6months and therefore more long term follow up would be required to further investigate this.

The relationship between facial asymmetry and age of surgical correction did show a reasonable degree of correlation for the landmark Cheilion only, whilst the remaining bilateral landmarks did not indicate a significant correlation. However, after application of the Bonferroni correction this was no longer significant. Although the sample size is relatively small these results do indicate that post-operative facial asymmetry does not correlate with age of follow up or early or later surgical intervention. Similar previous studies have also been unable to find a correlation between the degree of facial asymmetry and the time elapsed between surgery and follow up, as well as a correlation between facial asymmetry and the timing of surgery.[9,11]

7.7: Comparison of current findings to a population of children under 16 years in the North West of England

A more appropriate comparison of the findings in this study can be made to another current DDSc project being carried out at the University of Liverpool by Carty et al. [130] which is assessing the degree of soft tissue facial asymmetry in a standard population of children under 16 years from the North West of England. The study consisted of 3D imaging of 107 individuals (57 males: 50 females) with a mean age of 7 years and a range of 0-14yrs. 3D imaging was carried out using the same static 3dMDhead system imaging pod which was used in the current UCS project. The researcher carrying out the study looking at the standard population also acted as the second observer for the inter-observer reliability testing and the same twenty two anthropometric landmarks were identified on the images in both studies. The samples were not matched for factors such as age and gender

therefore, statistical analysis between the two samples was not conducted. However, due to the same methods having been employed in both studies some comparison can be made.

A similar trend was found in both populations with asymmetry generally increasing as you move away from the cranium. The lowest AI in the mid-facial landmarks was observed in both studies for the ladmark Nasion with a median AI of 0.60mm (IQR 0.24mm, 1.04mm) for the "standard" population and a slightly lower AI in the UCS population of 0.49mm (IQR 0.26mm, 1.03mm). However with the exception of Nasion and Glabella the AI for the mid-facial landmarks was higher in the UCS population in comparison to the "standard" population where only one of the landmarks showed an asymmetry score of greater than 1mm. This contrasts with the current UCS study where all but two landmarks had an asymmetry score of greater than 1mm and the greatest asymmetry was seen for the landmark Pogonion, which was almost three times greater in the UCS sample (Table 19).

When comparing the bilateral paired landmarks the asymmetry in both populations is also seen to increase as you move from the middle to lower face. Similar to the mid-facial landmarks, the UCS population shows more asymmetry when compared to a standard North West England child population. The greatest asymmetry in both groups is evident around the mouth with Crista Philtri in the standard population showing an asymmetry of 2.09mm and Cheilion 2.56mm. In comparison the asymmetry for the UCS children is much higher with an asymmetry of 6.21mm and 7.11mm for the landmarks Crista Philtri and Cheilion respectively (Table 20). This highlights that while a similar trend in the distribution of soft tissue asymmetry is evident there is a higher degree of asymmetry in a post-operative UCS cohort. This comparison coincides with the findings of Owall et al.[11] who found that only 10% of children with UCS who underwent FOAR in infancy had a degree of craniofacial asymmetry which was within the range of asymmetry observed in a control group.[11]

Despite the differences seen in asymmetry using the Asymmetry Index between the two populations comparing the findings for the paired t tests for the linear and surface measurements similar trends are noted. In both studies for the linear measurements significant differences were found for the landmarks Exocanthion and Cheilion. In contrast however significant differences for landmarks Endocanthion and Crista Philtri were found in the standard child population whereas these were not statistically significant in the UCS study. Similarly significant differences were found in the surface measurements for Exocanthion and Palpebrale Inferius in both studies, with the addition of Cheilion in the standard child population. This was not found, however, to be statistically significant in the UCS population. A possible explanation is that the sample size for the UCS population was small and therefore the study may not be significantly powered to find a difference.

Landmark	Asymmetry Index median in mm (IQR) child population NW England	Asymmetry Index median in mm (IQR) current UCS study
Glabella	0.62 (0.27, 1.16)	0.62 (0.24,0.98)
Nasion	0.60 (0.24, 1.04)	0.5 (0.26, 1.03)
Pronasale	0.74 (0.36, 1.27)	1.66 (0.87,2.52)
Subnasale	0.82 (0.36, 1.37)	2.13 (1.54, 3.15)
Labrale Superius	0.86 (0.47, 1.59)	3.11 (2.42, 4.02)
Stomion	0.90 (0.40, 1.60)	3.20 (2.36, 3.87)
Labrale Inferius	0.98 (0.42, 1.70)	3.30 (2.53, 4.86)
Pogonion	1.08 (0.56, 1.75)	3.40 (1.78, 5.50)

Table 19. Comparison of median asymmetry index and IQR for current study and child population under 16 years in North West of England.[130]

Landmark	Asymmetry Index median in mm (IQR) child population NW England	Asymmetry Index median in mm (IQR) current UCS study
Endocanthion	1.56 (1.15, 2.42)	2.33 (1.49, 3.19)
Exocanthion	2.16 (1.41, 3.34)	3.52 (2.25, 5.12)
Palpebrale Superius	1.68 (1.23, 3.29)	2.30 (1.33, 3.17)
Palpebrale Inferius	1.56 (1.06, 2.22)	2.84 (1.81, 3.42)
Alare	1.94 (1.27, 2.73)	4.22 (3.02, 6.07)
Crista Philtri	2.09 (0.63, 3.46)	6.21 (4.63, 7.55)
Cheilion	2.56 (1.69, 3.65)	7.11 (4.69, 8.94)

Table 20. Comparison of median asymmetry index and IQR for current study and child population under 16 years in North West of England.[130]

7.8: Limitations of the study

Alder Hey Craniofacial Unit is one of four Craniofacial Units in the United Kingdom and has between three and thirteen cases of UCS per year. Due to the low prevalence of the condition of 0.8 to 1 per 10,000 live births and that the project was being carried out as a DDSc project, therefore had to be completed within a three year timeframe, it would have been very difficult to carry out the study prospectively and have sufficient subjects for imaging. As such the study was retrospective in nature, which may have introduced the potential of selection bias which is recognised in retrospective studies.

The images used were all taken from a single centre. This may affect the generalisability of the results. However, the centre is one of only four Craniofacial Units in the UK and therefore takes referrals from a large geographical area, covering all ethnicities and socioeconomic backgrounds.

Fifty eight participants were eligible for inclusion in the study however due to the quality of the static 3dMD head system images taken, eleven children had to be excluded. A further eleven patients were excluded following review of the clinical notes due to an associated syndrome, there being no post-operative imaging, or due to not having undergone FOAR. In total 36 participants were included in the study which although still a relatively low number is higher than previous research assessing 3D facial asymmetry in UCS patients.[9,11,18] This also reflects the low prevalence of the condition.

Missing data on the images particularly in the region of the ears, possibly as a result of the subject's hair casting shadow on the image or noise of the scanner, meant that landmarking in this region was more difficult. The subjects were also very young in age and therefore it is challenging to ensure that they remain motionless during imaging. Previous literature assessing the accuracy and precision of identifying landmarks have found that due to artefacts in the ear region repeatability was lower than for other landmarks.[21,22,122] Due to the potential for introducing landmarking error in this region in the current study landmarks on the ears were used only to reference plane the image. To try and secure the subjects hair off their face a head cap was worn during imaging. However, in many cases this was placed over the forehead resulting in it not being possible to analyse asymmetry on the participant's forehead.

There is an error of measurement associated with placement of landmarks. However intra and inter-observer repeatability was assessed and the mean difference was shown for the majority of landmarks to be less than 0.50mm and all of the landmarks had a mean difference of less than 1mm. This is comparable to the literature assessing the reliability of landmarking on 3dMD images.[20–22] Previous UCS studies with the 3dMD system [9,11] assessed intra-observer reliability only whereas in this current study both intra and inter-observer reliability was analysed. ICC and Bland and Altman plots were used and demonstrated that on the whole the errors were random and not systematic in nature.

The study was limited to post-operative facial asymmetry and the majority of participants had imaging at a single time point with a mean age at imaging of 5yrs 6 months. While no correlation was evident between age of imaging and facial asymmetry more long term follow up of these participants into adulthood would be beneficial to assess long term growth of this cohort.

7.9: Implications for Clinical Practice

The results of this study have implications for subjects with UCS. To the authors knowledge this is the first assessment of facial asymmetry using stereophotogrammetry in a UCS population in the United Kingdom. With a sample size of 36 participants, this study is also larger than previous studies using three-dimensional imaging to assess facial asymmetry in UCS patients who have undergone FOAR in infancy. While carried out at a single centre, Alder Hey Children's Hospital is one of only four craniofacial units in the UK and therefore receives referrals from a large area, increasing the generalisability of the findings.

The findings of this study are consistent with previous smaller studies which is that children with UCS who undergo fronto-orbital advancement and remodelling in infancy do continue to show middle and lower facial asymmetry. These findings will provide clinicians, particularly Craniofacial Surgeons, with information on the impact that FOAR has on facial growth and asymmetry. This information can also be provided to families of children with UCS to explain to them how the face is expected to grow after surgical intervention and to manage expectations following surgery.

Both intra-rater and inter-rater agreement was assessed in the current study. Much of the literature on the reliability and precision of landmarking 3dMD images only assess intra-rater reliability.[19,20,22] This is also the case in previous studies assessing facial asymmetry in UCS patients.[9] The findings of this study add to the evidence that 3dMD technology has high levels of both intra-rater and inter-rater reliability and therefore provides a viable option of imaging.

7.10: Implications for future research

This study was limited to assessment of post-operative imaging and future research comparing pre-operative to post-operative facial asymmetry using the 3dMD system in UCS patients would be of interest in order to assess the improvement in facial symmetry following FOAR. This would be of benefit to clinicians in order to be able to inform parents of the effect that FOAR will likely have on facial growth and symmetry.

Future projects to compare the UCS population in this study with the standard child population in the North West of England could be explored with matching of the samples. This would facilitate statistical analysis between the two populations and would provide further information which would be of use for clinicians in discussing FOAR and future growth with UCS families.

The sample size, although larger than previous studies, was still relatively small and the mean age of the subjects in this study was only 5 ½ years. More long term follow up of these individuals with static 3dMD head system imaging and a larger sample size would provide further information on how facial asymmetry changes with age and growth and the need for any surgical revision in adulthood.

Chapter 8: Conclusions

- The findings of this study demonstrate that subjects with Unicoronal synostosis who undergo Fronto- Orbital Advancement and Remodelling in infancy show consistent soft tissue craniofacial asymmetry post-operatively.
- Soft tissue facial asymmetry shows features similar to that of the untreated UCS phenotype.
- Fronto-Orbital Advancement and Remodelling does not change the direction of facial growth in a UCS population with direction of facial rotation continuing towards the unfused side.
- No relationship was found between age of three dimensional imaging and age of surgical correction on facial asymmetry
- Similar to “standard” child populations, facial asymmetry increases as you move superiorly to inferiorly, although the amount of facial asymmetry is greater in UCS patients in comparison to “standard” individuals.

References:

1. Ghali GE, Sinn DP, Tantipasawasin S. Management of nonsyndromic craniosynostosis. *Atlas of Oral and Maxillofacial Surgery Clinics of North America* 2002;10:1–41.

2. Ciurea AV, Toader C. Genetics of craniosynostosis: review of the literature. *Journal of Medicine and Life* 2009;2(1):5–17.

3. Cobourne M, DiBiase A. *Handbook of Orthodontics*. 1st ed. London: Elsevier Ltd; 2009: 70-71.

4. Cornelissen M, Ottelander BD, Rizopoulos D, Van der Hulst R, Mink van der Molen A, Van der Horst C, et al. Increase of prevalence of craniosynostosis. *Journal of Cranio-Maxillo-Facial Surgery* 2016;44:1273-1279.

5. Camargos IS, Metzler P, Persing J, Alcon A, Steinbacher DM. Nasal soft-tissue and vault deviation in unicoronal synostosis. *Journal of Plastic, Reconstructive & Aesthetic Surgery* 2015;68(5):615–21.

6. Meara JG, Burvin R, Bartlett RA, Mulliken JB. Anthropometric study of synostotic frontal plagiocephaly: before and after fronto-orbital advancement with correction of nasal angulation. *Plastic and Reconstructive Surgery* 2003;112(3):731–8.

7. Eva Š, Horn F, Neščáková E, Kabát M, Petrík M, Trnka. Anthropometry of craniosynostosis. *Neurologia I Neurochirurgia Polska* 2015;49(4): 229-238.

8. Kreiborg S, Bjork A. Craniofacial asymmetry of a dry skull with plagiocephaly. *European Journal of Orthodontics* 1981;3:195–203.

9. Oh AK, Wong J, Ohta E, Rogers GF, Deutsch CK, Mulliken JB. Facial Asymmetry in Unilateral Coronal Synostosis: Long-Term Results after Fronto-orbital Advancement. *Plastic and Reconstructive Surgery* 2008;121: 555-562.

10. Ursitti F, Fadda T, Papetti L, Pagnoni M, Nicita F, Iannetti G, et al. Evaluation and management of nonsyndromic craniosynostosis. *Acta Paediatrica* 2011;100(9):1185–94.

11. Owall L, Dervann TA, Larsen P, Hove HD, Hermann NV, Bøgeskov L, et al. Facial Asymmetry in Children with Unicoronal Synostosis Who Have Undergone Craniofacial Reconstruction in Infancy. *The Cleft Plate-Craniofacial Journal* 2016;53(4):385-93.

12. Hansen M, Padwa BL, Scott RM, Stieg PE, Mulliken JB. Synostotic frontal plagiocephaly: anthropometric comparison of three techniques for surgical correction. *Plastic and Reconstr uctive Surgery* 1997;100(6):1387–95.

13. Rhodesô G, Yoshikawa S, Palermoô R, Simmonsá LW, Peters M, Lee K, et al. Perceived health contributes to the attractiveness of facial symmetry , averageness , and sexual dimorphism. *Perception* 2007;36:1244–53.

14. McCarthy J, Glasberg SB, Cutting CB, Epstein FJ, Grayson BH, Ruff G, et al. Twenty-year experience with early surgery for craniosynostosis: I. Isolated craniofacial synostosis--results and unsolved problems. *Plastic and Reconstructive Surgery* 1995;96(2):272–83.

15. Bartlett SP, Whitaker LA, Marchac D. The operative treatment of Isolated Craniofacial Dysostosis (Plagiocephaly): A Comparison pf the Unilateral and Bilateral Techniques. *Plastic and Reconstructive Surgery* 1990;85(5):677-683.

16. Marchac D, Renier D. Craniofacial Surgery for Craniosynostosis Improves Facial Growth: A Personal Case Review. *Annals of Plastic Surgery* 1985;14(1):43–54.

17. Weinzweig J, Whitaker LA, Craniofacial Surgery 1- Congenital. Plastic Surgery Secrets Plus. 2nd ed. Mosby: Elsevier Ltd; 2010: 196–211.

18. Becker DB, Fundakowski CE, Govier DP, Deleon VB, Marsh JL, Kane AA. Long-term osseous morphologic outcome of surgically treated unilateral coronal craniosynostosis. *Plastic and Reconstructive Surgery* 2006;117(3):929–35.

19. Weinberg SM, Naidoo S, Govier DP, Martin RA, Kane AA, Marazita ML. Anthropometric precision and accuracy of digital three-dimensional photogrammetry: comparing the Genex and 3dMD imaging systems with one another and with direct anthropometry. The *Journal of Craniofacial Surgery* 2006;17(3):477–83.

20. Wong JY, Oh AK, Ohta E, Hunt AT, Rogers GF, Mulliken JB, et al. Validity and reliability of craniofacial anthropometric measurement of 3D digital photogrammetric images. *Cleft Palate-Craniofacial Journal* 2008;45(3):232–9.

21. Aldridge K, Boyadjiev SA, Capone GT, DeLeon VB, Richtsmeier JT. Precision and error of three-dimensional phenotypic measures acquired from 3dMD photogrammetric images. *American Journal of Medical Genetics Part A* 2005;138 A(3):247–53.

22. Aynechi N, Larson BE, Leon-Salazar V, Beiraghi S. Accuracy and precision of a 3D anthropometric facial analysis with and without landmark labeling before image acquisition. *Angle Orthodontist* 2011;81(2):245–52.

23. Aviv RI, Rodger E, Hall CM. Craniosynostosis. *Clinical Radiology* 2002;57(2):93–102

24. Lenton KA, Nacamuli RP, Wan DC, Helms JA, Longaker MT. Cranial Suture Biology. *Current Topics in Developmental Biology* 2005;66:287–328.

25. Slater BJ, Lenton KA, Kwan MD, Gupta DM, Wan DC, Longaker MT. Cranial Sutures: A Brief Review. *Plastoc and Reconstructive Surgery* 2008;121(4):170e–178e.

26. Morriss-Kay GM, Wilkie AOM. Growth of the normal skull vault and its alteration in craniosynostosis: insights from human genetics and experimental studies. *Journal of Anatomy* 2005;207(5):637–53.

27. Ghali GE, Woerner JE, Dashow JE. 61 - Surgical Management of Craniosynostosis [Internet]. Third Edit. *Maxillofacial Surgery.* Elsevier Inc.; 2000. 853-869. Available from: http://dx.doi.org/10.1016/B978-0-7020-6056-4.00062-9

28. Kabbani H, Raghuveer T. Craniosynostosis. *American Family Physician* 2004;69(12): 2863-70.

29. Nagaraja S, Anslow P, Winter B. Craniosynostosis. *Clinical Radiology* 2013;68:284–92.

30. Ridgway EB, Weiner HL. Skull deformities. *Pediatric Clinics of North America* 2004;51(2):359–87.

31. Meikle MC. Remodeling the Dentofacial Skeleton : The Biological Basis of Orthodontics and Dentofacial Orthopedics. *Journal of Dental Research* 2007;86(1):12–244.

32. Garza RM, Khosla RK. Nonsyndromic craniosynostosis. *Seminars in Plastic Surgery* 2012;26(2):53–63.

33. Kimonis V, Gold J, Hoffman TL, Panchal J, Boyadjiev SA. Genetics of Craniosynostosis. Seminars in *Pediatric Neurology* 2007;14: 150-161.

34. French LR, Jackson I, Melton LJ. A population-based study of cranisynostosis. *Journal of Clinical Epidemiology* 1990;43(I):69–73.

35. Boulet SL, Rasmussen SA, Honein MA. A population-based study of craniosynostosis in metropolitan Atlanta, 1989-2003. *American Journal of Medical Genetics Part A* 2008;146(8):984–91.

36. Kweldam CF, Van Der Vlugt JJ, Van Der Meulen JJNM. The incidence of craniosynostosis in the Netherlands, 1997-2007. *Journal of Plastic Reconstructive & Aesthetic Surgery* 2011;64(5):583–8.

37. Lee HQ, Hutson JM, Wray AC, Lo PA, Chong DK, Holmes AD, et al. Changing Epidemiology of Nonsyndromic Craniosynostosis and Revisiting the Risk Factors. *The Journal of Craniofacial Surgery* 2012;23(5):1245–51.

38. Cohen Jr M. Craniosynostosis update 1987. *American Journal of Medical Genetics Supplement* 1988;4:99–148.

39. Lajeunie E, Le Merrer M, Bonaiti-Pellie C, Marchac D, Reiner D. Genetic study of scaphocephaly. *American Journal of Medical Genetics* 1996;62(3):282–5.

40. Goodrich JT. Skull base growth in craniosynostosis. *Child's Nervous System* 2005;21(10):871–9.

41. Panchal J, Uttchin V. Management of Craniosynostosis. *Plastic and Reconstructive Surgey*. 2003;111(6):123–32.

42. Boyadjiev SA. Genetic Analysis of non-syndromic craniosynostosis. *Orthodontics & Craniofacial Research* 2007;10:291–306.

43. Lajeunie E, Le Merrer M, Marchac D, Renier D. Syndromal and nonsyndromal primary trigonocephaly: Analysis of a series of 237 patients. *American Journal of Medical Genetics* 1998;75(2):211–5.

44. Van Der Meulen J. Metopic synostosis. *Child's Nervous System* 2012;28(9):1359–67.

45. Weinzweig J, Kirschner RE, Farley A, Reiss P, Hunter J, Whitaker LA, et al. Metopic Synostosis: Defining the Temporal Sequence of Normal Suture Fusion and Differentiating It from Synostosis on the Basis of Computed Tomography Images. *Plastic and Reconstructive Surgery* 2003;112(5):1211–8.

46. Vu HL, Panchal J, Parker EE, Levine NS, Francel P. The timing of physiologic closure of the metopic suture: a review of 159 patients using reconstructed 3D CT scans of the craniofacial region. The *Journal of Craniofacial Surgery* 2001;12(6):527–32.

47. Tubbs RS, Blount JP, Jerry W. Preliminary Observations on the Association between Simple Metopic Ridging in Children without Trigonocephaly and the Chiari I Malformation. *Pediatric Neurosurgery* 2001;35:136–9.

48. Okada H, Gosain AK. Current approaches to management of nonsyndromic craniosynostosis. *Current Opinion in Otolaryngology & Head and Neck Surgery* 2012;20(4):310–7.

49. Rhodes JL, Tye GW, Fearon JA. Craniosynostosis of the lambdoid suture. *Seminars in Plastic Surgery* 2014;28(3):138–43.

50. Shahinian H, Jaekle R, Suh R, Jarrahy R, Aguilar V, Soojian M. Obstetrical factors governing the etiopathogenesis of lambdoid synostosis. *American Journal of Perinatology* 1998;15:281–6

51. Rocco C Di, Paternoster G. Anterior plagiocephaly : epidemiology , clinical findings , diagnosis, and classification . A review. *Child's Nervous System* 2012;28: 1413–22.

52. Lajeunie E, Le Merrer M, Bonaiti-Pellie C, Marchac D, Renier D. Genetic study of nonsyndromic coronal craniosynostosis. *American Journal of Medical Genetics* 1995;55(4):500–4.

53. Wilkie AOM, Byren JC, Hurst JA, Jayamohan J, Johnson D, Knight SJL et al. Prevalence and complications of single gene and chromosomal disorders in craniosynostosis. *Pediatrics* 2010;126(2):391-400.

54. Ko JM. Genetic syndromes associated with craniosynostosis. *Journal of Korean Neurosurgical Society* 2016;59(3):187–91.

55. Zakhary GM, Montes DM, Woerner JE, Notarianni C, Ghali GE. Surgical correction of craniosynostosis. A review of 100 cases. *Journal of Cranio-Maxillo-Facial Surgery* 2014;42(8):1684–91.

56. Persing, John A. M.D.; Jane, John A. M.D., Ph.D.; Shaffrey MMD. Virchow and the Pathogenesis of Craniosynostosis: A Translation of His Original Work. *Plastic & Reconstructive Surgery* 1989; 83(4):738–42.

57. Sharma RK. Craniosynostosis. *Indian Journal of Plastic Surgery* 2013;46(1):18-27.

58. Moss M. The Pathogenesis of Premature Cranial Synostosis in man. *Acta Anatomica (Basel)* 1959;37:351–70.

59. Babler W, Persing J, Persson K, Winn H, JA J, Rodeheaver G. Skull growth after coronal suturectomy, periosteotomy and dural transection. *Journal of Neurosurgery* 1982;56(4):529–35.

60. Passos-Bueno MR, Serti Eaacute AE, Jehee FS, Fanganiello R, Yeh E. Genetics of craniosynostosis: genes, syndromes, mutations and genotype-phenotype correlations. *Frontiers of Oral Biology* 2008;12:107–43.

61. Purushothaman R, Cox TC, Muga AM, Cunningham ML. Facial suture synostosis of newborn Fgfr1(P250R/+) and Fgfr2(S252W/+) mouse models of Pfeiffer and Apert syndromes. *Birth Defects Research Part A Clinical Moecular Teratology* 2011;91(7):1370–80.

62. Liu YH, Tang Z, Kundu RK, Wu L, Luo W, Zhu D, et al. Msx2 Gene Dosage Influences the Number of Proliferative Osteogenic Cells in Growth Centers of the Developing Murine Skull : A Possible Mechanism for MSX2 -Mediated Craniosynostosis in Humans. *Developmental Biology* 1999;274:260–74.

63. Alderman B, Lammer E, Joshua S, Cordero J, Ouimette D, Wilson M, et al. An epidemiologic study of craniosynostosis: risk indicators for the occurrence of craniosynostosis in Colorado. *American Journal of epidemiology* 1988;128(2):431–8.

64. Renier D, Sainte-Rose C, Marchac D, Hirsch JF. Intracranial pressure in craniostenosis. *Journal of Neurosurgery* 1982;57(3):370–7.

65. Bristol RE, Lekovic GP, Rekate HL. The effects of craniosynostosis on the brain with respect to intracranial pressure. *Seminars in Pediatrric Neurology* 2004;11(4):262–7.

66. Cornelissen MJ, Vlugt JJ Van Der, Willemsen JCN, Adrichem LNA Van, Mathijssen IMJ, Der Meulen JJNM Van. Unilateral versus bilateral correction of unicoronal synostosis : An analysis of long-term results. *Journal of Plastic, Reconstructive & Aesthetic Surgery* 2013;66(5):704–11.

67. Heuzé Y, Martínez-Abadías N, Stella JM, Senders CW, Boyadjiev SA, Lo LJ, et al. Unilateral and bilateral expression of a quantitative trait: Asymmetry and symmetry in coronal

craniosynostosis. *Journal of Experimental Zoology. Part B, Molecular and Developmental Evolution* 2012;318(2):109–22.

68. Johnson D, Wilkie AOM. Craniosynostosis. *European Journal of Human Genetics* 2011;19(4):369–76.

69. Seto ML, Hing AV, Chang J, Hu M, Kapp-Simon KA, Patel PK, et al. Isolated saggital and coronal craniosynostosis associated with TWIST box mutations. *American Journal of Medical Genetics. Part A* 2007;143A(7):678–86.

70. Kallen K. Maternal smoking and craniosynostosis. *Teratology* 1999;60(3):146–50.

71. Engel M, Castrillon-Oberndorfer G, Hoffmann J, Mühling J, Seeberger R, Freudlsperger C. Long-term results in nonsyndromatic unilateral coronal synostosis treated with fronto-orbital advancement. *Journal of Cranio-Maxillofacial Surgery* 2013;41(8):747–54.

72. Beckett JS, Persing JA, Steinbacher DM. Zygomatic dysmorphology in unicoronal synostosis. *Journal of Plastic, Reconstructive & Aesthetic Surgery* 2013;66(8):1096–1102.

73. Kane AA, Kim Y, Eaton A, Pilgram TK, Marsh JL, Zonneveld F, et al. Quantification of Osseous Facial Dysmorphology in Untreated Unilateral Coronal Synostosis. *Plastic and Reconstuctive Surgery* 2000;106:251–8.

74. Fishman RS. Hereditary premature closure of a coronal suture in the Abraham Lincoln family. *Gene* 2013;528(1):2–6.

75. Arvystas MG, Antonellis P, Justin AF. Progressive facial asymmetry as a result of early closure of the left coronal suture. *American Journal of Orthodontics* 1985;87(3):240–6.

76. Farkas LG, Katic MJ, Forrest CR. Anthropometric proportion indices in the craniofacial regions of 73 patients with forms of isolated coronal synostosis. *Annals of Plastic Surgery* 2005;55(5):495–9.

77. Snyder H, Ph D, Pope AW, Ph D. Psychosocial Adjustment in Children and Adolescents With a Craniofacial Anomaly : Diagnosis-Specific Patterns. *Cleft Palate Craniofacial Journal* 2010;47(3):264–72.

78. Khechoyan DY, Saber NR, Burge J, Fattah A, Drake J, Forrest CR, et al. Surgical outcomes in craniosynostosis reconstruction : The use of prefabricated templates in cranial vault remodelling. *Journal of Plastic, Reconstructive & Aesthetic Surgery* 2014;67(1):9–16.

79. Mesa JM, Fang F, Muraszko KM, Buchman SR. Reconstruction of unicoronal plagiocephaly with a hypercorrection surgical technique. *Neurosurgical Focus* 2011;31(2):1-8.

80. Selber JC, Brooks C, Kurichi JE, Temmen T, Sonnad SS, Whitaker LA. Long-Term Results following Fronto-Orbital Reconstruction in Nonsyndromic Unicoronal Synostosis. *Plastic and Reconstructive Surgery* 2008;121(5):251e–260e.

81. Wall SA, Goldin JH, Hockley AD, Wake MJC, Poole MD, Briggs M. Fronto-orbital re-operation in craniosynostosis. *British Journal of Plastic Surgery* 1994;47:180-184.

82. Whitaker LA, Bartlett SP, Schut L, Bruce D. Craniosynostosis: an analysis of the timing, treatment, and complications in 164 consecutive patients. *Plastic and Reconstructive Surgery* 1987;80(2):195–206.

83. Raposa-Amaral CE, Denadai R, Ghizoni E, Buzzo CL, Raposa-Amaral CA. Facial Changes After Early Treatment of Unilateral Coronal Synostosis Question the Necessity of Primary Nasal Osteotomy. *Journal of Craniofacial Surgery* 2015;26(1):141–6.

84. Severt TR, Proffit WR. The prevalence of facial asymmetry in the dentofacial deformities population at the University of North Carolina. *International Journal of Adult Orthodontics and Orthognathic Surgery*. 1997;12(3):171–6.

85. Collett BR, Gray KE, Kapp-simon KA, Birgfeld C, Cunningham M, Rudo-stern J, et al. Laypersons ' Ratings of Appearance in Children With and Without Single-Suture Craniosynostosis. *The Journal of Craniofacial Surgery* 2013;24(4):1331–5.

86. Bishara SE, Burkey PS, Kharouf JG. Dental and facial asymmetries: a review. *The Angle Orthodontist* 1994;64(2):89–98.

87. Farkas LG, Cheung G. Facial asymmetry in healthy North American Caucasians. An anthropometrical study. *The Angle Orthodontist* 1981;51:70–7.

88. Ferrario VF, Sforza C, Miani Jr. A, Serrao G. A three-dimensional evaluation of human facial asymmetry. *Journal of Anatomy* 1995;186(Pt 1):103–10.

89. Vig PS, Hewitt AB. Asymmetry of the human facial skeleton. *The Angle Orthodontist* 1975;45(2):125–9.

90. Cohen JA, Zaidel DW. The Face , Beauty, And Symmetry: Perceiving Asymmetry In Beautiful Faces. *The International Journal of neuroscience* 2005;115:1165–73.

91. Thiesen G, Gribel BF, Freitas MPM. Facial asymmetry: a current review. *Dental Press Journal of Orthodontics* 2015;20(6):110–25.

92. Fischer B. Asymmetries of the Dentofacial Complex. *The Angle Orthodontist* 1954;24:179–92.

93. Peck S, Peck L, Kataja M. Skeletal asymmetry in esthetically pleasing faces. *The Angle Orthodontist* 1991;61(1):43–8.

94. Ferrario VF, Sforza C, Miani A. Craniofacial morphometry by photographic evaluations. *American Journal of Orthodontics and Dentofacial Orthopedics* 1993;103:327-37.

95. Blackburn K, Schirillo J. Emotive hemispheric differences measured in real-life portraits using pupil diameter and subjective aesthetic preferences. *Experimental Brain Research* 2012;219:447–55.

96. Alqattan M, Djordjevic J, Zhurov AI, Richmond S. Comparison between landmark and surface-based three-dimensional analyses of facial asymmetry in adults. *European Journal of Orthodontics 2015*;37(1):1–12.

97. Lu KH. Harmonic Analysis of the Human Face. *Biometrics* 1965;21(2):491–505.

98. Farkas L. Anthropometry of the Head and Face. 2nd edition. New York:Raven Press; 1994. 71-77 p.

99. Stefanovic N, El H, Chenin DL, Glisic B, Palomo JM. Three-dimensional pharyngeal airway changes in orthodontic patients treated with and without extractions. *Orthodontics and Craniofacial Research* 2013;16(2):87–96.

100. Wang TT, Wessels L, Hussain G, Merten S. Discriminative Thresholds in Facial Asymmetry : A Review of the Literature. *Aesthetic Surgery Journal* 2017;37(4):375–85.

101. Hohman MH, Kim SW, Heller ES, Frigerio A, Heaton JT, Hadlock TA. Determining the threshold for asymmetry detection in facial expressions. *Laryngoscope* 2014;124(4):860–5.

102. Meyer-marcotty P, Stellzig-eisenhauer A, Bareis U, Hartmann J, Kochel J. Three-dimensional perception of facial asymmetry. *European Journal of Orthodontics* 2011;33:647–53.

103. Kwak KH, Kim Y, Nam HJ, Kim SS, Park SB, Son WS. Differences Among Deviations , Genders, and Observers in the Perception of Eye and Nose Asymmetry. *Journal of Oral and Maxillofacial Surgery* 2015;73(8):1606–14.

104. Chu EA, Farrag TY, Ishii LE, Byrne PJ. Threshold of Visual Perception of Facial Asymmetry in a Facial Paralysis Model. *Archives of Facial Plastic Surgery* 2011;13(1):14–19.

105. Hajeer MY, Ayoub AF, Millett DT. Three-dimensional assessment of facial soft-tissue asymmetry before and after orthognathic surgery. *British Journal of Oral and Maxillofacial Surgery* 2004;42(5):396–404

106. Matteson SR. 3D-CT evaluation of facial asymmetry. *Oral Surgery, Oral Medicine, Oral Pathology, Oral Radiology, and Endodontology* 2005;99(2):212–20.

107. Farkas LG, Bryson W, Tech B, Klotz J. Is photogrammetry of the face reliable? *Plastic and reconstructive surgery* 1980;66(3): 346–55.

108. Karatas OH, Toy E. Three-dimensional imaging techniques: A literature review. *European Journal of Dentistry* 2014;8(1):132–40.

109. Scarfe WC, Farman AG, Sukovic P. Clinical Applications of Cone-Beam Computed. *Journal (Canadian Dental Association)* 2006;72(1):75–80.

110. Littlefield TR, Kelly KM, Cherney JC, Beals SP, Pomatto JK, et al. Technical Strategies, Development of a new three-dimensional cranial imaging system. *The Journal of Craniofacial Surgery* 2004;15(1):175–81.

111. Kusnoto B, Evans CA. Reliability of a 3D surface laser scanner for orthodontic applications. *American Journal of Orthodontics and Dentofacial* Orthopedics 2002;122(4):342–8.

112. Kau CH, Cronin AJ, Richmond S. A three-dimensional evaluation of postoperative swelling following orthognathic surgery at 6 months. *Plastic and Reconstructive Surgery* 2007;119(7):2192–9.

113. Papadopoulos MA, Christou PK, Athanasios E, Boettcher P, Zeilhofer HF, Sader R, et al. Three-dimensional craniofacial reconstruction imaging. *Oral Surgery Oral Medicine Oral Pathology Oral Radiology* 2002;93(4):382–93.

114. Kau CH, Richmond S, Zhurov AI, Knox J, Chestnutt I, Hartles F, et al. Reliability of measuring facial morpholgy with a 3-dimensional laser scanning system. *American Journal of Orthodontics and Dentofacial Orthopedics* 2005;128:424–30.

115. Hajeer M, Ayoub A, Millett D, Bock M, Siebert JP. Three-dimensional imaging in orthognathic surgery: the clinical application of a new method. *The International Journal of Adult Orthodontics and Orthognath Surgery* 2002;17(4):318–30.

116. Tzou CHJ, Artner NM, Pona I, Hold A, Placheta E, Kropatsch WG, et al. Comparison of three-dimensional surface-imaging systems. *Journal of Plastic, Reconstructive & Aesthetic Surgery* 2014;67(4):489–97.

117. Nguyen C, Nissanov J, Öztürk C, Nuveen M, Tuncay O. Three-dimensional imaging of the craniofacial complex. *Clinical Orthodontics and Research* 2000;3:46–50.

118. Srivastava D, Singh H, Mishra S, Sharma P, Kapoor P, Chandra L. Facial asymmetry revisited: Part I- diagnosis and treatment planning. *Journal of Oral Biology and Craniofacial Research* 2018; 8(1):7-14.

119. Lane C, Harrell Jr W. Completing the 3-dimensional picture. *American Journal of Orthodontics*

and Dentofacial Orthopedics 2008;133(4):612–20.

120. De Menezes M, Rosati R, Ferrario VF, Sforza C. Accuracy and reproducibility of a 3-dimensional stereophotogrammetric imaging system. *Journal of Oral and Maxillofacial Surgery* 2010;68(9):2129–35.

121. 3dMD [Internet]. Atlanta: [updated 2015; cited 2017 Nov 1]. Available from: www.3dmd.com.

122. Plooij JM, Swennen GRJ, Rangel FA, Maal TJJ, Schutyser FAC, Bronkhorst EM, et al. Evaluation of reproducibility and reliability of 3D soft tissue analysis using 3D stereophotogrammetry. *International Journal of Oral and Maxillofacial Surgery* 2009;38(3):267–73.

123. Schaaf H, Pons-Kuehnemann J, Malik CY, Streckbein P, Preuss M, Howaldt HP, et al. Accuracy of three-dimensional photogrammetric images in non-synostotic cranial deformities. *Neuropediatrics* 2010;41(1):24–9.

124. Ort R, Metzler P, Kruse AL, Matthews F, Zemann W, Grätz KW, et al. The Reliability of a Three-Dimensional Photo System- (3dMDface-) Based Evaluation of the Face in Cleft Lip Infants. *Plastic Surgery International* 2012;2012:1–8.

125. Huang CS, Liu XQ, Chen YR. Facial asymmetry index in normal young adults. *Orthodontics and Craniofacial Research* 2012;16(2):97-104.

126. Djordjevic J, Pirttiniemi P, Harila V, Heikkinen T, Toma AM, Zhurov AI, et al. Three-dimensional longitudinal assessment of facial symmetry in adolescents. *European Journal of Orthodontics* 2013;35(2):143–51.

127. Darby LJ, Millett DT, Kelly N, McIntyre GT, Cronin MS. The effect of smiling on facial asymmetry in adults: a 3D evaluation. *Australian Orthodontic Journal* 2015;31:132–7.

128. Bugaighis I, Mattick CR, Tiddeman B, Hobson R. 3D asymmetry of operated children with oral clefts. *Orthodontics & Craniofacial Research* 2015;31(2):132–7.

129. Miller SF, Weinberg SM, Nidey NL, Defay DK, Maraazitaa ML, Wehby GL, et al. Exploratory genotype-phenotype correlations of facial form nd asymmetry in unafected relatives of children with non-syndromic cleft lip and/or palate. *Journal of Anatomy* 2014;224:688–709.

130. Carty O, Flannigan N, Burnside G, Dominguez-Gonzalez S. Study on Facial Asymmetry in Children Under 16 years from the North West of England using Three-dimensional Images (3dMD). *Unpublished thesis type* Liverpool Univ, Liverpool. 2018.

131. Bland JM, Altman DG. Statistical methods for assessing agreement between two methods of clinnical measurement. *International Journal of Nursing Studies* 2010;47(8):931–6.

132. Mccluskey A, Lalkhen AG. Statistics I : data and correlations. *Continuing Education in Anaesthesia, Critical Care and Pain* 2007;7(3):95–9.

133. Mccluskey A, Lalkhen AG. Statistics II : Central tendency and spread of data. *Continuing Education in Anaesthesia, Critical Care and Pain* 2007;7(4):127–30.

Appendix 1: Ethics and Regulatory Approval

Alder Hey Children's NHS Foundation Trust

Alder Hey Children's NHS Foundation Trust
Clinical Research Business Unit
2nd Floor
INSTITUTE IN THE PARK
Eaton Road
Liverpool
L12 2AP

Tel: 0151 252 5570

Dr Susana Dominguez-Gonzalez

Consultant Orthodontist

Alder Hey Children's NHS Foundation Trust

Date: 5th December 2017

Dear Dr Dominguez-Gonzalez,

Re: Headspace and facial symmetry projects

Thank you for discussing with me your Headspace and facial symmetry projects.

I write to confirm in my capacity as Director of Research that Alder Hey that both your projects do not
Require REC or HRA approval.

I wish you every success with your studies.

Best wishes.

Yours sincerely

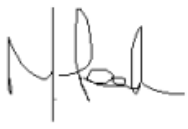

Professor Matthew Peak
Director of Research for Alder Hey

Appendix 2: Panel assessment form

Pt number	Initials	Image number	Date	Include=Y Exclude=N	Why exclude?

Appendix 3: Bland and Altman Plots Intra-observer reliability

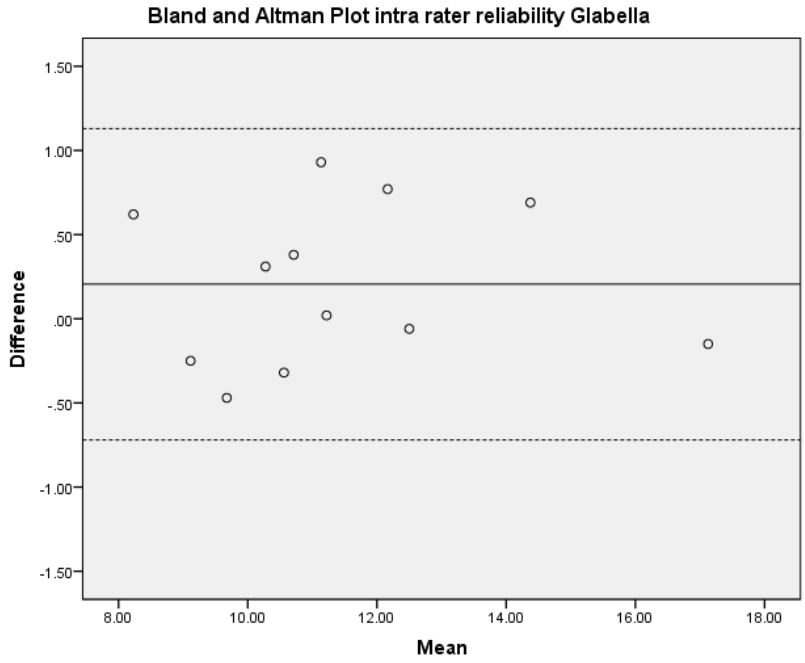

Bland and Altman Plot for EB intra-observer agreement for Glabella - Nasion; mean difference 0.21mm, 95% Limits of agreement = -0.72 to 1.13 mm

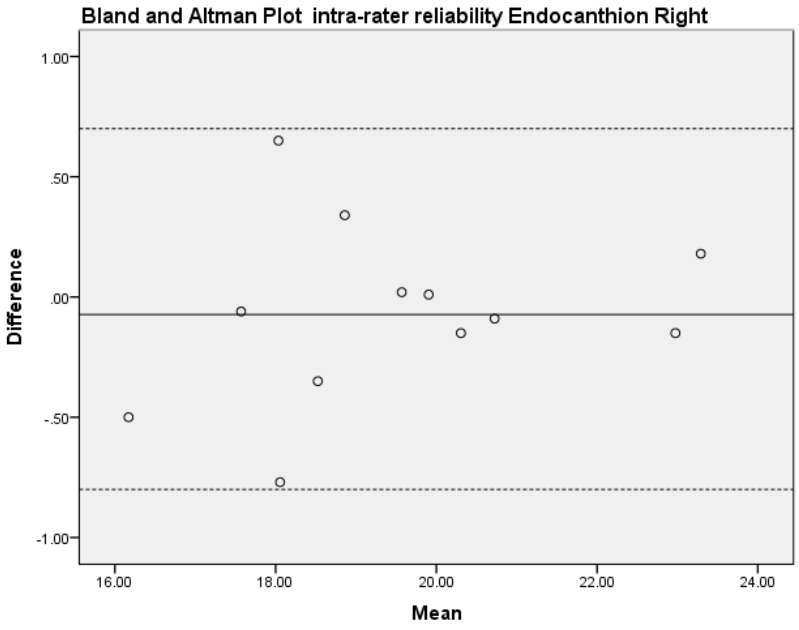

Bland and Altman Plot for EB intra-observer agreement for Endocanthion Right - Nasion; mean difference -0.07mm, 95% Limits of agreement = -0.80 to 0.66mm

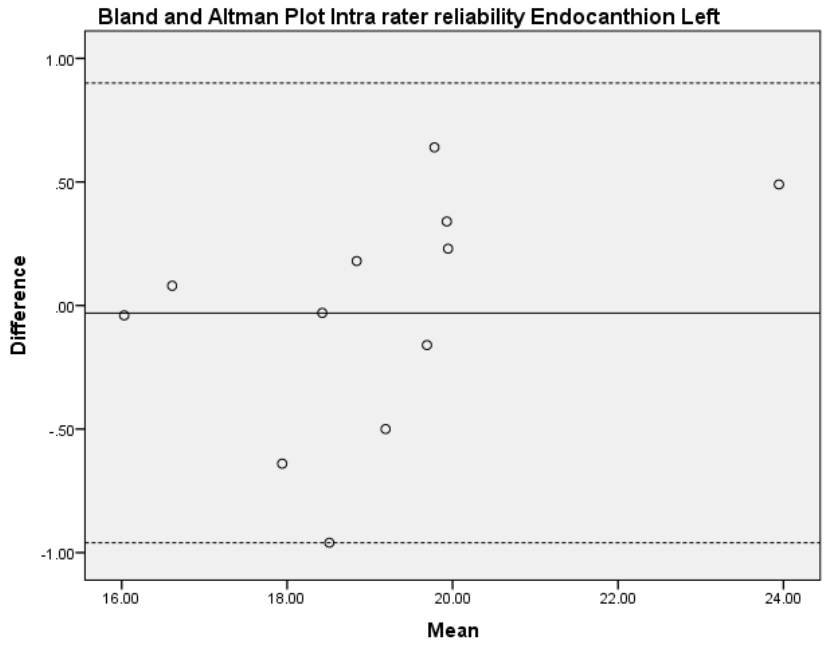

Bland and Altman Plot for EB intra-observer agreement for Endocanthion Left - Nasion; mean difference -0.03mm, 95% Limits of agreement = -0.96 to 0.90mm

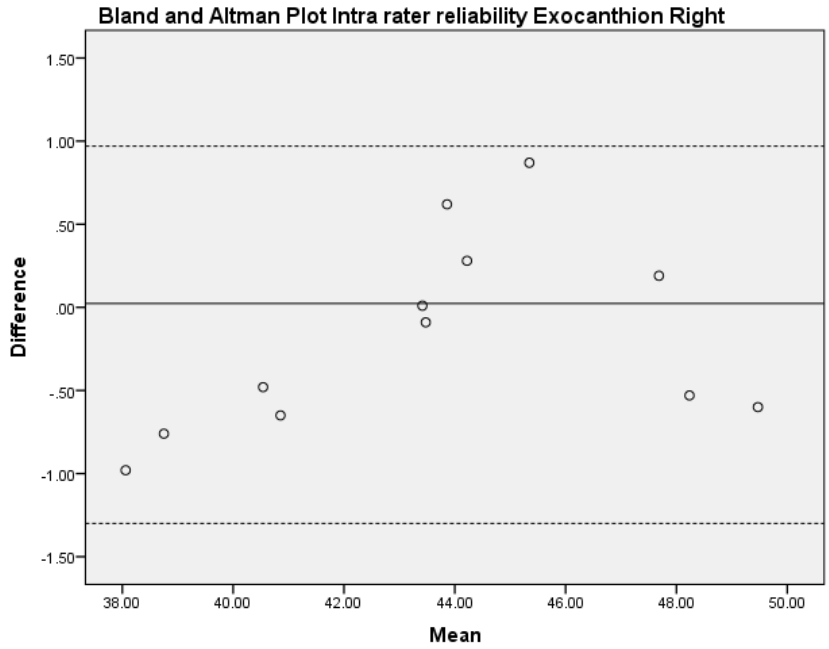

Bland and Altman Plot for EB intra-observer agreement for Exocanthion Right - Nasion; mean difference 0.21mm, 95% Limits of agreement = -1.32 to 0.96mm

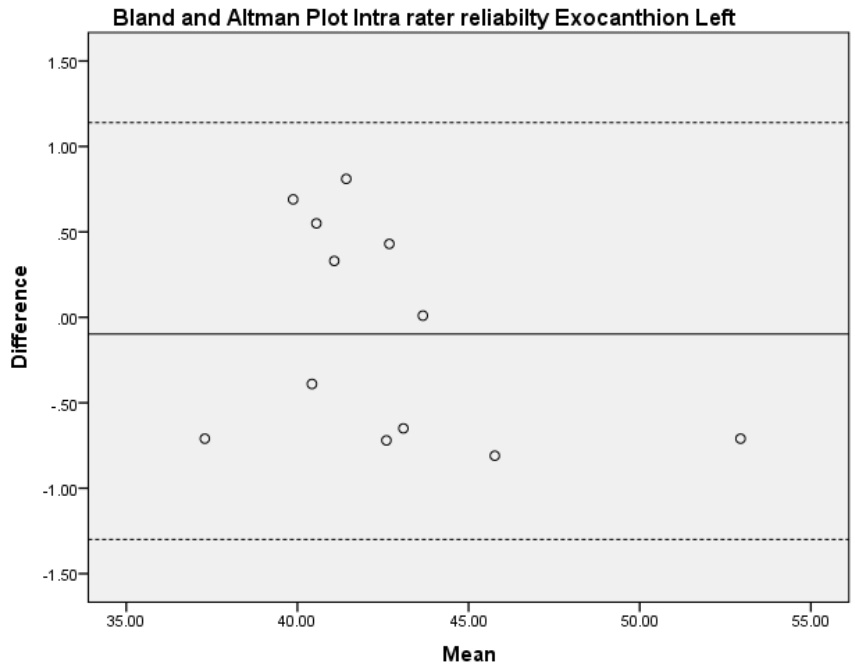

Bland and Altman Plot for EB intra-observer agreement for Exocanthion Left - Nasion; mean difference -0.10mm, 95% Limits of agreement = -1.33 to 1.14mm

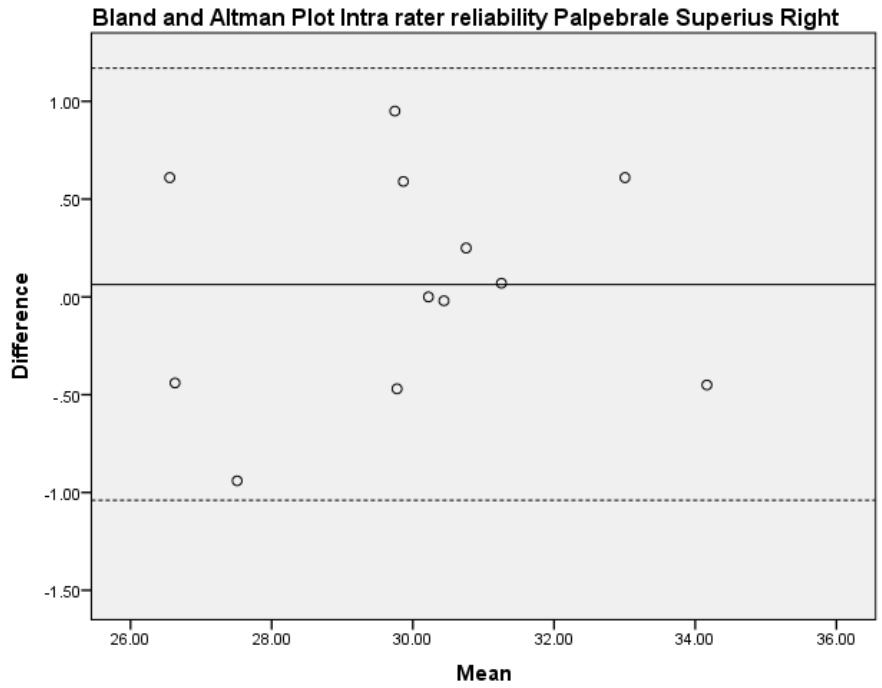

Bland and Altman Plot for EB intra-observer agreement for Palpebrale Superius Right- Nasion; mean difference 0.06mm, 95% Limits of agreement = -1.04 to 1.17mm

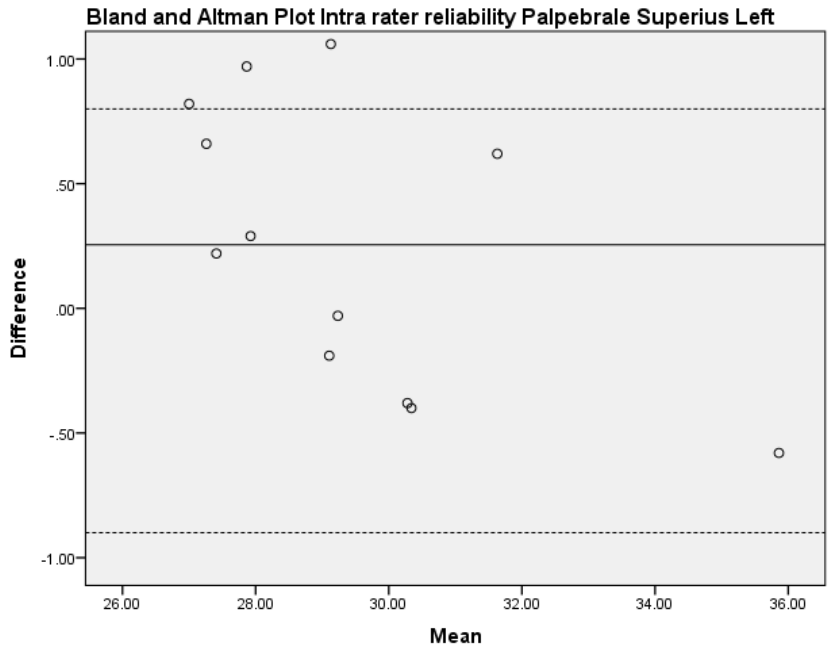

Bland and Altman Plot for EB intra-observer agreement for Palpebrale Superius Left- Nasion; mean difference 0.26, 95% Limits of agreement = -0.86mm to 0.80mm

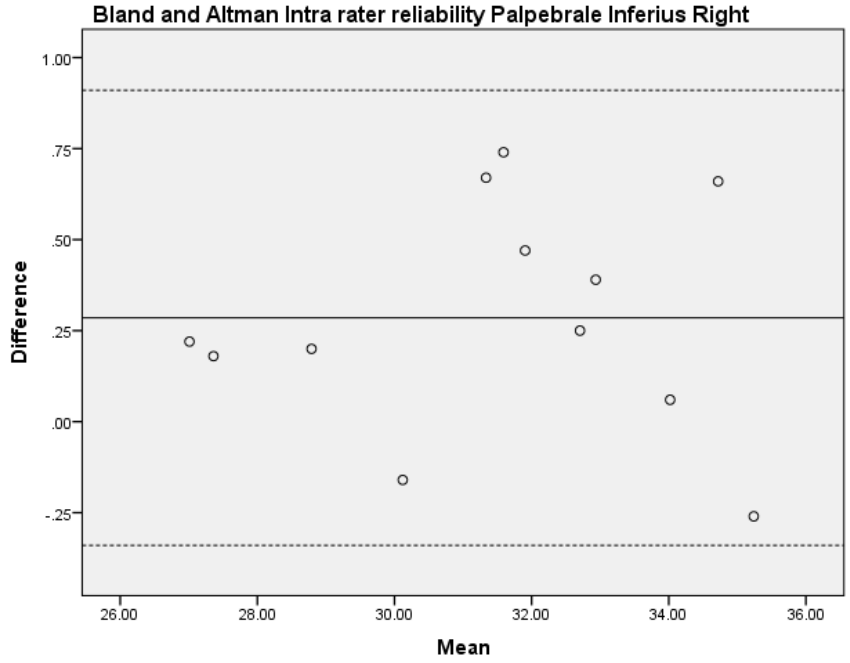

Bland and Altman Plot for EB intra-observer agreement for Palpebrale Inferius Right - Nasion; mean difference 0.30, 95% Limits of agreement = -0.34mm to 0.91mm

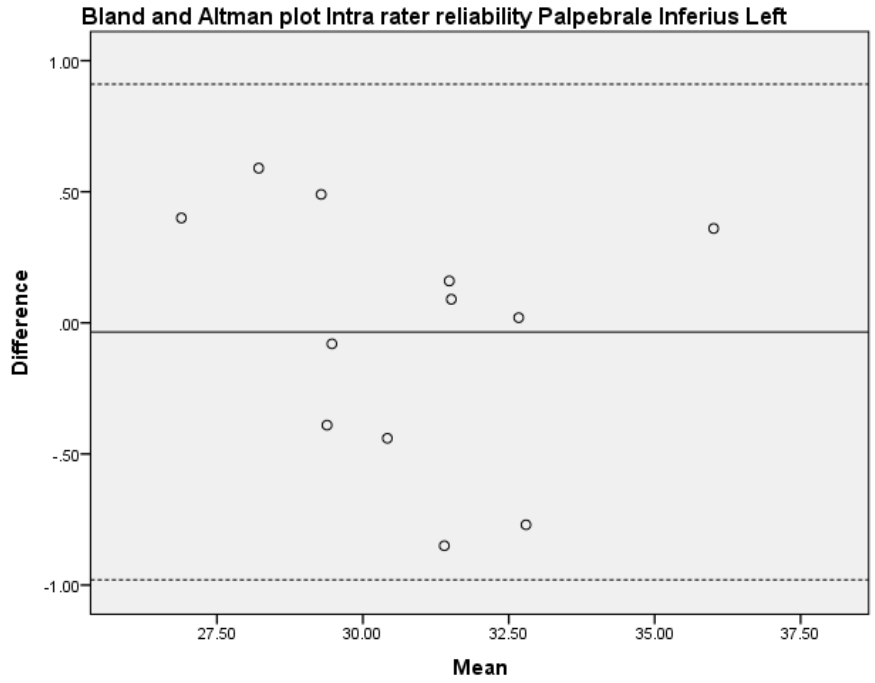

Bland and Altman Plot for EB intra-observer agreement for Palpebrale Inferius Left - Nasion; mean difference -0.04mm, 95% Limits of agreement = -0.98 to 0.91mm

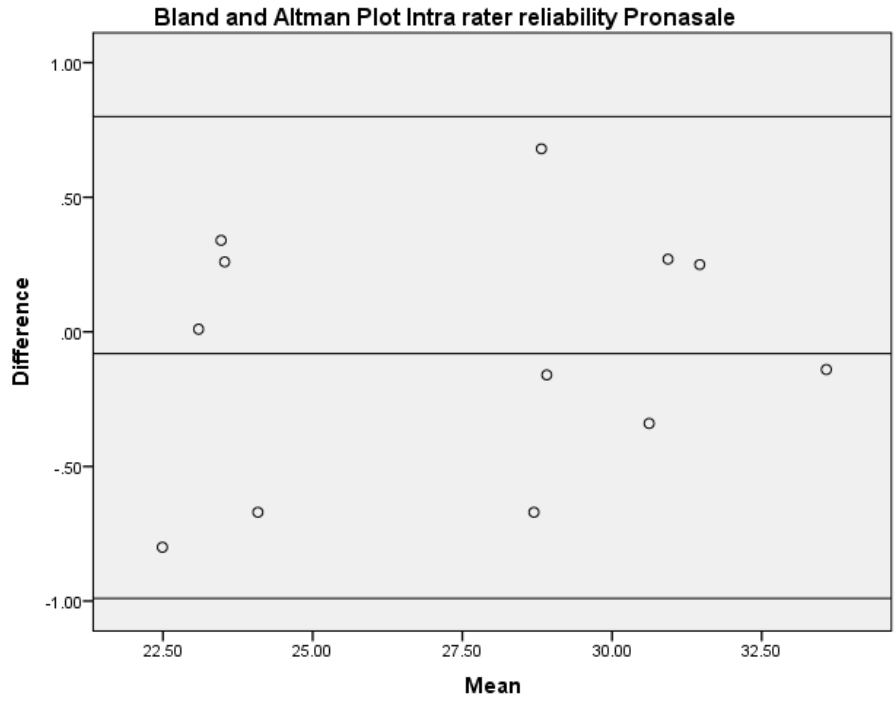

Bland and Altman Plot for EB intra-observer agreement for Pronasale - Nasion; mean difference -0.08mm, 95% Limits of agreement = -0.99 to 0.83mm

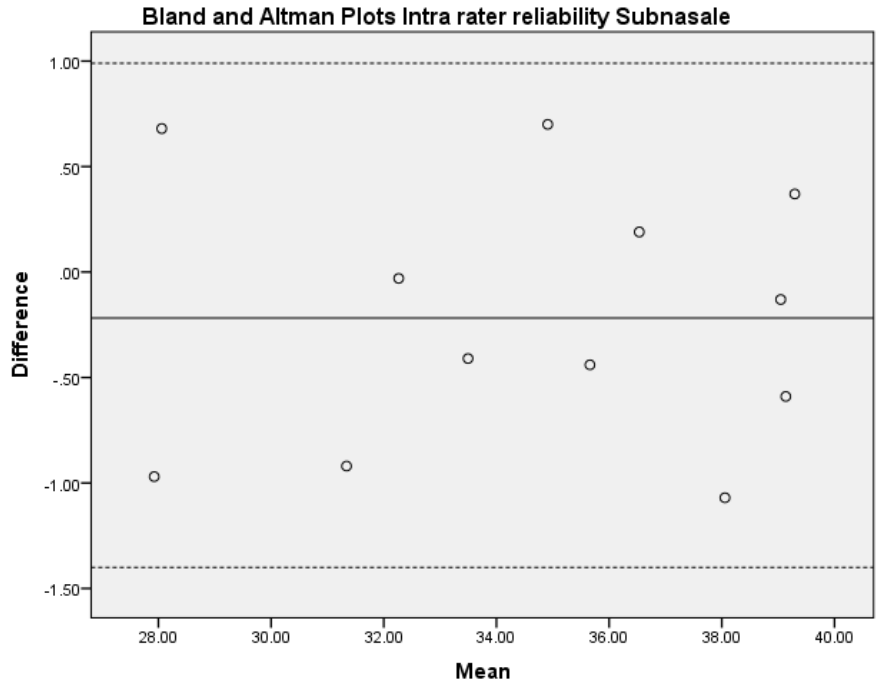

Bland and Altman Plot for EB intra-observer agreement for Subnasale - Nasion; mean difference -0.22mm, 95% Limits of agreement = -1.43 to 0.99mm

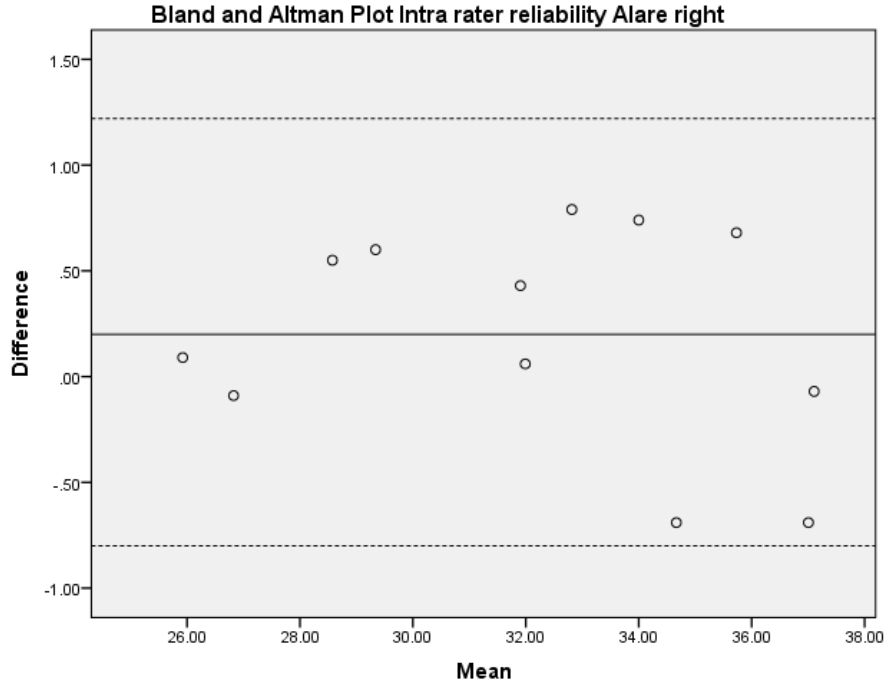

Bland and Altman Plot for EB intra-observer agreement for Alare Right - Nasion; mean difference 0.20mm, 95% Limits of agreement = -0.82 to 1.22mm

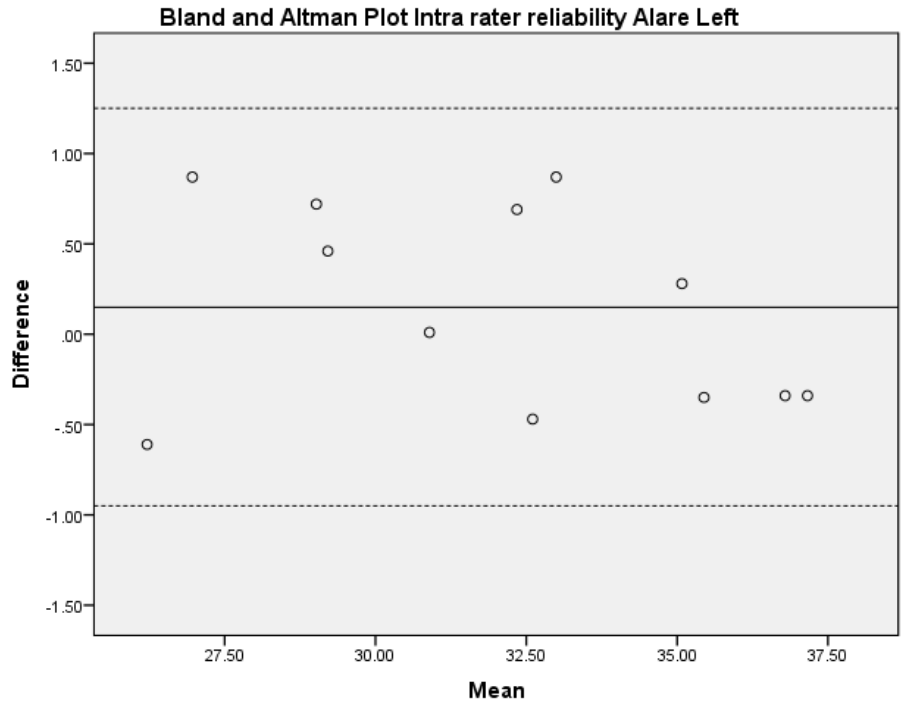

Bland and Altman Plot for EB intra-observer agreement for Alare Left - Nasion; mean difference 0.15mm, 95% Limits of agreement = -0.95 to 1.25mm

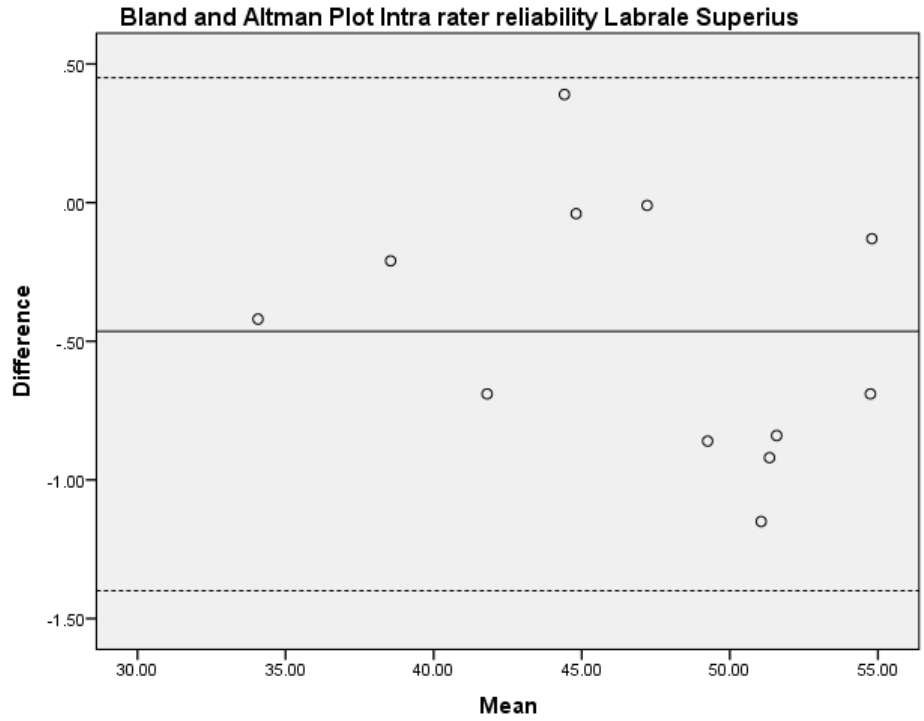

Bland and Altman Plot for EB intra-observer agreement for Labrale Superius - Nasion; mean difference -0.46mm, 95% Limits of agreement = -1.37 to 0.45mm

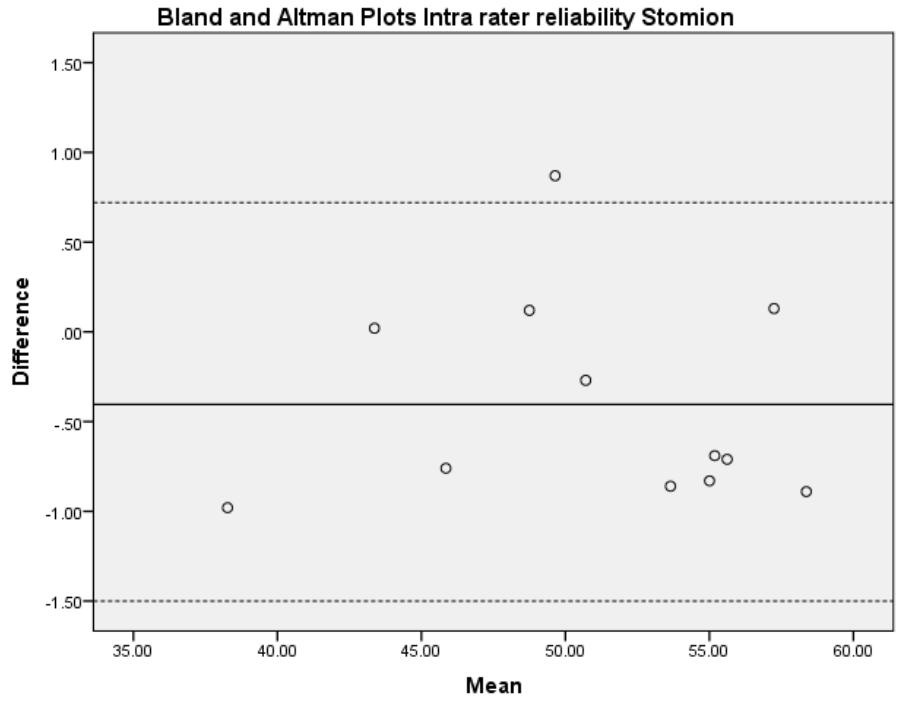

Bland and Altman Plot for EB intra-observer agreement for Stomion - Nasion; mean difference -0.40mm, 95% Limits of agreement = -1.53 to 0.72mm

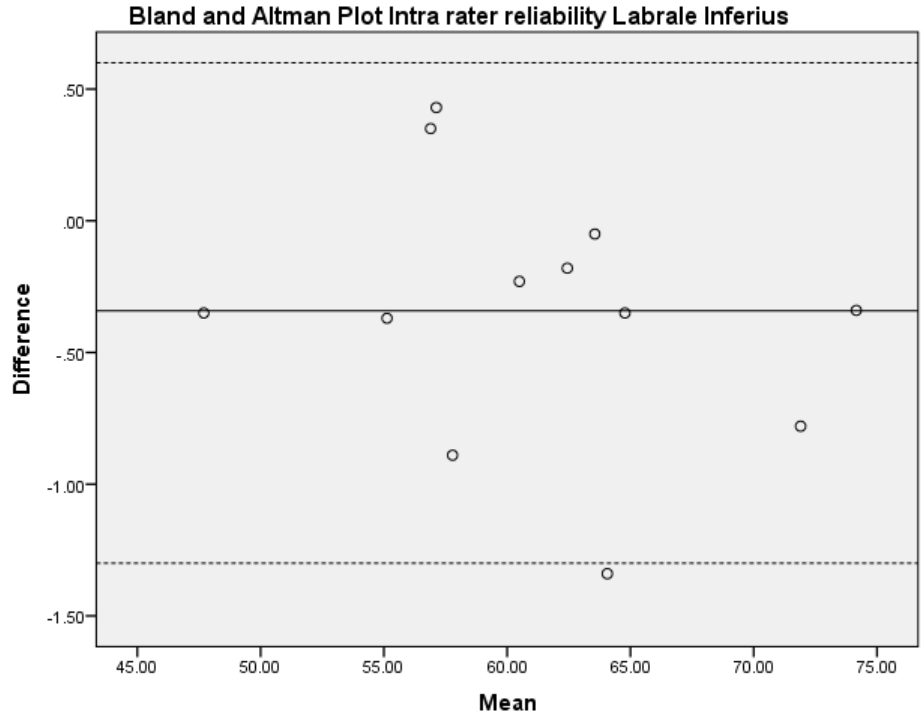

Bland and Altman Plot for EB intra-observer agreement for Labrale Inferius - Nasion; mean difference -0.34mm, 95% Limits of agreement = -1.31 to 0.63mm

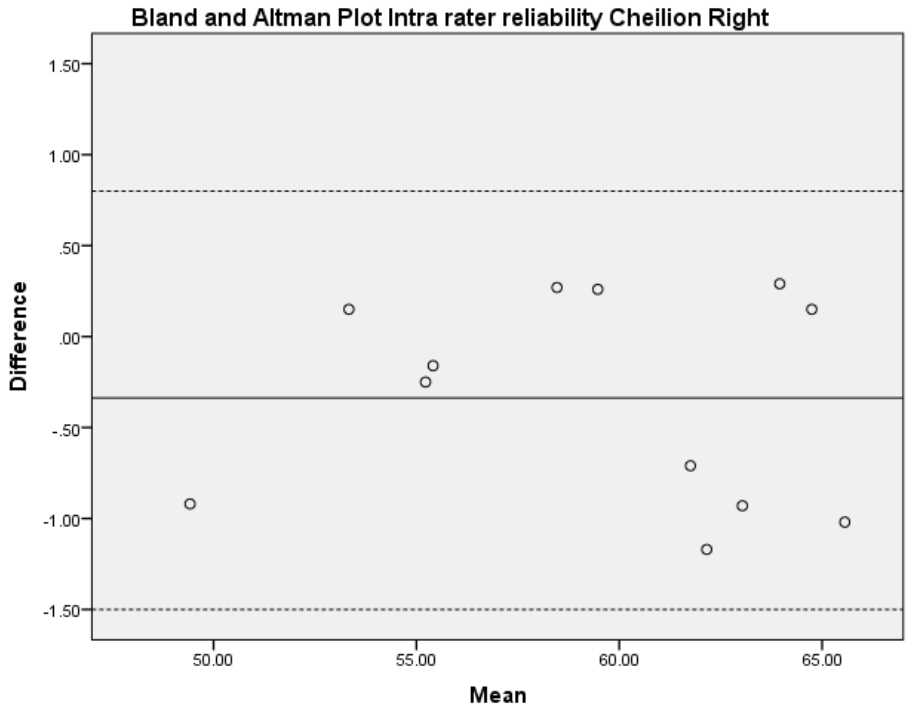

Bland and Altman Plot for EB intra-observer agreement for Cheilion Right - Nasion; mean difference -0.34mm, 95% Limits of agreement= -1.46 to 0.79mm

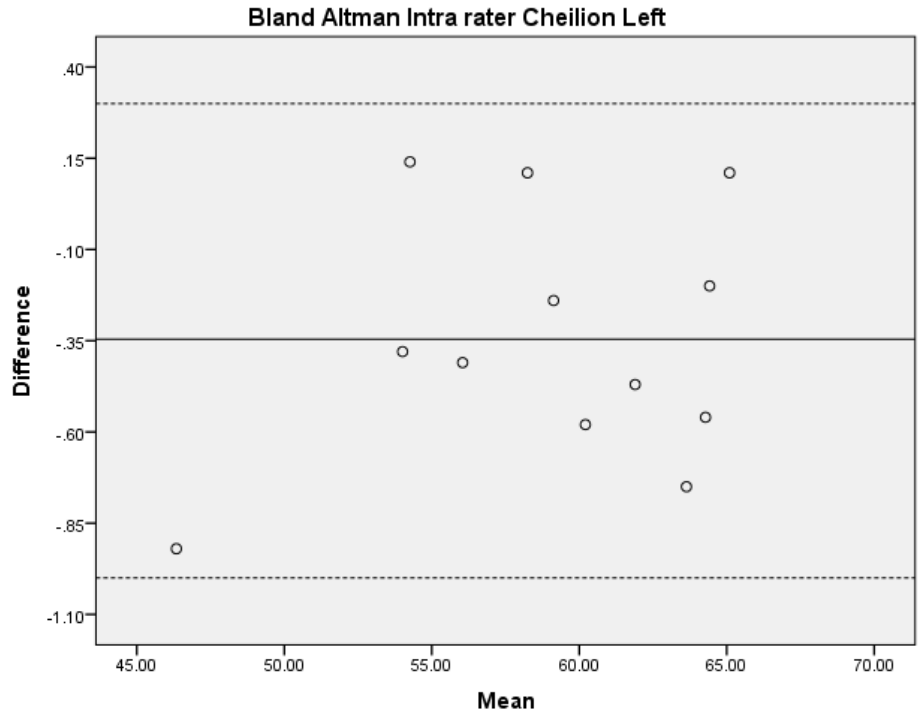

Bland and Altman Plot for EB intra-observer agreement for Cheilion Left - Nasion; mean difference -0.35mm, 95% Limits of agreement= -1.02 to 0.33mm

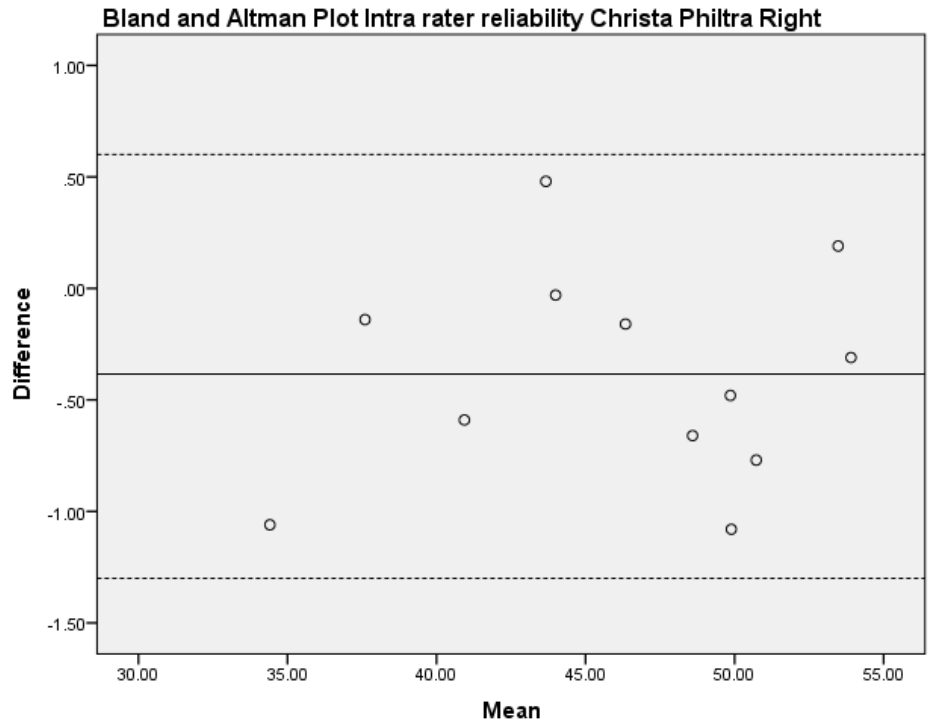

Bland and Altman Plot for EB intra-observer agreement for Christa Philtra Right - Nasion; mean difference -0.38mm, 95% Limits of agreement = -1.33 to 0.56mm

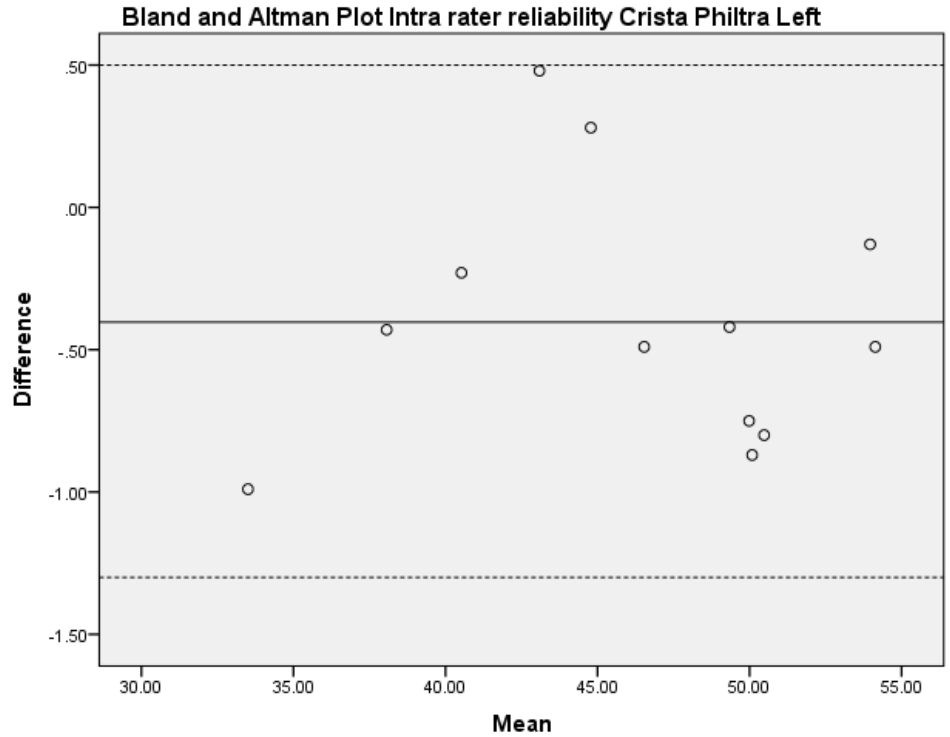

Bland and Altman Plot for EB intra-observer agreement for Christa Philtra Left - Nasion; mean difference -0.40mm, 95% Limits of agreement= -1.28 to 0.47mm

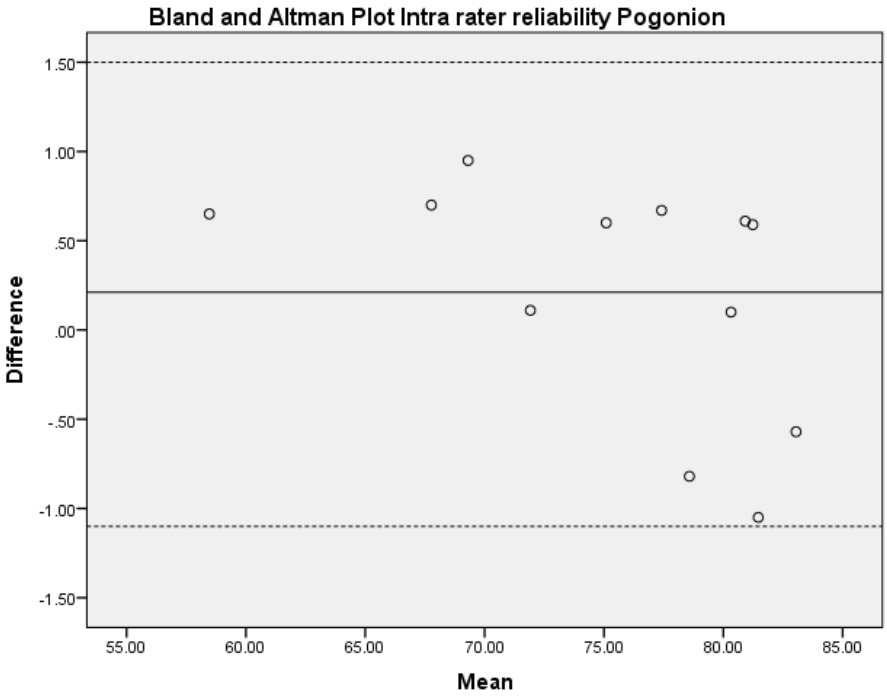

Bland and Altman Plot for EB intra-observer agreement for Pogonion - Nasion; mean difference 0.21mm, 95% Limits of agreement = -1.10 to 1.52mm

Appendix 4: Bland and Altman Plots Inter-observer reliability

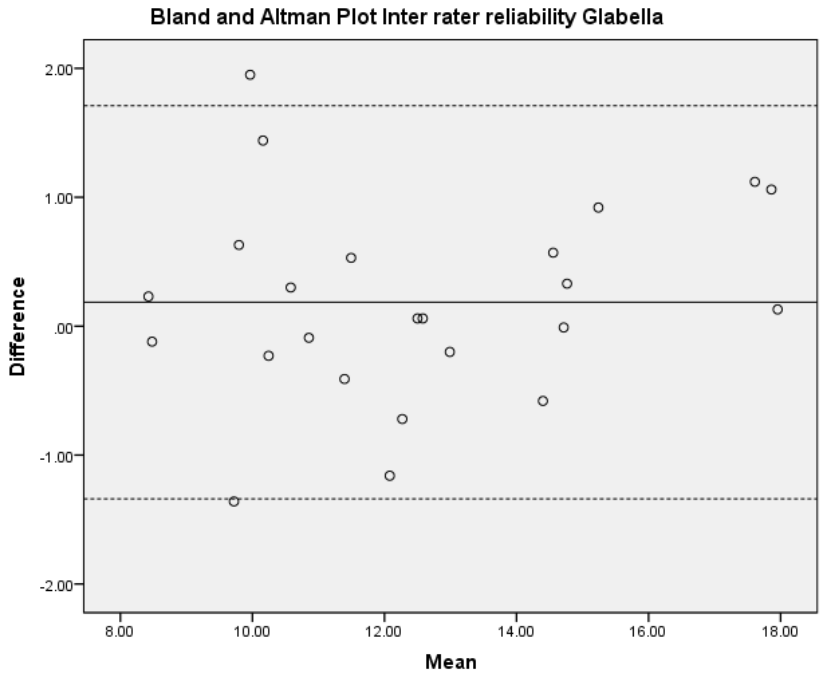

Bland and Altman Plot for inter-observer agreement for Glabella - Nasion; mean difference 0.19mm, 95% Limits of agreement = -1.34 to 1.71mm

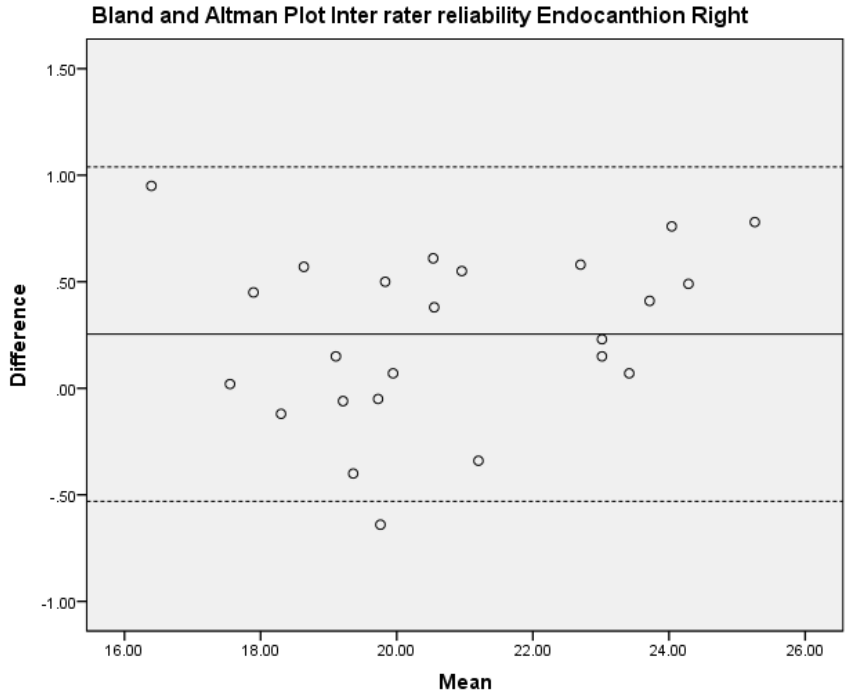

Bland and Altman Plot for inter-observer agreement for Endocanthion Right - Nasion; mean difference 0.25mm, 95% Limits of agreement = -0.53 to 1.04mm

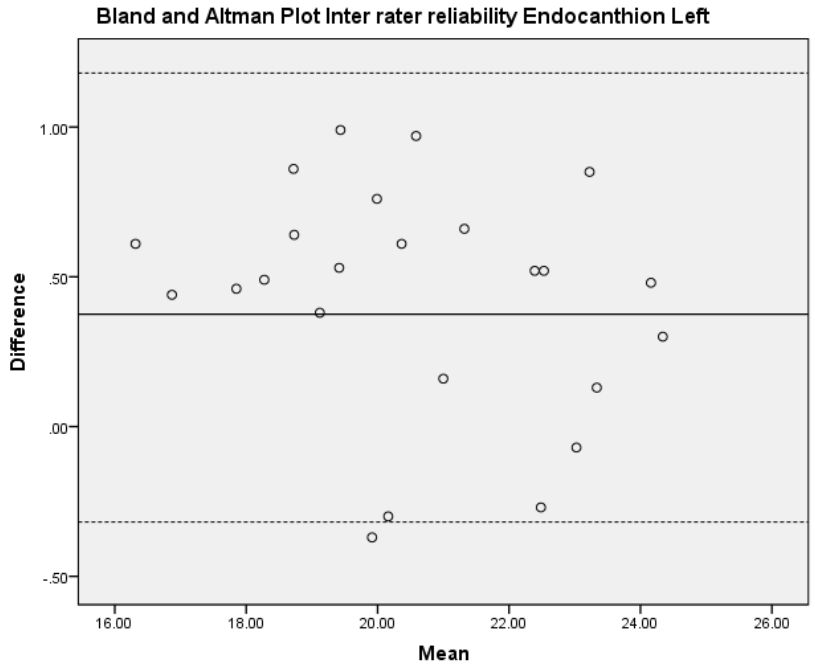

Bland and Altman Plot for inter-observer agreement for Endocanthion Left - Nasion; mean difference 0.43mm, 95% Limits of agreement = -0.32 to 1.18mm

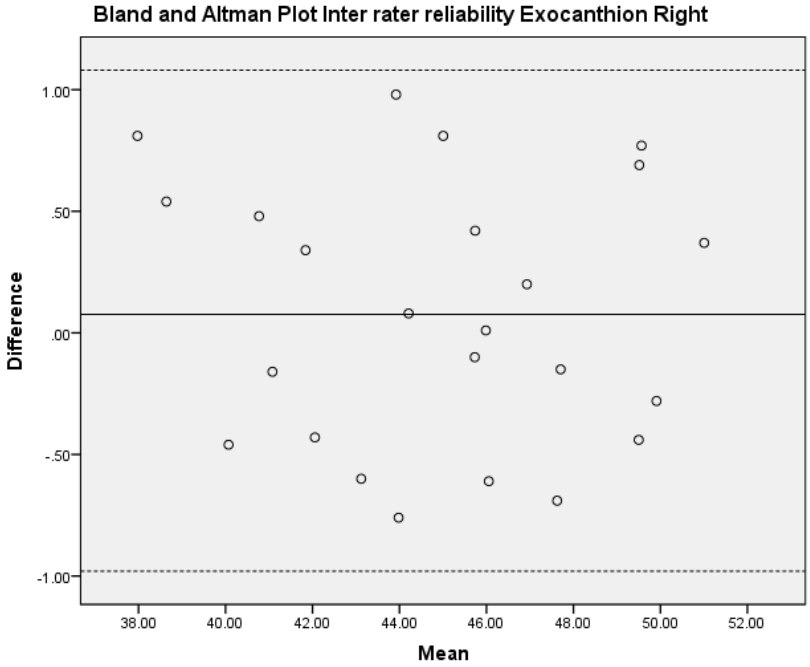

Bland and Altman Plot for inter-observer agreement for Exocanthion Right - Nasion; mean difference 0.08mm, 95% Limits of agreement = -0.98 **to** 1.08mm

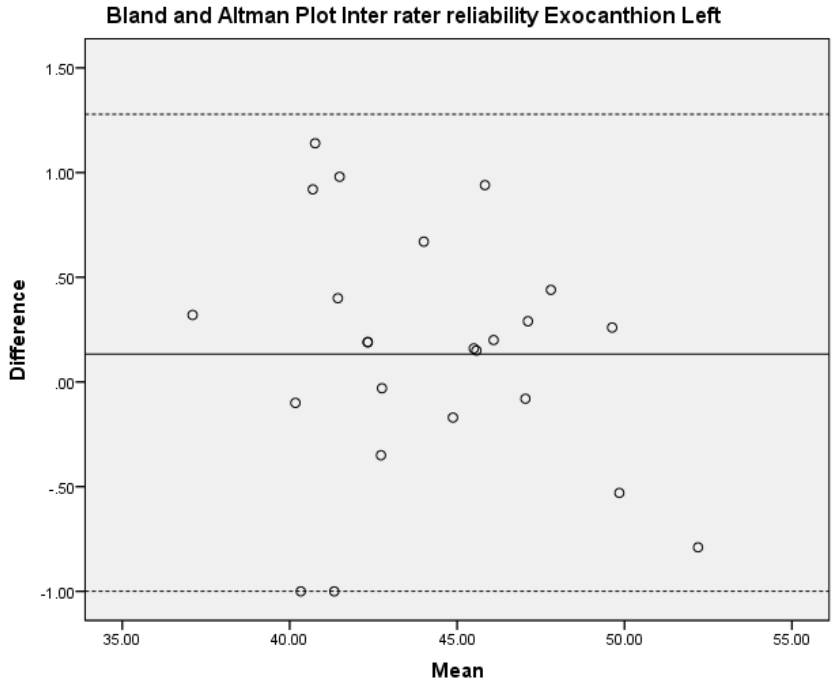

Bland and Altman Plot for inter-observer agreement for Exocanthion Left - Nasion; mean difference 0.13mm, 95% Limits of agreement = -1.01 to 1.28mm

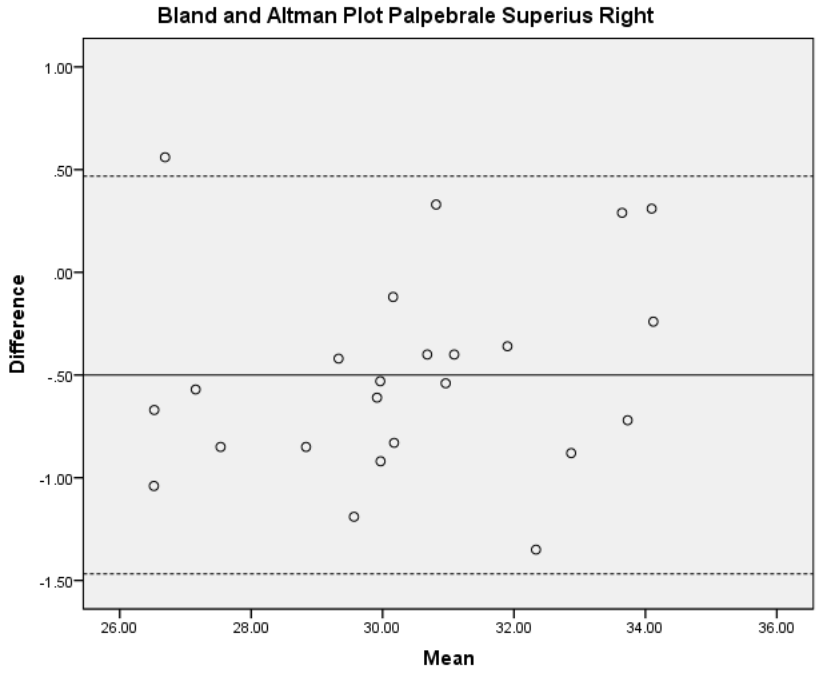

Bland and Altman Plot for inter-observer agreement for Palpebrale Superius Right - Nasion; mean difference -0.50mm, 95% Limits of agreement = -1.47 to 0.47mm

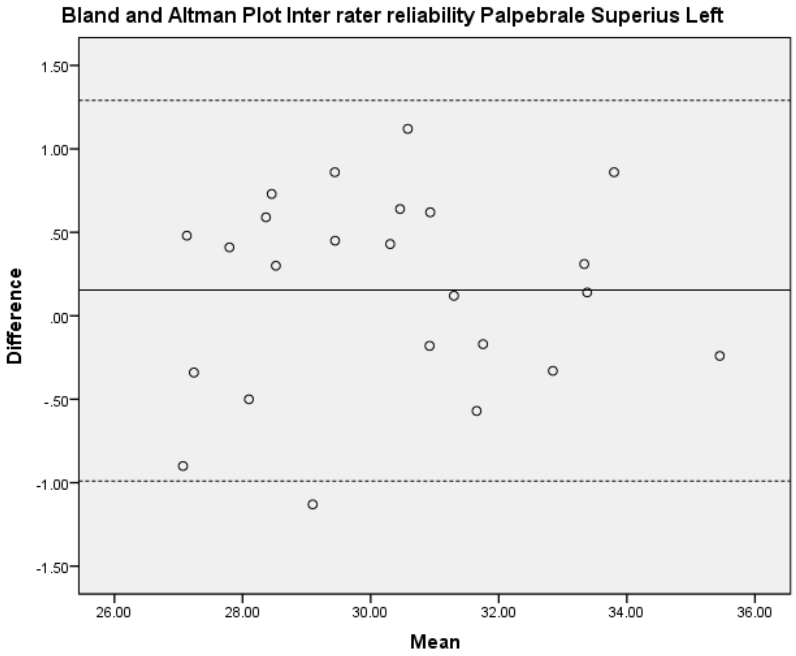

Bland and Altman Plot for inter-observer agreement for Palpebrale Superius Left - Nasion; mean difference 0.15mm, 95% Limits of agreement = -0.99 to 1.30mm

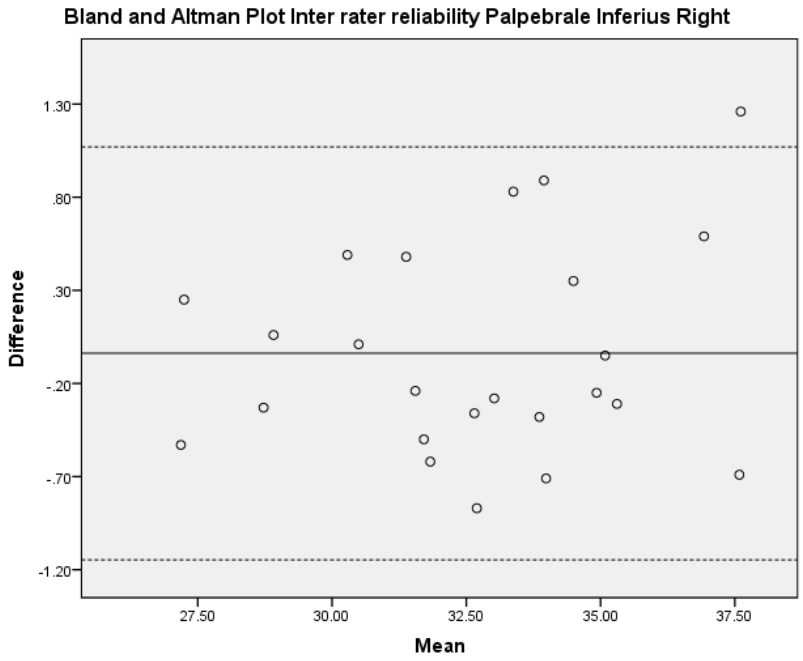

Bland and Altman Plot for inter-observer agreement for Palpebrale Inferius Right - Nasion; mean difference -0.04mm, 95% Limits of agreement = -1.15 to 1.07mm

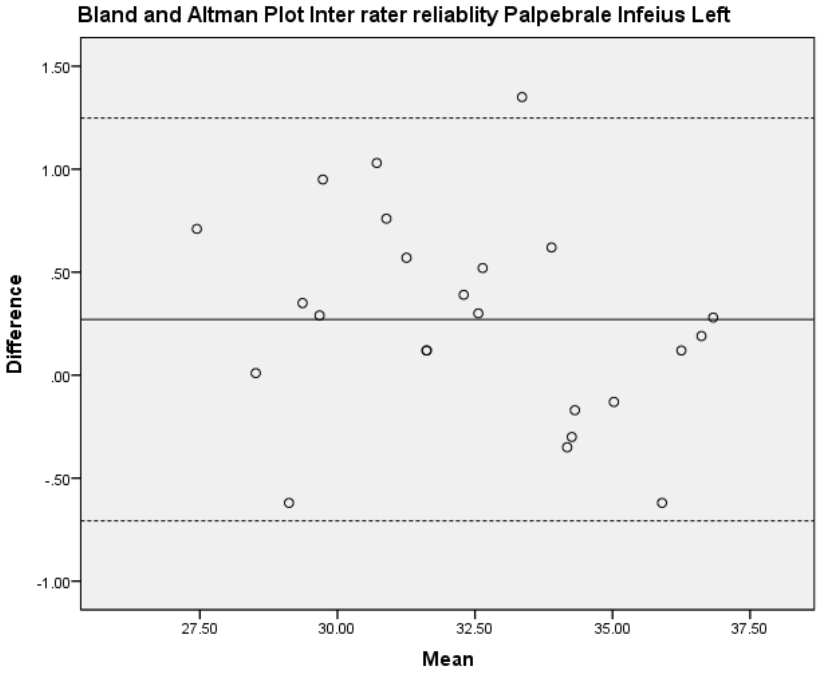

Bland and Altman Plot for inter-observer agreement for Palpebrale Inferius Left - Nasion; mean difference 0.27mm, 95% Limits of agreement = -0.71 to 1.25mm

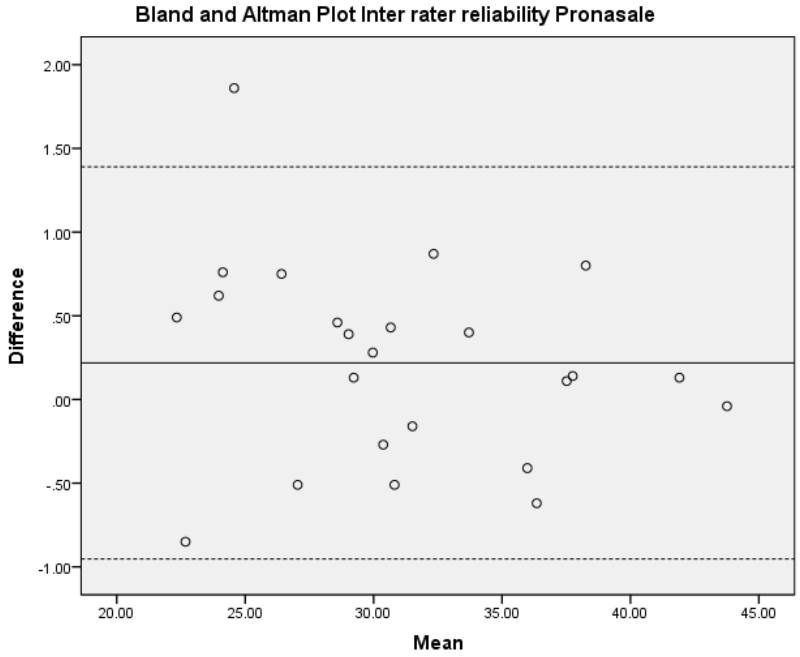

Bland and Altman Plot for inter-observer agreement for Pronasale - Nasion; mean difference 0.22mm, 95% Limits of agreement = -0.95 to 1.39mm

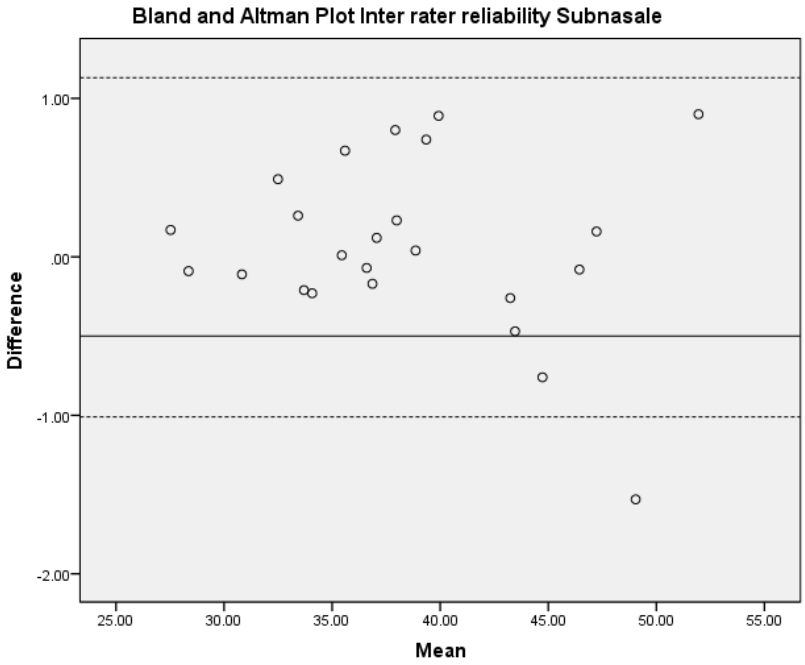

Bland and Altman Plot for inter-observer agreement for Subnasale - Nasion; mean difference 0.06mm, 95% Limits of agreement = -1.01 to 1.14mm

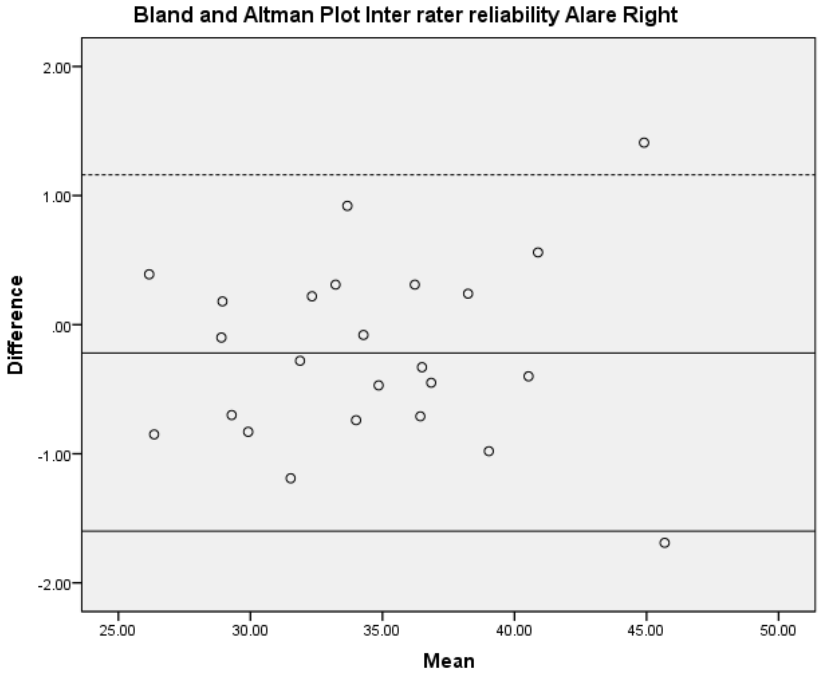

Bland and Altman Plot for inter-observer agreement for Alare Right - Nasion; mean difference -0.22mm, 95% Limits of agreement = -1.60 to 1.16mm

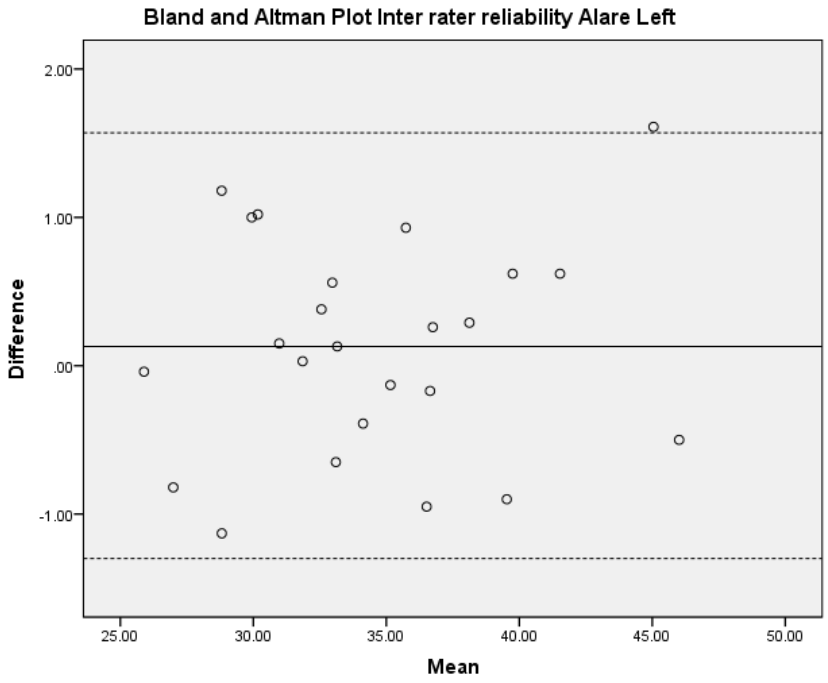

Bland and Altman Plot for inter-observer agreement for Alare Left - Nasion; mean difference 0.13mm, 95% Limits of agreement -1.31 to 1.57mm

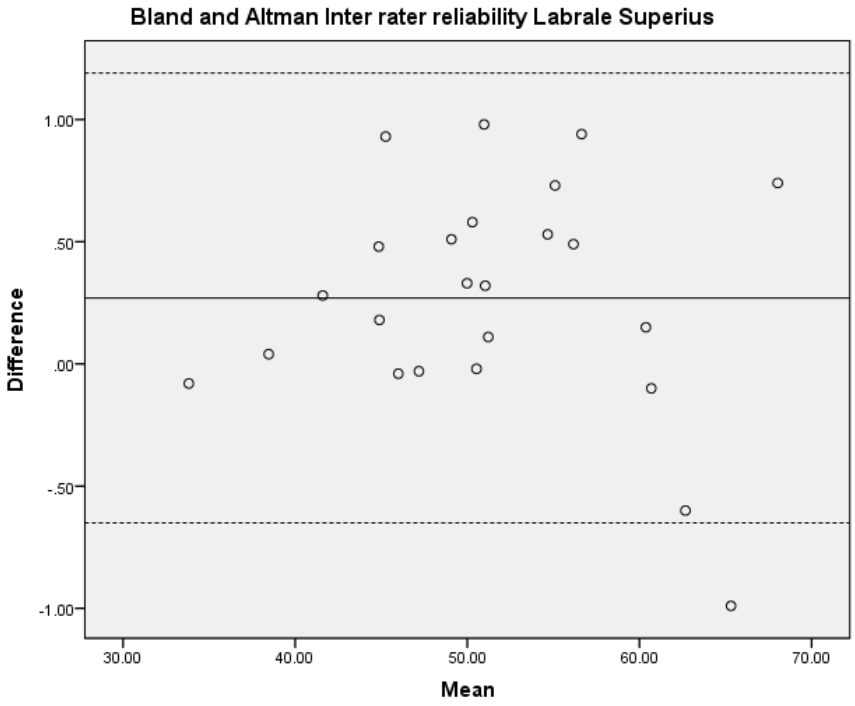

Bland and Altman Plot for inter-observer agreement for Labrale Superius - Nasion; mean difference 0.30mm, 95% Limits of agreement = -0.66 to 1.19mm

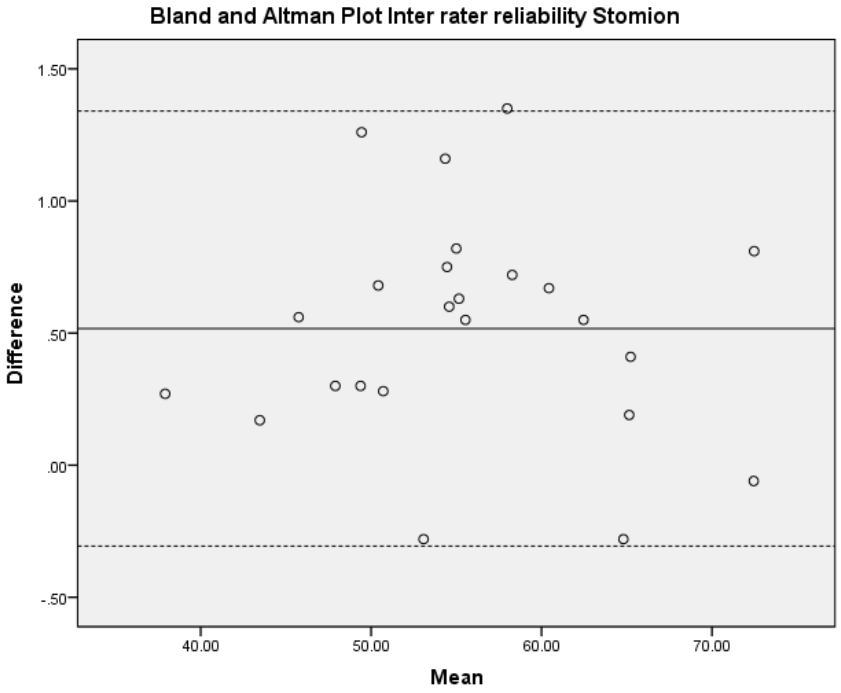

Bland and Altman Plot for inter-observer agreement for Stomion - Nasion; mean difference 0.52mm, 95% Limits of agreement = -0.31 to 1.34mm

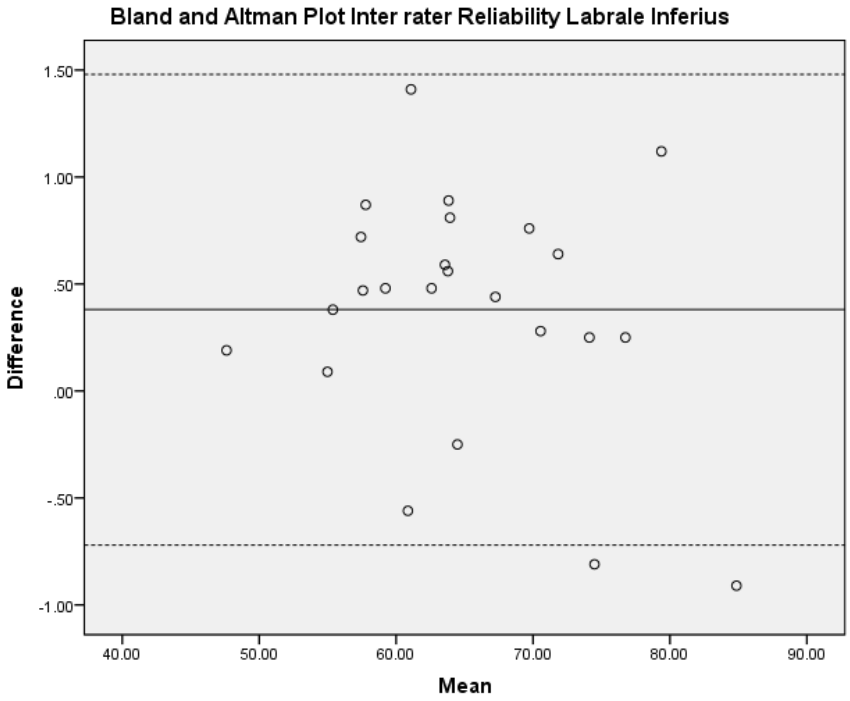

Bland and Altman Plot for inter-observer agreement for Labrale Inferius - Nasion; mean difference 0.38mm, 95% Limits of agreement = -0.72 to 1.48mm

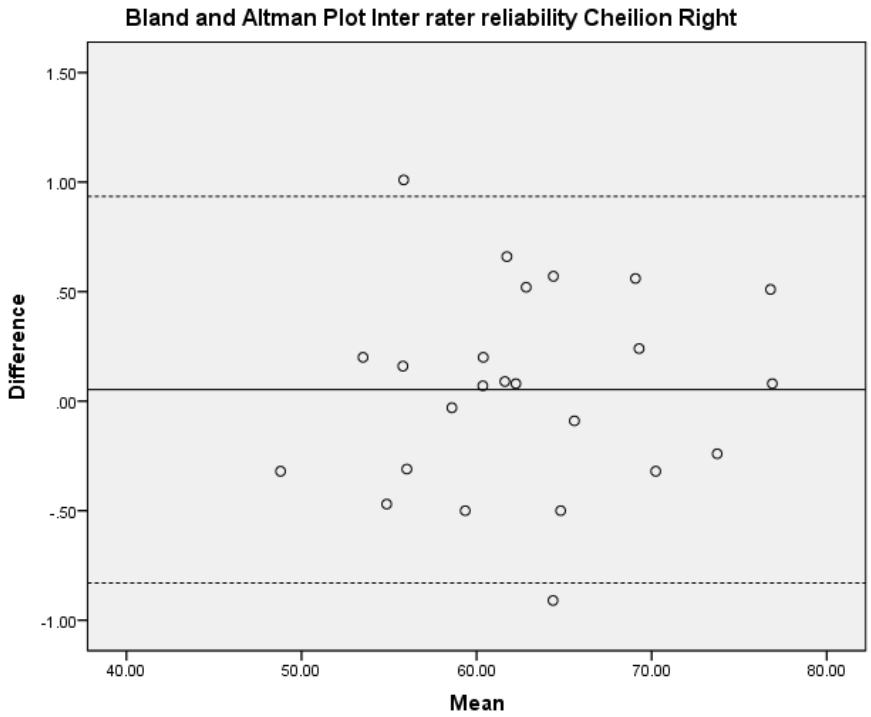

Bland and Altman Plot for inter-observer agreement for Cheilion Right - Nasion; mean difference 0.05mm, 95% Limits of agreement = -0.83 to 0.94mm

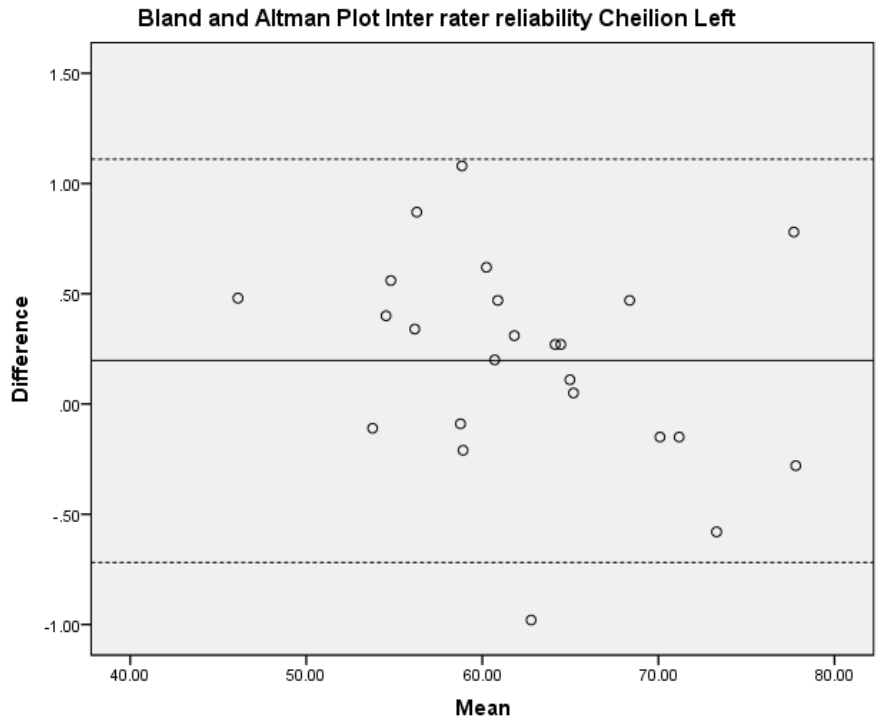

Bland and Altman Plot for inter-observer agreement for Cheilion Left - Nasion; mean difference 0.20mm, 95% Limits of agreement = -0.72 to 1.11mm

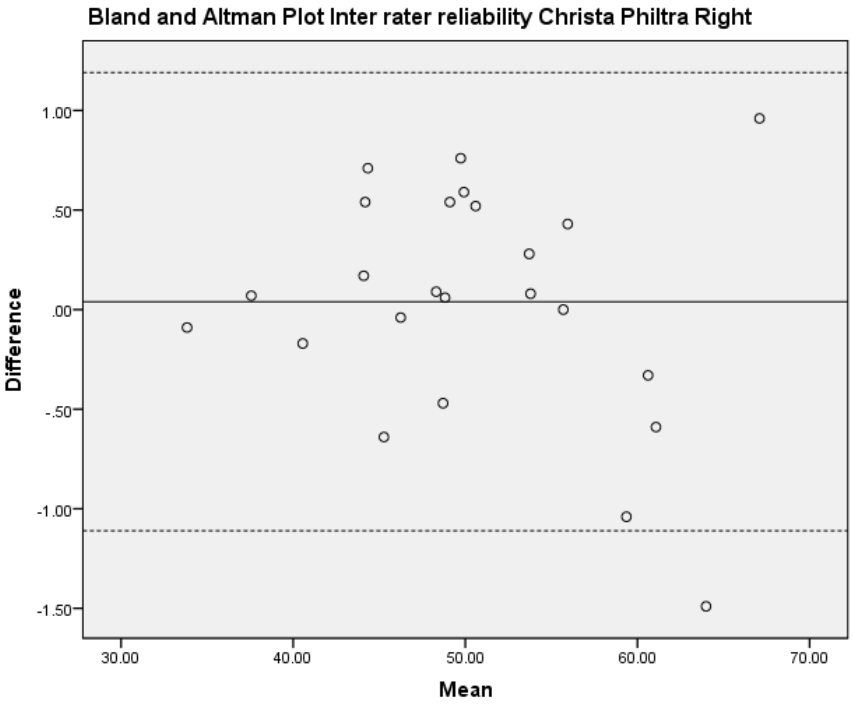

Bland and Altman Plot for inter-observer agreement for Christa Philtra Right - Nasion; mean difference 0.04mm, 95% Limits of agreement = -1.11 to 1.19mm

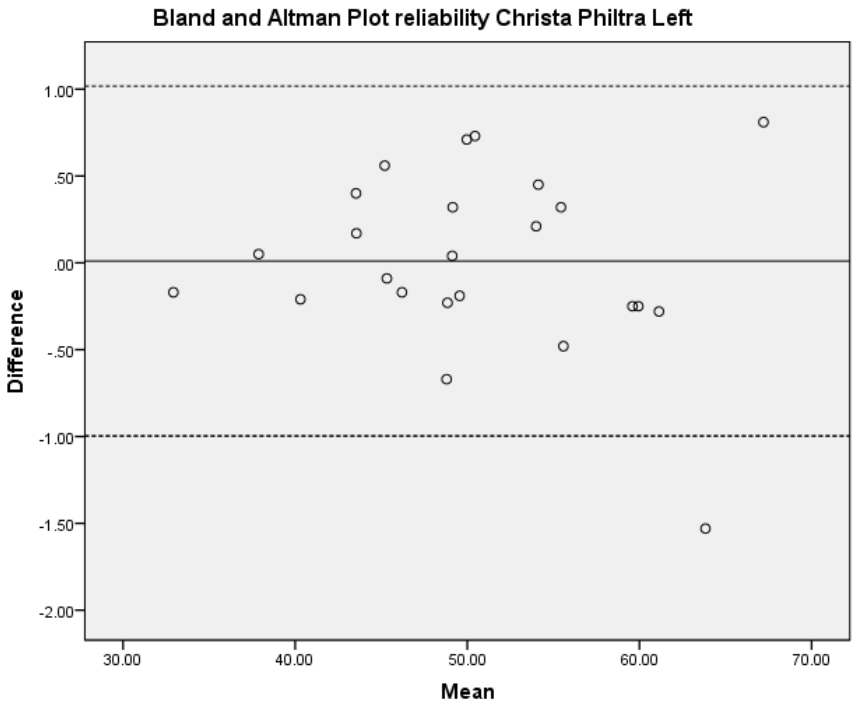

Bland and Altman Plot for inter-observer agreement for Christa Philtra Left - Nasion; mean difference 0.01mm, 95% Limits of agreement = -1.00 to 1.02mm

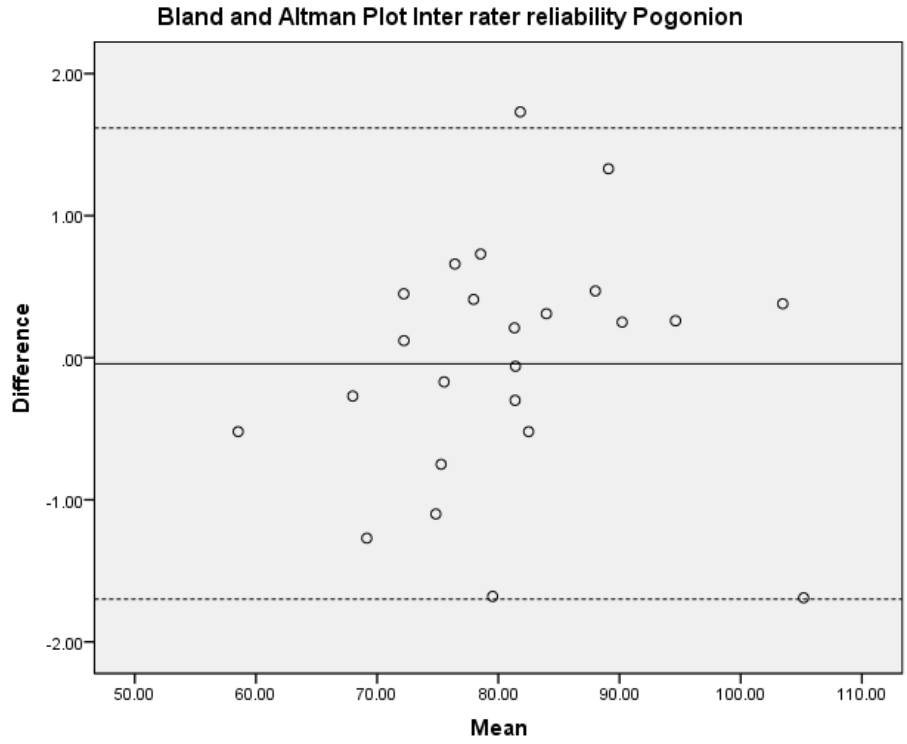

Bland and Altman Plot for inter-observer agreement for Pogonion - Nasion; mean difference -0.04mm, 95% Limits of agreement = -1.70 to 1.62mm

Appendix 5: Histograms and Shapiro-Wilk tests demonstrating distribution of data for mid-facial landmarks in x direction (mediolateral plane)

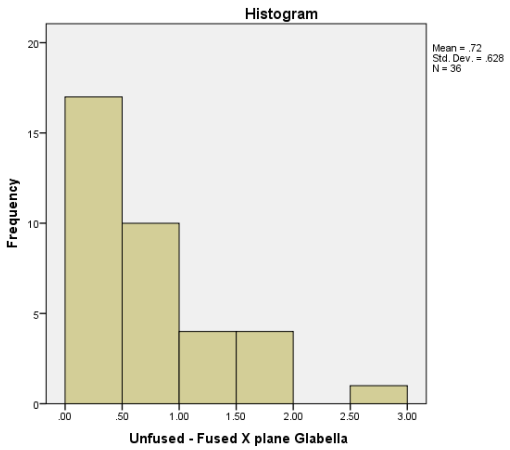

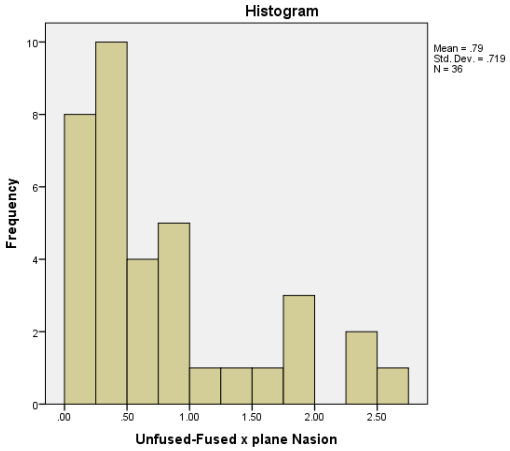

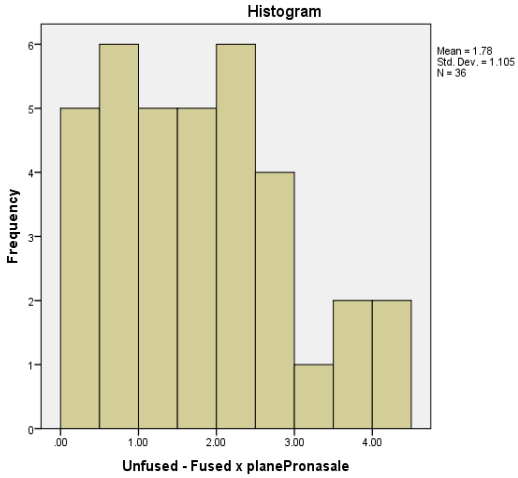

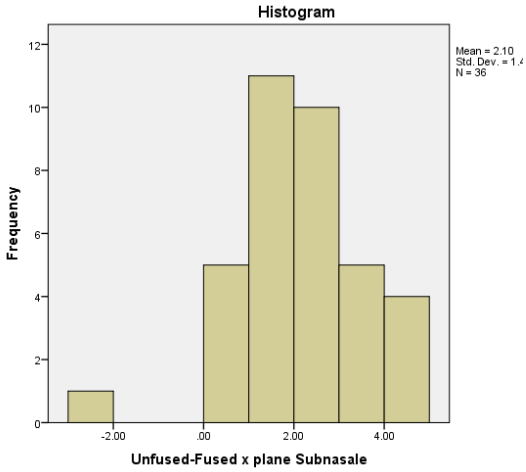

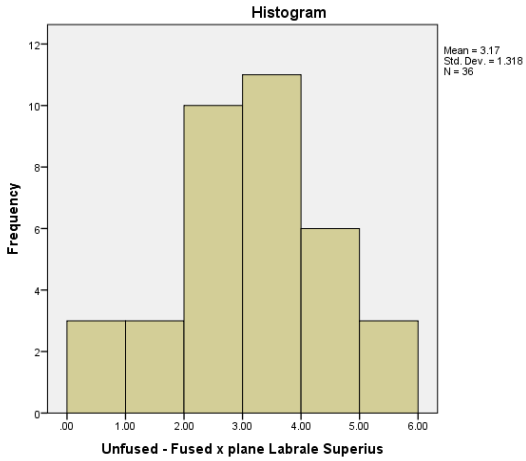

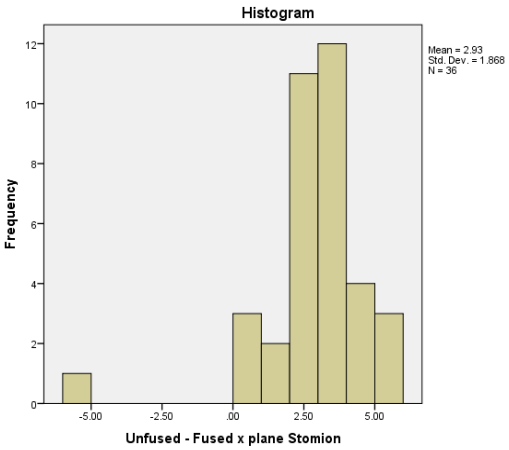

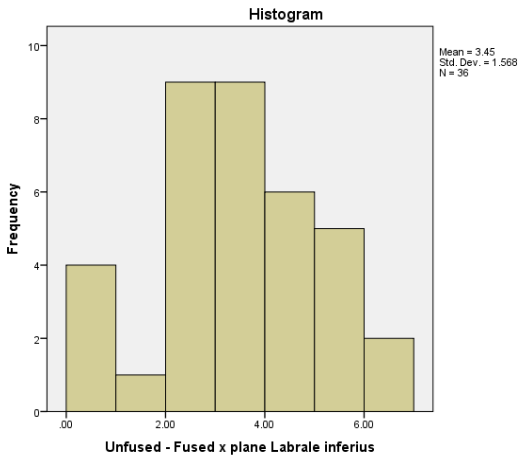

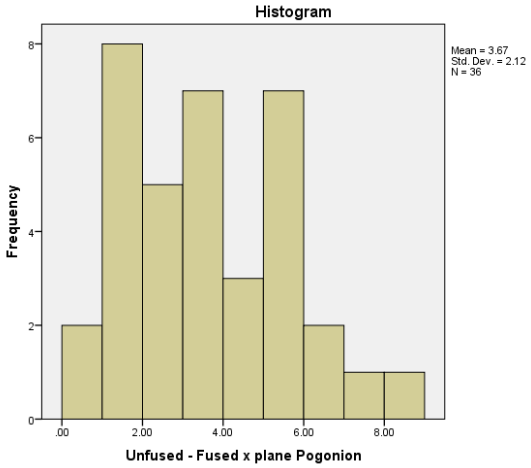

	Shapiro-Wilk		
Landmark	Statistic	Df	Sig.
Glabella	0.876	36	0.001
Nasion	0.842	36	<0.001
Pronasale	0.936	36	0.037
Subnasale	0.925	36	0.018
Labrale Superius	0.959	36	0.197
Stomion	0.986	36	0.915
Labrale Inferius	0.971	36	0.452
Pogonion	0.816	36	<0.001

Appendix 6: Histograms and Shapiro-Wilk tests showing distribution of data for bilateral landmarks in x co-ordinate plane (mediolateral plane)

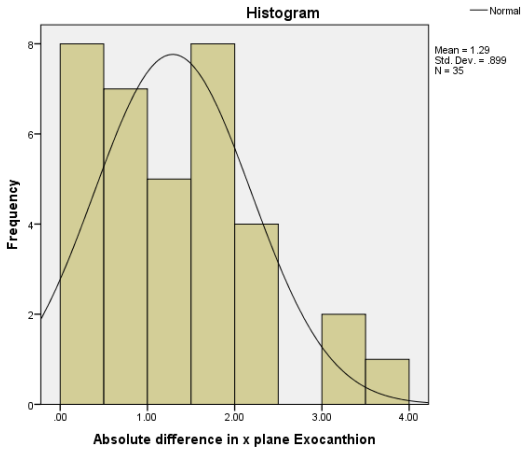

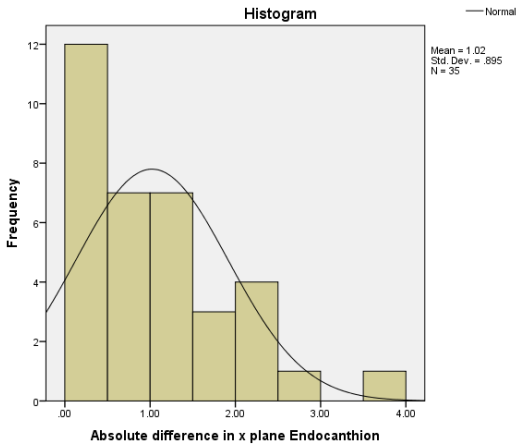

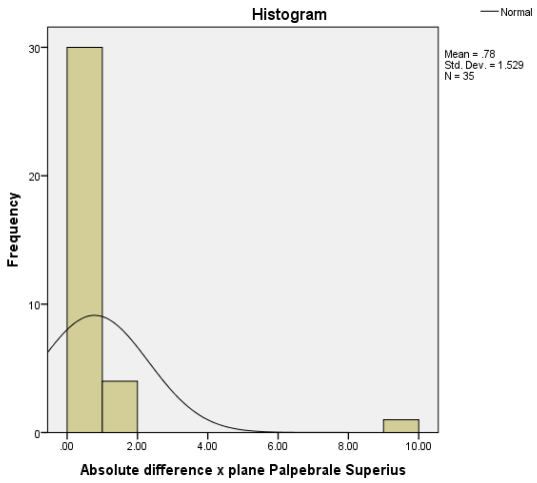

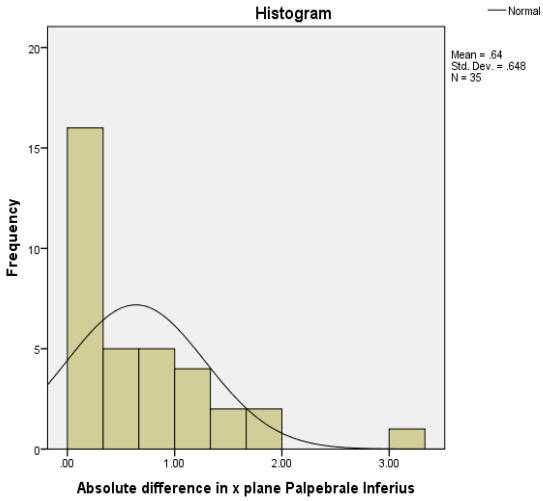

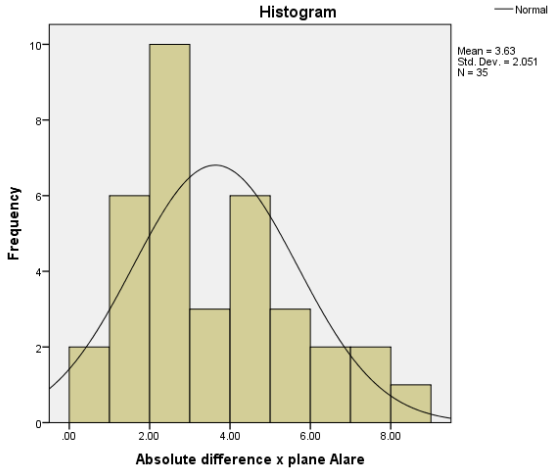

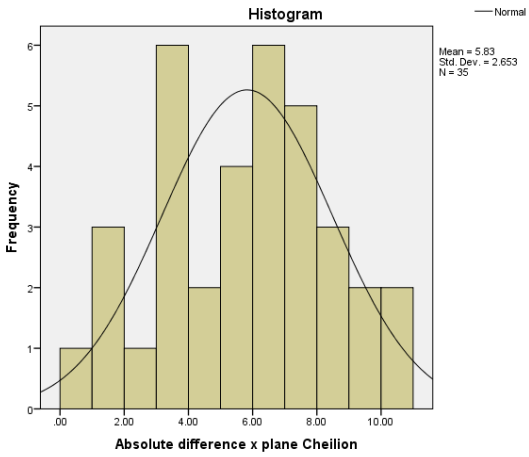

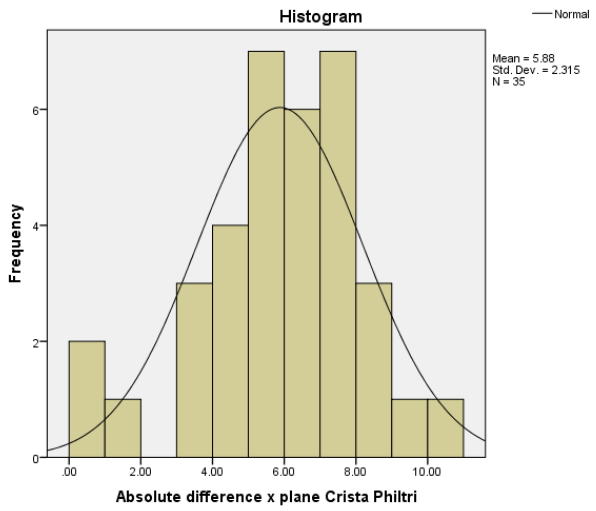

	Shapiro-Wilk		
Landmark	Statistic	df	Sig.
Exocanthion	0.933	35	0.033
Endocanthion	0.885	35	0.002
Palpebrale Superius	0.388	35	<0.001
Palpebrale Inferius	0.826	35	<0.001
Alare	0.940	35	0.055
Cheilion	0.972	35	0.507
Crista Philtri	0.963	35	0.289

Appendix 7: Histograms and Shapiro-Wilk tests showing distribution of data for bilateral landmarks in y co-ordinate plane (Superior Inferior Plane)

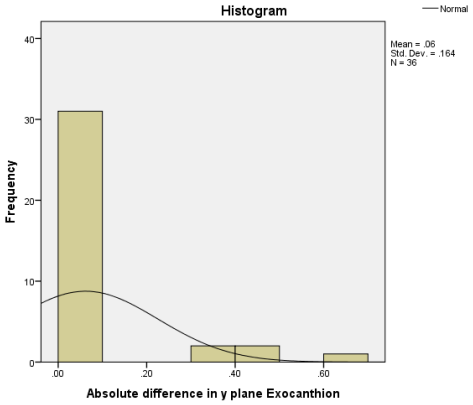

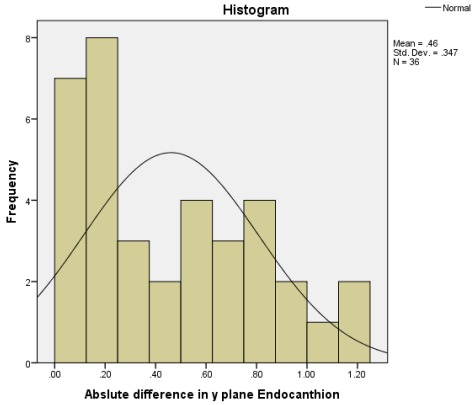

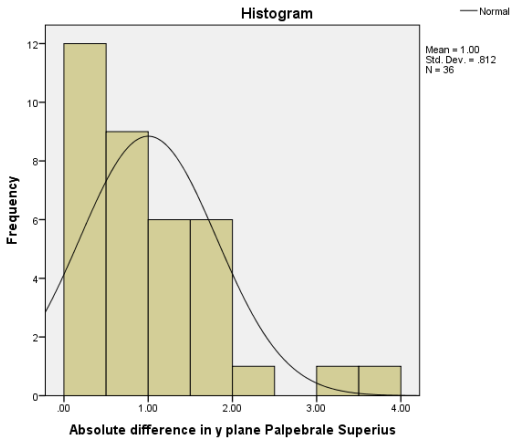

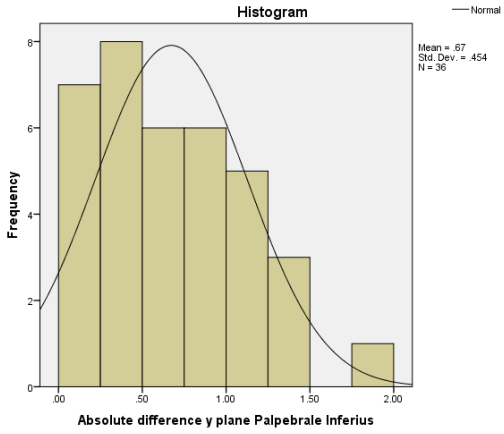

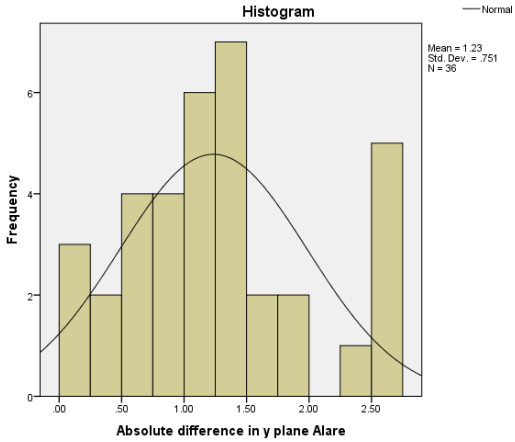

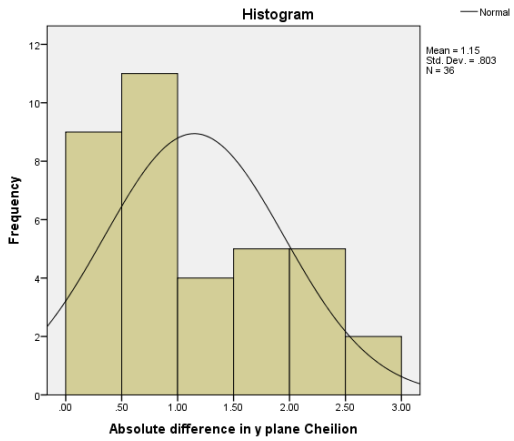

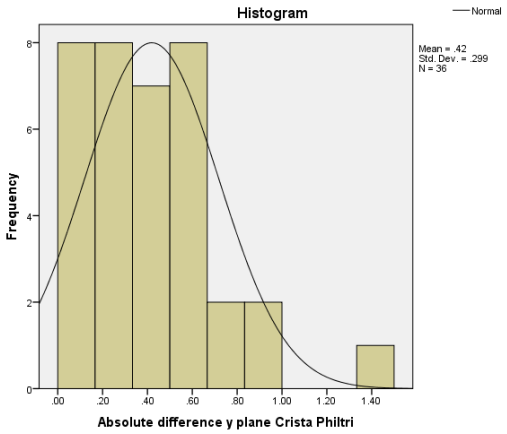

	Shapiro-Wilk		
Landmark	Statistic	df	Sig.
Exocanthion	0.434	36	<0.001
Endocanthion	0.919	36	0.012
Palpebrale Superius	0.882	36	<0.001
Palpebrale Inferius	0.963	36	0.270
Alare	0.936	36	0.037
Cheilion	0.932	36	0.028
Crista Philtri	0.920	36	0.012

Appendix 8: Histograms and Shapiro-Wilk tests showing distribution of data for bilateral landmarks in z co-ordinate plane (Anteroposterior Plane)

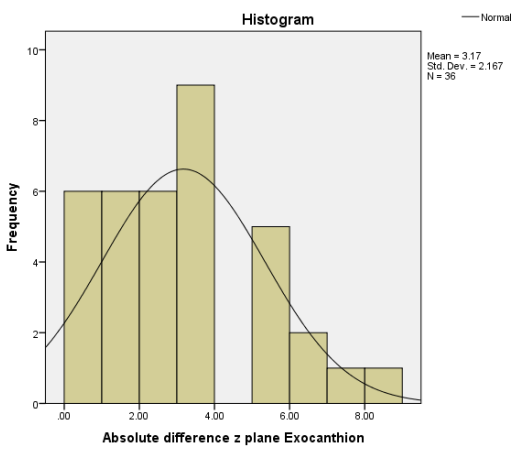

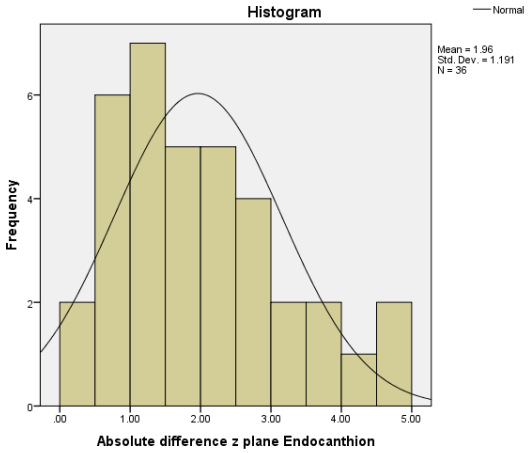

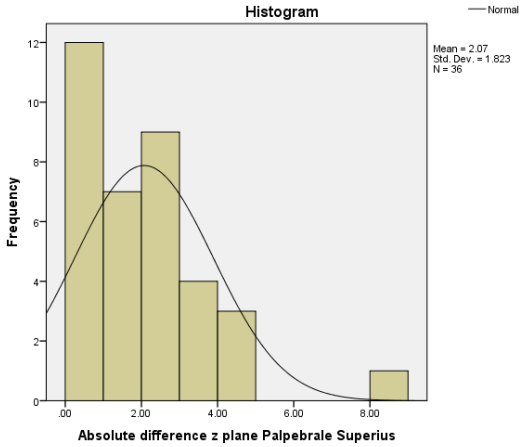

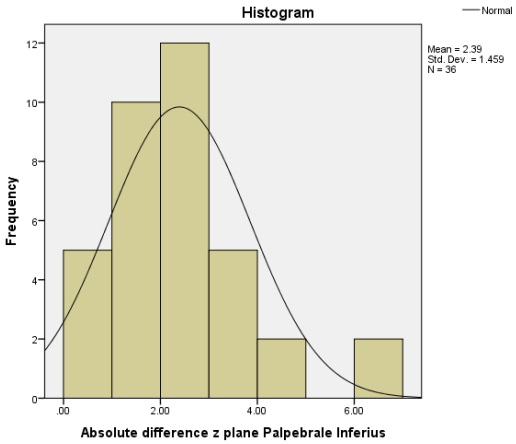

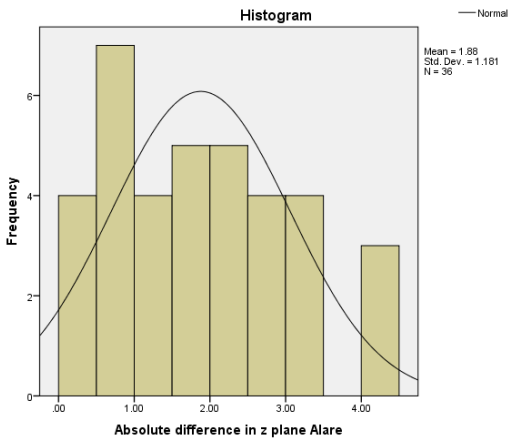

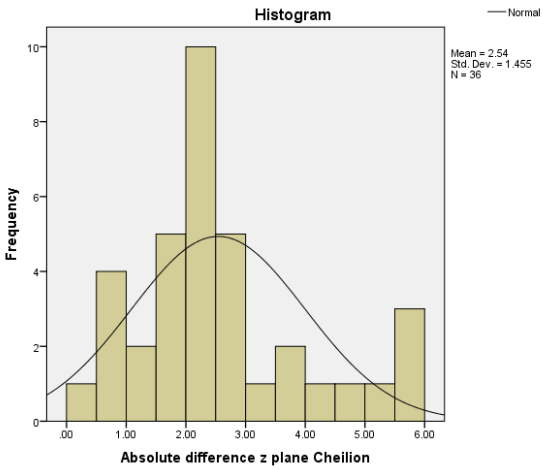

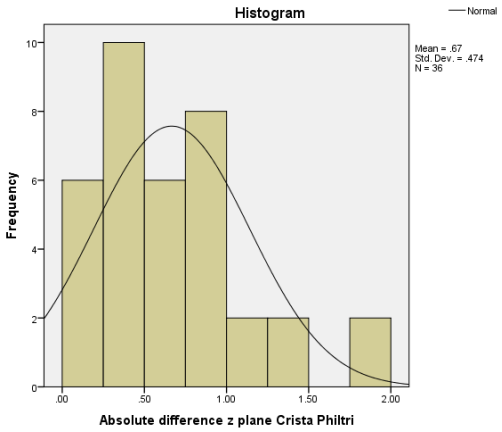

	Shapiro-Wilk		
Landmark	Statistic	df	Sig.
Exocanthion	0.936	36	0.037
Endocanthion	0.957	36	0.170
Palpebrale Superius	0.861	36	<0.001
Palpebrale Inferius	0.938	36	0.043
Alare	0.956	36	0.159
Cheilion	0.912	36	0.007
Crista Philtri	0.956	36	0.159

Appendix 9: Histograms and Shapiro-Wilk tests showing distribution of data for bilateral landmarks Euclidean distance/ linear measurements

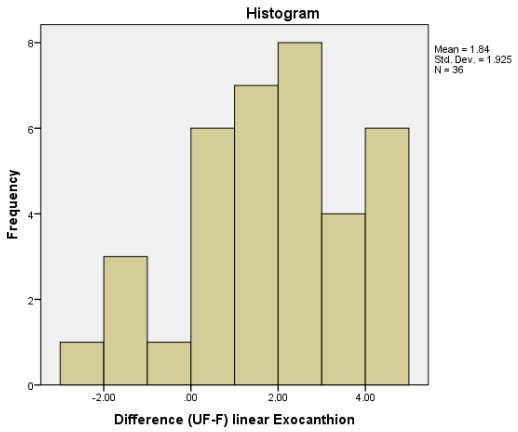

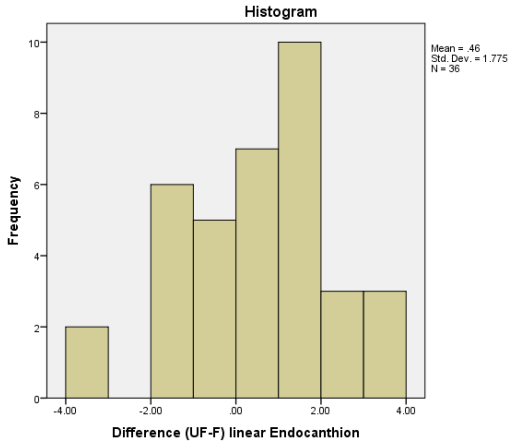

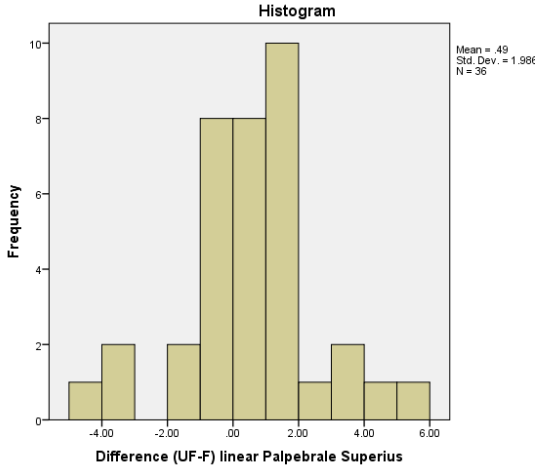

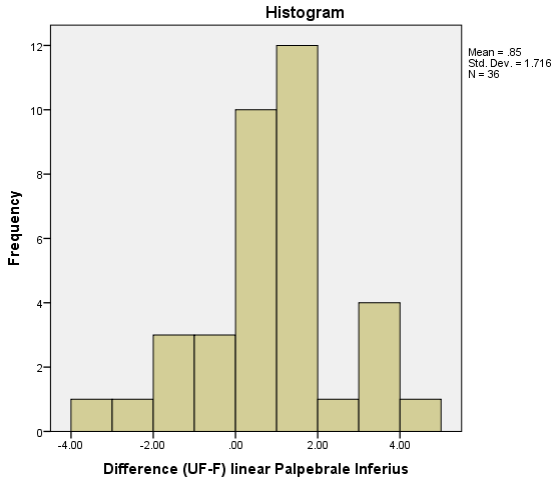

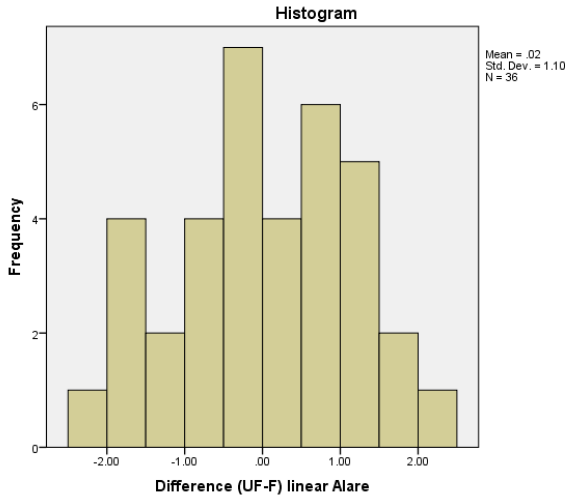

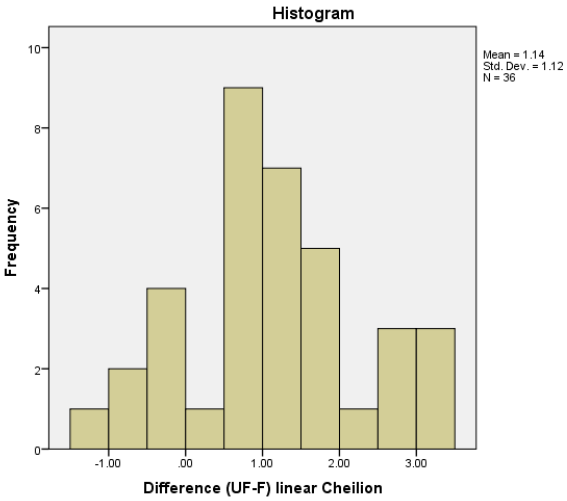

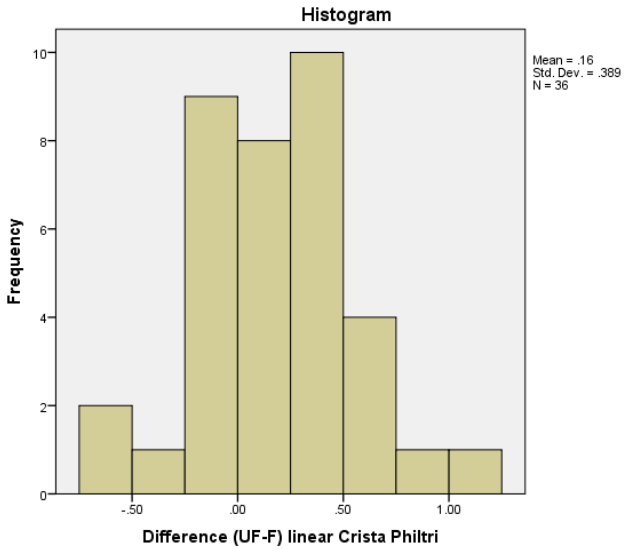

	Shapiro-Wilk		
Landmark	Statistic	df	Sig.
Exocanthion	0.967	36	0.344
Endocanthion	0.985	36	0.889
Palpebrale Superius	0.965	36	0.304
Palpebrale Inferius	0.972	36	0.486
Alare	0.982	36	0.795
Cheilion	0.966	36	0.322
Crista Philtri	0.988	36	0.955

Appendix 10: Histograms and Shapiro-Wilk tests showing distribution of data for bilateral landmarks surface measurements

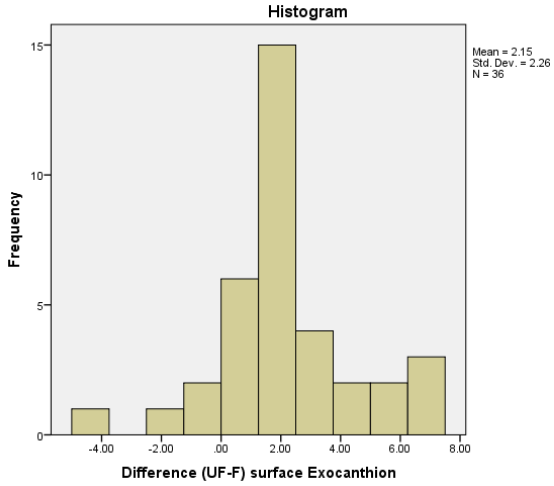

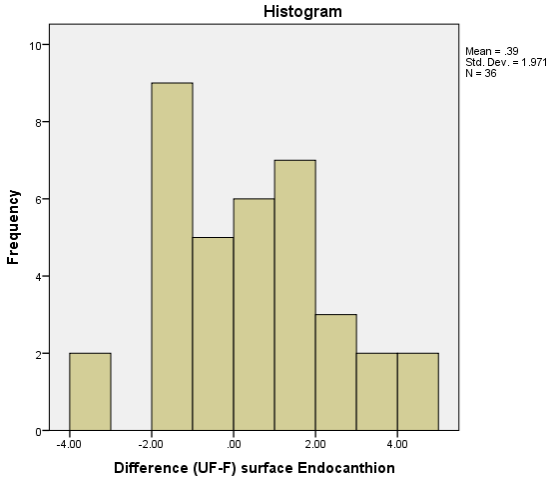

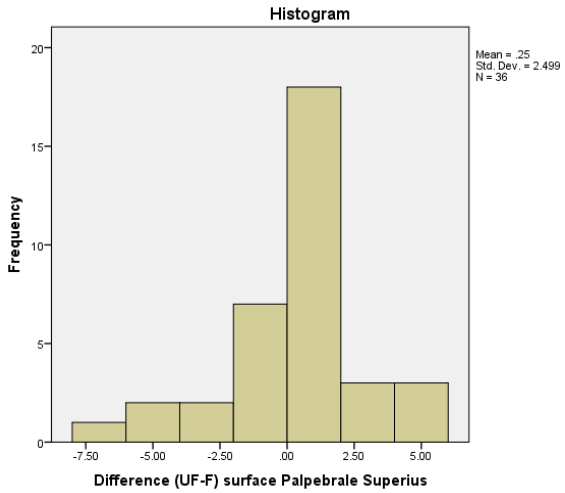

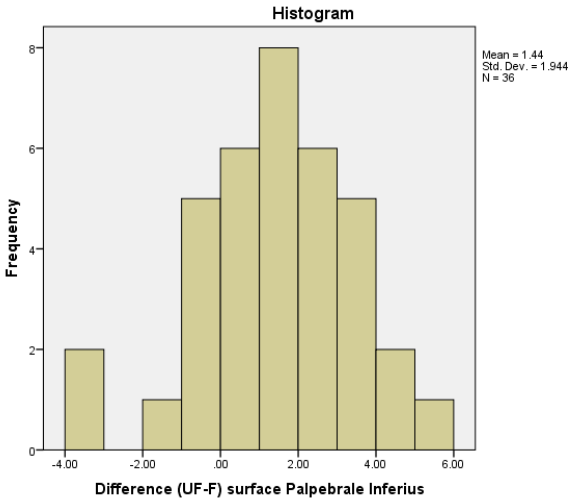

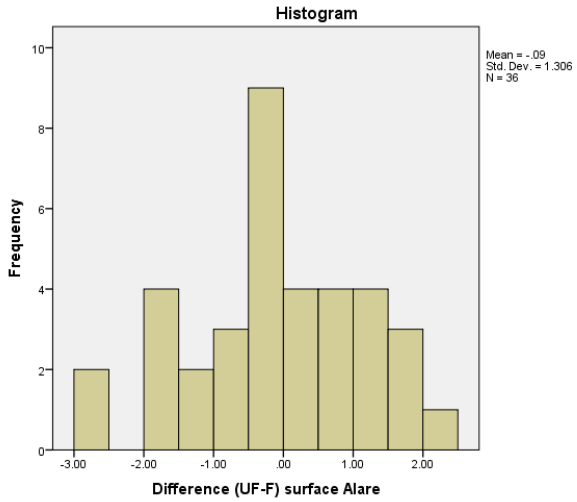

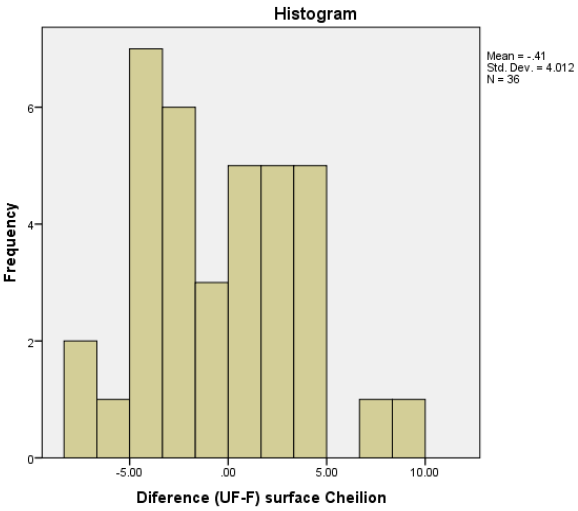

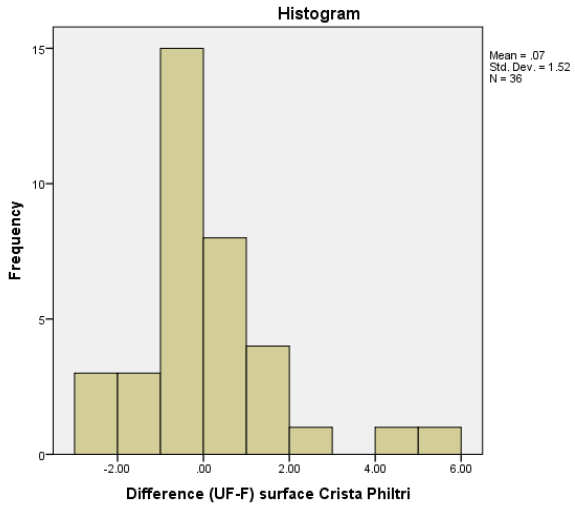

	Shapiro-Wilk		
Landmark	Statistic	df	Sig.
Exocanthion	0.946	36	0.081
Endocanthion	0.979	36	0.708
Palpebrale Superius	0.941	36	0.053
Palpebrale Inferius	0.977	36	0.658
Alare	0.978	36	0.682
Cheilion	0.966	36	0.322
Crista Philtri	0.983	36	0.850